Structural Principles for Dynamics of Glass Networks

by

Linghong Lu

BSc, Yunnan University, 2002
MSc, Yunnan University, 2005

A Dissertation Submitted in Partial Fulfillment of the
Requirements for the Degree of

MASTER OF SCIENCE

in the Department of Mathematics and Statistics

Structural Principles for Dynamics of Glass Networks

by

Linghong Lu

BSc, Yunnan University, 2002
MSc, Yunnan University, 2005

Supervisory Committee

Dr. Roderick Edwards, Supervisor (Department of Mathematics and Statistics)

Dr. Reinhard Illner, Member (Department of Mathematics and Statistics)

Dr. Christopher Bose, Member (Department of Mathematics and Statistics)

Dr. Nikitas J. Dimopoulos, Member (Department of Electrical and Computer Engineering)

Dr. Tomas Gedeon, External Examiner (Montana State University)

Supervisory Committee

Dr. Roderick Edwards, Supervisor (Department of Mathematics and Statistics)

Dr. Reinhard Illner, Member (Department of Mathematics and Statistics)

Dr. Christopher Bose, Member (Department of Mathematics and Statistics)

Dr. Nikitas J. Dimopoulos, Member (Department of Electrical and Computer Engineering)

Dr. Tomas Gedeon, External Examiner (Montana State University)

Abstract

Gene networks can be modeled by piecewise-linear (PL) switching systems of differential equations, called Glass networks after their originator. Networks of interacting genes that regulate each other may have complicated interactions. From a 'systems biology' point of view, it would be useful to know what types of dynamical behavior are possible for certain classes of network interaction structure.

A useful way to describe the activity of this network symbolically is to represent it as a directed graph on a hypercube of dimension n where n is the number of elements in the network. Our work here is considering this problem backwards, i.e. we consider different types of cycles on the n-cube and show that there exist parameters, consistent with the directed graph on the hypercube, such that a periodic orbit exists.

For any simple cycle on the n-cube with a non-branching vertex, we prove by construction that it is possible to have a stable periodic orbit passing through the corresponding orthants for some sets of focal points F in Glass networks. When the simple cycle on the n-cube doesn't have a non-branching vertex, a structural principle is given to determine whether it is possible to have a periodic orbit for some focal points. Using a similar construction idea, we prove that for self-intersecting cycles where the vertices revisited on the cycle are not adjacent, there exist Glass

networks which have a periodic orbit passing through the corresponding orthants of the cycle. For figure-8 patterns with more than one common vertex, we obtain results on the form of the return map (Poincaré map) with respect to how the images of the returning cones of the 2 component cycle intersect the returning cone themselves. Some of these allow complex behaviors.

Table of Contents

List of Tables

List of Figures

Acknowledgements

I would like to take this opportunity to express my heart-felt gratitude to a number of people for different sorts of assistance they have provided me in making this thesis a reality.

First and foremost, I am greatly indebted to my academic advisor Dr. Rod Edwards, for his boundless help during my study, for his valuable directions and enlightening suggestions, and for his generosity in spending his precious time reading, discussing and improving my thesis. Without his help, the completion of my thesis would be impossible.

I am very grateful to all the teachers and professors who taught me and gave me inspiring lectures on various subjects that have helped to widen my point of view during my study in the University of Victoria.

I feel fortunate to have shared my graduate experience with so many wonderful fellow students: Angus Argyle, Tony Deng, Shelly Hsieh, Terry Lee, Bibo Liu, Maryam Namazi, Beiyan Ou, Reinel Sospedra Alfonso, Xiaolong Yang and so many more. Their camaraderie has been invaluable and I look forward to their continued friendships and collaborations.

Last, but not least, my sincere appreciation goes to my parents. It is their understanding and endless support that gave me strong motivation to finish my graduate study abroad.

Chapter 1

Introduction

In the context of Network theory, the term "complex network" refers to a network (graph) that has certain non-trivial topological features that do not occur in simple networks. Most social, biological, and technological networks (as well as certain network-driven phenomena) can be considered complex by virtue of non-trivial topological structure.

Since complex networks are often characterized by their tremendous sizes and the nonlinear interaction between their components, it is hard to develop general techniques which may be used to get their asymptotic behavior.

In gene networks, genetic regulatory elements called transcription factors can control the transcription of proteins. They bind to the DNA turning "on" and "off" the synthesis of specific mRNA according to their concentrations. Then the mRNA sequence is translated into an amino acid sequence which forms a protein.

After an article by Jacob and Monod [1] from the early 1960s about genetic regulatory elements, many researchers have worked on mathematical models to predict the dynamical behavior of gene networks ([26]-[29]).

In 1973, Glass and Kauffman [2] proposed a mapping obtained from the logical structure of the networks to study the qualitative properties of continuous biochemical control networks. In the following years, many nice results about this mapping came along including the development and dynamical analysis of this mapping. In 1974 [3], techniques were given to classify biological networks into classes having similar structure and therefore possibly similar qualitative dynamics. In this paper, Glass used directed edges in n-cubes (hypercubes in n dimensions) to represent the state transition diagrams of n variable systems. We see from later papers that this idea is a very useful way to describe the activity of the network symbolically.

When the continuous threshold functions in the differential equations are replaced by step functions, the equations become piecewise linear (PL equations). The general

form of PL equations called Glass networks (after their originator) is the following.

Let x_1, x_2,..., x_n be real variables and suppose positive constants θ_1, θ_2, ..., θ_n are given. Then

$$\dot{x}_i = -\alpha x_i + G_i(\tilde{x}_1, \tilde{x}_2, \ldots, \tilde{x}_n), \quad i = 1, \ldots, n,$$

where $\alpha > 0$ and

$$\tilde{x}_i = \begin{cases} a & \text{if} \quad x_i < \theta_i, \\ b & \text{if} \quad x_i > \theta_i. \end{cases}$$

Let $y_i = \alpha(x_i - \theta_i)$, $s = \alpha t$ and $F_i(\tilde{y}_1, \tilde{y}_2, \ldots, \tilde{y}_n) = G_i(\tilde{x}_1, \tilde{x}_2, \ldots, \tilde{x}_n) - \alpha\theta_i$, where $\tilde{y}_i = (\tilde{x}_i - a)/(b - a)$ and replacing the time variable s by t again, the original glass network is transformed as

$$\dot{y}_i = -y_i + F_i(\tilde{y}_1, \tilde{y}_2, \ldots, \tilde{y}_n), \quad i = 1, \ldots, n, \tag{1.1}$$

where

$$\tilde{y}_i = \begin{cases} 0 & \text{if} \quad y_i < 0, \\ 1 & \text{if} \quad y_i > 0. \end{cases} \tag{1.2}$$

These theoretical models have been in use for at least 30 years ([2], [9]), but the technology to conduct experiments has only recently been developed. In 2000 ([19], [20]), experimental results about the construction of genetic circuits, based on simple mathematical models, showed that the mathematical model predicts the behavior of the synthetic network very well. This is a great motivation to researchers working on genetic networks. H. De Jong ([10], [31]) uses the general piecewise-linear approach to simulate the initiation of sporulation in bacillus subtilis and the carbon starvation response in Escherichia coli. Moreover, researchers are making some changes to the general PL model ([22], [24]) to make the model more realistic.

Although Glass networks have aroused researchers' interest and have been widely discussed for years, most previous work ([11]-[18], [22], [24], [25]) started from given PL equations and the corresponding state transition diagrams called n-cube (introduced below in Section 2.2). Some researchers tried to classify networks and get the qualitative dynamical behavior of the PL equations by considering the structure of n-cube without knowing the equation ([3]-[8]). One of the most important contributions is about a certain configuration called "cyclic attractor". In [8], Glass and Pasternack proved that for the associated PL equation, all trajectories in the regions of phase space corresponding to the cyclic attractor either (i) approach a unique

stable limit cycle attractor, or (ii) approach the origin, in the limit $t \to \infty$, and an algebraic criterion is given to distinguish the two cases.

The result about the cyclic attractor is very nice, but how about other state transition diagrams with cycles but without cyclic attractors, which certainly exist since there is only one cyclic attractor on the 3-cube and three cyclic attractors on the 4-cube considering the geometric symmetries.

In this thesis, we will consider this problem backwards, i.e. we consider different types of cycles on the n-cube and show that there exist F_i in Eq. (1.1), consistent with the directed graph on the hypercube, such that a periodic orbit or a complex dynamical behavior can exist. Since most previous results are about the existence of periodic orbits ([8], [11], [12], [24]) or chaos ([16], [18]) for a *given* gene network, the results in this thesis explore Glass networks in a totally different way.

A brief description of the organization of this thesis is as follows.

In Chapter 2, we introduce the mathematical model (Glass Networks) which is used to model gene regulatory networks. All the needed mathematical background is given in this chapter including the linear fractional maps, the n-cube, the structural equivalence classes and some results from other researchers' work.

In Chapter 3, by construction of suitable focal points, we obtain the existence and stability of periodic orbits on simple cycles. Examples are given to illustrate the construction idea.

In Chapter 4, we focus on a more complicated cycle on the n-cube, a figure-8 cycle. Using some results from Chapter 3, we get the existence and stability of simple figure-8 orbits on figure-8 cycles by construction of focal points. Moreover, we generalize the result to cycles with multiple self-intersection but where the vertices revisited are not adjacent.

In Chapter 5, we focus on figure-8 patterns with two or more adjacent common vertices. We deal with only 2 cycles, A and B, in this configuration and focus on the possible patterns of the images of the respective returning cones. By controlling the image types, we are able to get very complex dynamical behavior for a given figure-8 pattern on the n-cube.

In the last chapter, Chapter 6, we give a summary of all the work in this thesis and discuss some future work.

Chapter 2

Background

2.1 Glass Networks

Throughout the article, we consider Glass networks expressed in the form

$$\dot{y}_i = -y_i + F_i(\tilde{y}_1, \tilde{y}_2, \ldots, \tilde{y}_n), \qquad i = 1, \ldots, n, \tag{2.1}$$

where

$$\tilde{y}_i = \begin{cases} 0 & \text{if} \quad y_i < 0, \\ 1 & \text{if} \quad y_i > 0. \end{cases}$$

Despite the discontinuity in the functions on the right-hand side of the equations, they are actually just very simple first-order differential equations in each given orthant in the form

$$\dot{y}_i = -y_i + f_i,$$

where $f_i = F_i(\tilde{y})$ is constant. Solving this ODE with initial point, $y(0)$, we get

$$y_i(t) = f_i + (y_i(0) - f_i)e^{-t}. \tag{2.2}$$

This expression shows that $y_i(t)$ approaches f_i exponentially, and since the decay rate is the same for each i, $y = (y_1, y_2, \ldots, y_n)^T$ approaches $f = (f_1, f_2, \ldots, f_n)^T$ in a straight line (T denotes the matrix transpose).

In vector form

$$y(t) = f + (y(0) - f)e^{-t},$$

where

$$f = F(\tilde{y}) = (F_1(\tilde{y}), F_2(\tilde{y}), \ldots, F_n(\tilde{y}))^T.$$

We will call f the focal point of the orthant considered. And of course, as soon as any y_i changes sign, i.e. crosses boundary 0, $\tilde{y}$ changes and the focal point changes

to the corresponding value.

In the following analysis, we always assume

Condition 2.1.1. $F_i \neq 0, \quad \forall i \quad \forall \tilde{y}$

and, except in Chapter 5,

Condition 2.1.2. $\text{sign}(F_i(\tilde{y}_1, \ldots, \tilde{y}_i = 0, \ldots, \tilde{y}_n)) = \text{sign}(F_i(\tilde{y}_1, \ldots, \tilde{y}_i = 1, \ldots, \tilde{y}_n))$.

Condition 2.1.1 states that the focal point of each orthant is in the interior of some orthant. Condition 2.1.2 states that the sign of F_i does not depend on $\tilde{y}_i$. Under Condition 2.1.2, when y_i changes sign, the transition across a boundary where $y_i = 0$ and $y_j \neq 0$, $j \neq i$ is unambiguous and the trajectory at the boundary is simply the continuous extension of the two pieces defined on either side of it. Otherwise, trajectories on the two sides flow towards or away from the boundary, and Mestl et al. [12] call the boundary a 'black wall' or 'white wall', respectively. Condition 2.1.2 corresponds to effective autoregulation in the network [21].

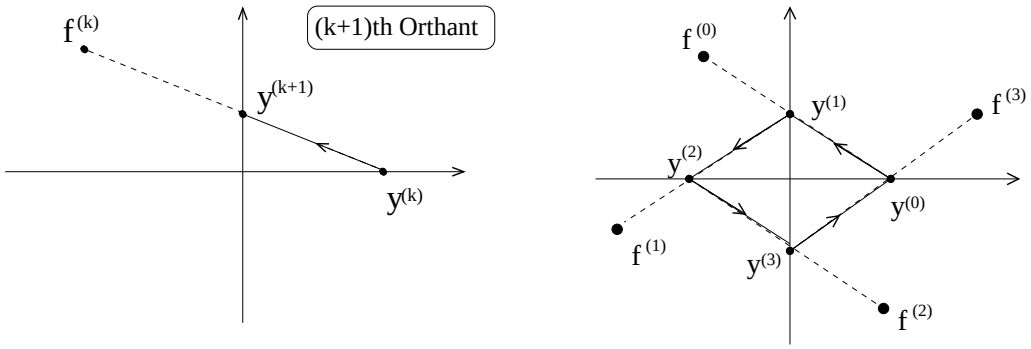

Figure 2.1: Notation illustrations in 2-D.

If the trajectories do not enter an orthant containing its own focal point (in this case, the trajectory will simply approach its focal point asymptotically), the trajectories for an n-dimensional network (n-net) may be specified by a discrete mapping on the $(n-1)$-dimensional boundaries with a fractional linear form. Let $f^{(k)}$ be the focal point associated with the $(k+1)$th orthant being entered and $y^{(k+1)}$ be the $(k+1)$th orthant boundary crossing on a trajectory which is the boundary on leaving the $(k+1)$th orthant (See Fig. 2.1 for illustration), we have the mapping from one boundary to the next in each variable as

$$y_i^{(k+1)} = \frac{f_i^{(k)} y_j^{(k)} - f_j^{(k)} y_i^{(k)}}{y_j^{(k)} - f_j^{(k)}}, \quad i = 1, \ldots, n, \tag{2.3}$$

where j is the index of the variable that switches on exiting the $(k+1)$th orthant along the trajectory, i.e., $y_j^{(k+1)} = 0$. Mapping (2.3) can also be represented as an operator ($M^{(k)} : \mathbb{R}^n \to \mathbb{R}^n$):

$$y^{(k+1)} = M^{(k)} y^{(k)} = \frac{B^{(k)} y^{(k)}}{1 + \langle \psi^{(k)}, y^{(k)} \rangle}, \tag{2.4}$$

where

$$B^{(k)} = I - \frac{f^{(k)} e_j^T}{f_j^{(k)}}, \quad \psi^{(k)} = \frac{-e_j}{f_j^{(k)}}, \tag{2.5}$$

j is the index of the variable that switches on exiting the $(k+1)$th orthant along the trajectory, e_j denotes the standard basis vector in $\mathbb{R}^n$, and the angle brackets denote the Euclidean inner product ($\langle \psi, y \rangle = \psi^T y$).

It is easy to check that the composition of fractional linear mappings is again a fractional linear mapping of the same form. In general, the mapping of a trajectory passing through m orthants can be represented as

$$My^{(0)} = \frac{B^{(m,0)} y^{(0)}}{1 + \langle \psi^{(m,0)}, y^{(0)} \rangle}, \tag{2.6}$$

where

$$B^{(m,0)} = B^{(m-1)} \dots B^{(1)} B^{(0)}, \quad \psi^{(m,0)} = \psi^{(0)} + \sum_{k=1}^{m-1} B^{(k,0)^T} \psi^{(k)}. \tag{2.7}$$

2.2 The n-Cube

A useful way to describe the activity of the network symbolically is to represent it as a directed graph on a hypercube of dimension n where n is the number of elements in the network (hereafter called an n-cube). We will use one example to show how the state transition diagram for a network can be represented as a digraph on a hypercube.

Define

$$\tilde{x}_i = \begin{cases} 0 & \text{if} \quad x_i < 0, \\ 1 & \text{if} \quad x_i > 0, \end{cases} \qquad i = 1, 2.$$

Consider the Glass network

$$\begin{aligned} &\dot{x}_i = -x_i + F_i, \qquad i = 1, 2, \\ &F_1 = 1 - 2\tilde{x}_2, \quad F_2 = 1 - 2\tilde{x}_1. \end{aligned} \tag{2.8}$$

The focal point structure of (2.8) is given in Table 2.1. System (2.8) is used to model

two mutually inhibitory elements see Fig. (2.2).

Orthant ($\tilde{x}$)	F
0 0	1 1
0 1	-1 1
1 0	1 -1
1 1	-1 -1

Table 2.1: Focal point structure of System (2.8).

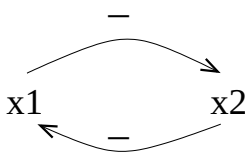

Figure 2.2: The interaction of two elements which is modeled by (2.8).

Orthant ($\tilde{x}$)	G
0 0	1 1
0 1	0 1
1 0	1 0
1 1	0 0

Table 2.2: Truth table for the mutually inhibitory network of Fig. 2.2 where $\text{sign}(F) = 2G - 1$.

Solving the above PL equations, we get (in each orthant)

$$x_i(t) = F_i + (x_i(0) - F_i)e^{-t}, \quad i = 1, 2, \tag{2.9}$$

Note that we use $\tilde{x}$ in each orthant to label the corresponding vertex on the 2-cube. Since there is a one-to-one correspondence from $\tilde{x}$ to the orthants in phase space, and also from the orthants in phase space to the vertices on the n-cube, $\tilde{x}$ defines the vertices. Furthermore, we can clearly see the connection between the vertex and the orthant from the label. For example vertex 01 represents the orthant where $x_1 < 0$ and $x_2 > 0$, while vertex 11 represents the orthant where $x_1 > 0$ and $x_2 > 0$.

In Fig. 2.3 (a), there are two fixed points, $(-1, 1)$ and $(1, -1)$. Trajectories starting in orthant 00, for example, have two choices depending on where they start. For a trajectory starting in the upper part of orthant 00, it will be approaching its focal point $(1, 1)$ in a straight line, but as soon as it leaves orthant 00, it will approach

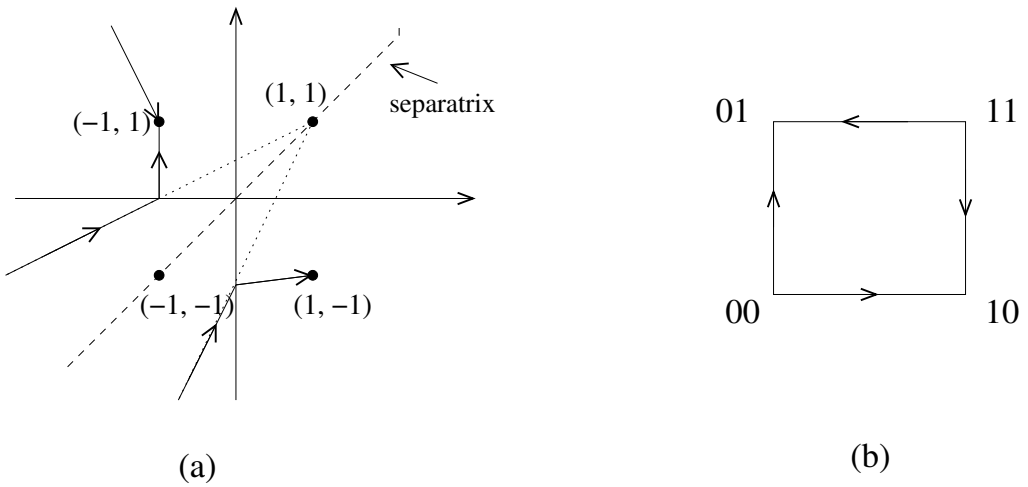

Figure 2.3: (a). Phase space for Eq. (2.8) with bistable behavior. (b). Digraph on the 2-cube for Eq. (2.8).

the focal point of orthant 01, and stay there forever since $(-1, 1)$ is a fixed point. Similarly, a trajectory starting in the lower part of orthant 00 will end up at $(1, -1)$. Using vertices of the 2-cube to represent the orthants in phase space and directed edges to represent the transition of trajectories, we get Fig. 2.3 (b), the digraph on the 2-cube for Eq. (2.9). We can see the bistable behavior of this system on the 2-cube very well.

Using the good properties of piecewise linear equations, we obtain a digraph on the n-cube, which represents the possible activities of the network symbolically. For some simple cases, we can get the n-cube from a diagram of the interactions between genes. For example, we get Fig. 2.3 (b) from Fig. 2.2 directly without knowing the focal points since we can get a truth table (Table 2.2) from Fig. 2.2. There are some important results about the relation between 'wiring diagrams' like Fig. 2.2 and the structure of the state space diagram. For example, Snoussi [30] claimed that cyclic attractors exist in the state space diagram if and only if there is a negative feedback loop embedded in the network. Some papers are about the relation between 'wiring diagrams' and dynamical behaviors. For example, the biological roles of individual positive loops (multistationarity, differentiation) and negative loops (homeostasis, with or without oscillations, buffering of gene dosage effect) are discussed in [33].

On the n-cube, we call a periodic sequence of vertices with the edges between successive vertices directed from one to the next one in sequence as a **cycle**.

Usually, the digraph on the n-cube for a given wiring diagram is not unique. For example, the wiring diagram in Figure 2.4 has different digraphs on the n-cube even

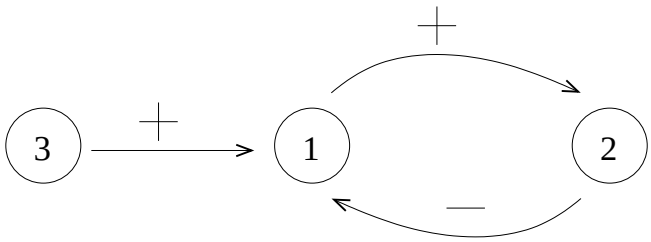

Figure 2.4: Wiring diagram for a 3-net which has at least two different digraphs on the n-cube.

though it is under the same functional form of interaction:

$$\begin{aligned} \dot{x}_1 &= -x_1 - (2\tilde{x}_2 - 1) + a(2\tilde{x}_3 - 1), \\ \dot{x}_2 &= -x_2 + (2\tilde{x}_1 - 1), \\ \dot{x}_3 &= -x_3 + 1. \end{aligned} \tag{2.10}$$

The focal point structure of this system is

Orthant $(\tilde{x})$			$F(\tilde{x}$		
0	0	0	1-a	-1	1
0	0	1	1+a	-1	1
0	1	0	-1-a	-1	1
0	1	1	-1+a	-1	1
1	0	0	1-a	1	1
1	0	1	1+a	1	1
1	1	0	-1-a	1	1
1	1	1	-1+a	1	1

Table 2.3: Focal point structure of System (2.10).

When $a > 1$, we have 3-cube (a) in Figure 2.5. Orthant 111 is globally attracting and there are no cycles on this 3-cube. When $0 < a < 1$, we have 3-cube (b) in Figure 2.5. In this case, there are two cycles on the 3-cube, $101 - 111 - 011 - 001$ and $100 - 110 - 010 - 000$.

One state transition diagram can only correspond to 2 wiring diagram (or more) if ineffective (weak) connections are added or removed. For example, if

$$F_1 = 1 - 2\tilde{x}_3, \quad F_2 = 2\tilde{x}_1 - 1, \quad F_3 = 2\tilde{x}_2 - 1$$

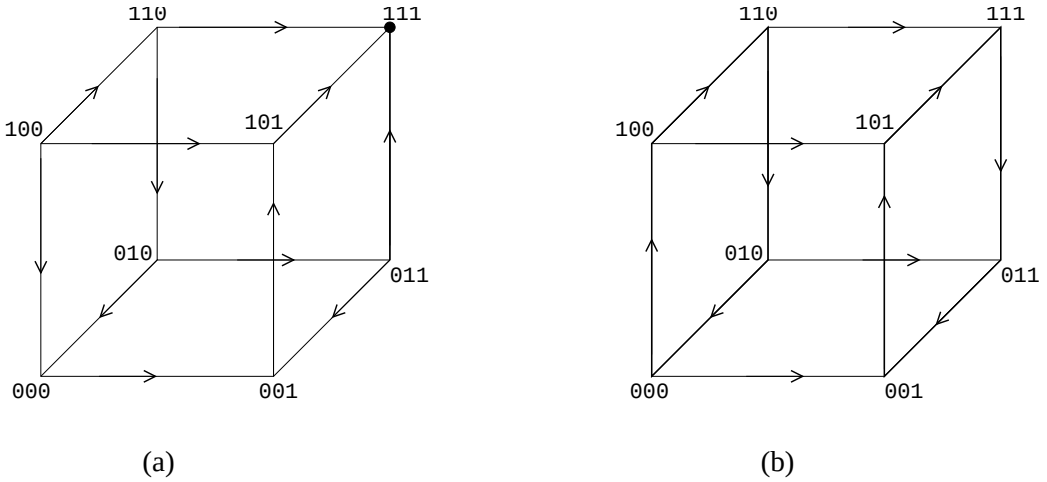

Figure 2.5: Two different state transition digraphs for the same wiring diagram Figure 2.4.

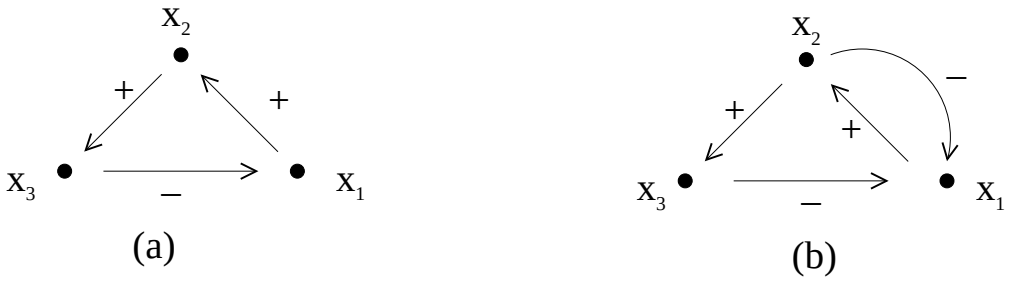

Figure 2.6: Two different 3-net wiring diagrams.

for Figure 2.6 (a) and

$$F_1 = 1 - 2\tilde{x}_3 - 2\tilde{x}_2\tilde{x}_3, \quad F_2 = 2\tilde{x}_1 - 1, \quad F_3 = 2\tilde{x}_2 - 1$$

for Figure 2.6 (b), then these two wiring diagrams have the same digraph on the n-cube.

Having the n-cube as an analysis technique, we will first use it to classify Glass networks into classes [3, 4]. The basic idea is simple, and we will use two-variable networks to illustrate the idea. In all two-variable Glass networks, we have 16 different state transition digraphs on the 2-cube as shown in Fig. 2.7. Although these 16 2-cubes are different, they can often be superimposed by application of some combination of symmetry operations, such as reflections, rotations and inversions of the n-cube. If two networks are identical under some symmetry operation of the n-cube, they will be called **structurally equivalent**. The number of structural equivalence classes is four for the two-variable Glass networks as shown in Fig. 2.8:

From a dynamical perspective, the qualitative features are the same provided

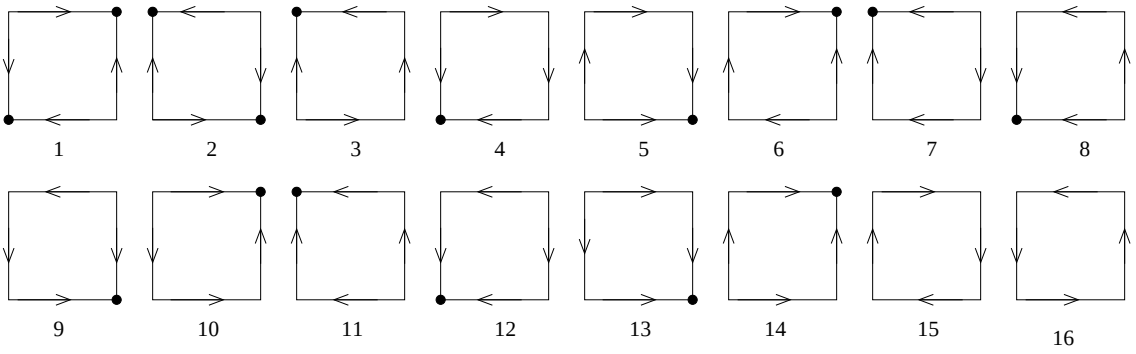

Figure 2.7: All the 16 different state transition digraphs for two-variable Glass networks.

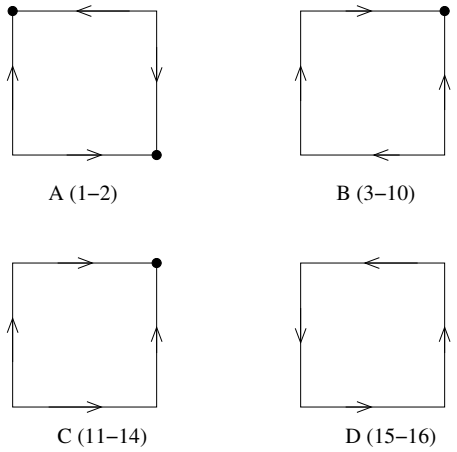

Figure 2.8: The structural equivalence classes for two-variable Glass networks. The number in the parentheses refers to Fig. 2.7, and we classify them into classes.

the focal points are chosen in an identical fashion. The definition of Structural Equivalence Class is one of the most important features used in our main theorems. For example, in order to simplify the notation and make the general idea clear, we may assume the first orthant on a cycle is the positive orthant, i.e. $x_i > 0, \forall i$.

The above information gives a general idea of PL equations including the calculation formula and the introduction of the n-cube. Note that a cycle of directed edges on the n-cube does not necessarily imply that there is a corresponding sequence of trajectory segments for the system of differential equations. In order to get the dynamical behavior of more complex networks from the n-cube, we need to consider which part of a boundary will contain trajectories that follow a given sequence of orthants and return to that boundary. There are cases for which the domain of definition for a cycle map may in fact be empty, or may be the entire starting boundary.

In the following, we will give the formula which determines the domain of each cycle (if it exists). The domains of definition of cycles are, in fact, cones by Eq. (2.12),

Eq. (2.13) and Prop. 2.3.3 below. We call the domain the **returning cone** of the cycle under consideration.

Let the $(n-1)$-dimensional orthant boundaries crossed on a specified cycle be denoted $\mathcal{O}^k$, with the starting boundary at $k=0$. $\mathcal{O}^k$ is divided into regions corresponding to the possible exit variables, where the possible exit variables in each orthant are those for which the sign of $y_i^{(k)}$ differs from the sign of $f_i^{(k)}$, the focal point for the orthant entered through $\mathcal{O}^k$. We know that trajectories in Glass networks are formed from piecewise-linear segments between orthant boundaries in phase space, with sharp changes of direction at the boundaries. From a given starting point on one boundary, $y(0)$, the next boundary crossing occurs at the earliest time that one of the y_i reaches 0. From Eq. (2.2), this time is the minimum of

$$t_i = \log\left(1 - \frac{y_i(0)}{f_i}\right)$$

over i such that $y_i(0)$ differs in sign from f_i. For later reference, the passage time at step k is the minimum of

$$t_i^{(k)} = \log\left(1 - \frac{y_i^{(k-1)}}{f_i^{(k-1)}}\right) \tag{2.11}$$

over i such that $y_i^{(k-1)}$ differs in sign from $f_i^{(k-1)}$.

From Eq. (2.11) it is clear that at any step y_j will cross before y_i if $0 > (y_j/f_j) > (y_i/f_i)$. With one such linear inequality for each alternate exit variable at each step, we then map all of them back to the starting boundary by Eq. (2.4). The returning cone, C, for the cycle is

$$C = \{y \in \mathcal{O}^{(0)} | Ry > 0\}, \tag{2.12}$$

where R is a matrix with one row for each alternate exit variable around the cycle, being the row vector

$$R_i = -\frac{e_i^T}{f_i^{(k)}} B^{(k)} B^{(k-1)} \dots B^{(0)} \tag{2.13}$$

in each case (refer to [17] for details of the calculations).

2.3 Previous Results

As a reference and to make this thesis stand on its own independently, we state without proof some important results on Glass networks in general, and results for some particular given Glass networks.

Proposition 2.3.1. [17] *The denominator,* $1+\langle\psi^{(m,0)}, y^{(0)}\rangle$*, in Eq. (2.6) corresponds to the exponential of the time taken to follow the portion of the trajectory described by the sequence of orthant boundary crossings and is thus* > 1*.*

Proposition 2.3.2. [17] *The mapping for a cycle is*

$$My = \frac{Ay}{1 + \langle\phi, y\rangle}, \tag{2.14}$$

where A *is* $(n-1)\times(n-1)$ $(A = B^{(m,0)}|_{(i)})$ *and* $\phi \in \mathbb{R}^{n-1}(\phi = \psi^{(m,0)}|_{(i)})$*.* $B^{(m,0)}$ *and* $\psi^{(m,0)}$ *are as indicated in Eq. (2.7).*

Proposition 2.3.3. [17] *Trajectories starting on the same ray through the origin remain on the same ray through the origin under the discrete mapping. Furthermore, trajectories from points on the same ray converge under the discrete mapping as* $t \to \infty$*.*

Proposition 2.3.4. [17] *If the mapping (Eq. (2.14)) for a specified cycle on the n-cube has a fixed point inside the cycle's returning cone, C (Eq. (2.12) and (2.13)), then the network has a periodic orbit passing through this point. Conversely, any periodic orbit of the network must pass through a fixed point in C for the corresponding cycle.*

Proposition 2.3.5. [17] *All non-zero fixed points of M (Eq. (2.14)) are eigenvectors of the matrix A.*

Proposition 2.3.6. [17] *If* v *is an eigenvector of* A*, corresponding to eigenvalue* $l \neq 0$*, such that* $\langle\phi, v\rangle \neq 0$*, then*

$$y^* = \frac{(l-1)v}{\langle\phi, v\rangle}$$

is a fixed point of M *and there is no other non-zero fixed point in the span of* v*.*

Proposition 2.3.7. [17] *A fixed point* y_i^* *of the discrete map (Eq. (2.14)) is asymptotically stable if the corresponding eigenvalue* λ_i *of the matrix* A *is the unique dominant one* $(\lambda_i > |\lambda_j|, j \neq i)$*; it is neurally stable if* λ_i *is dominant but* $\lambda_i = |\lambda_j|$ *for some* $j \neq i$*; and it is unstable otherwise.*

Proposition 2.3.8. [17] *The straight lines between fixed points (including the origin) are invariant manifolds under* M*.*

While there are many results on determining the dynamics of a given Glass network, there are few results on structural principles. The only clear example is the result on "cyclic attractor" [8] already mentioned. A vertex, not on a given cycle, which shares a common edge with a vertex of the cycle is **adjacent** to the cycle. A **cyclic attractor** is a cycle for which there are $(n-2)$ vertices adjacent to each vertex of the cycle and the edges from each adjacent vertex to the cycle are directed toward the cycle. An **n-dimensional cyclic attractor** is a cyclic attractor on an n-cube which is not contained on any lower dimensional sub-cube (Fig. 2.9 for example).

Theorem 2.3.1. [8] *Given an n-dimensional system of Eq. (2.1) in which the state transition diagram has an n-dimensional cyclic attractor, then one of the following two situations holds:*

1. *There is a stable limit cycle in phase space which passes through the orthants in the same sequence and order as the cyclic attractor in the state transition diagram. The trajectories through the points of orthants represented by vertices of the cyclic attractor and the points of boundaries represented by edges of the cyclic attractor asymptotically approach the limit cycle as $t \to \infty$.*

2. *The trajectories through the points of orthants and boundaries represented by the cyclic attractor asymptotically approach the origin as $t \to \infty$.*

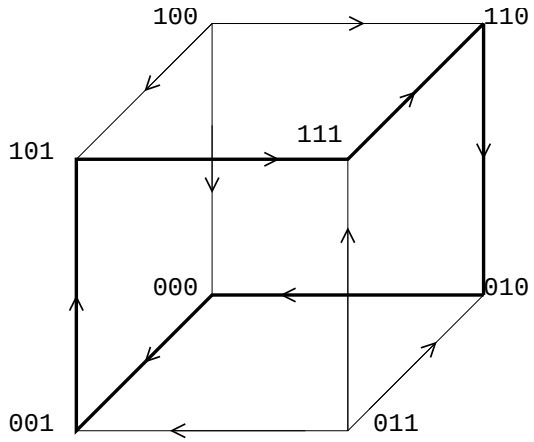

Figure 2.9: The state transition diagram for the cyclic attractor in $\mathbb{R}^3$.

In Chapter 3, we will get more general results about the existence of periodic orbits.

Among the results about the dynamics of a given Glass network, most of them are about the existence of periodic orbits ([11, 12, 17, 24]). Researchers are also working

on the existence of complex dynamical behaviors in the Glass networks ([16, 18]). The existence of a chaotic attractor has never been proven in the Glass network, but a general method by which the existence of an attractor on which the dynamics is aperiodic for a given Glass network has been presented in ([18]). In Chapter 5, starting from the domains and images of two cycles A and B, we will obtain structural principles for the existence of complex dynamics.

2.4 Notation

From now on, since a directed edge connecting to a vertex represents a variable in the corresponding orthant, we call a variable an **entry variable** for the orthant if the corresponding directed edge is pointing inwards. Similarly, we call a variable an **exit variable** if the corresponding directed edge is pointing outwards .

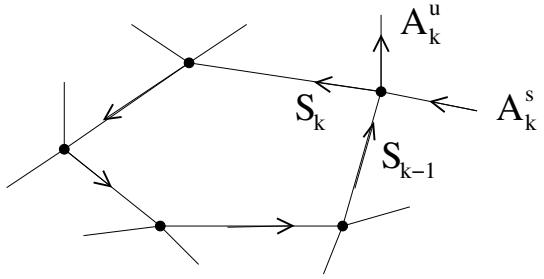

Figure 2.10: Illustration for notation.

In order to make the description and reference clear, we use the following notation (see Figure 2.10 for illustration):

1. Let s_k denote the index of the switching variable on the cycle at step k, i.e., the variable that switches on exiting the orthant;

2. Let A_k^s denote the set of indices of **alternate entry variable(s)**, i.e. entry variable(s) excluding s_{k-1}, at the kth orthant on the cycle;

3. Let A_k^u denote the set of indices of **alternate exit variable(s)**, i.e. exit variable(s) excluding s_k, at the kth orthant on the cycle.

Chapter 3

Existence and Stability of Periodic Orbits on Simple Cycles

Given a digraph on the n-cube, if all the vertices on a cycle are distinct in one period, then we call this cycle a **simple cycle**. Each vertex with the least number of outgoing arrows on the cycle is called a **critical vertex**. In this section, we consider the case when there is only one outgoing arrow connecting to each critical vertex, namely, the one on the direction of the cycle. This kind of vertex is called a **non-branching vertex**. For example in Fig. 3.1, the cycle in bold is a simple cycle, and vertex 111 is a critical vertex with only one outgoing arrow. Therefore the cycle in bold is a simple cycle with a non-branching critical vertex.

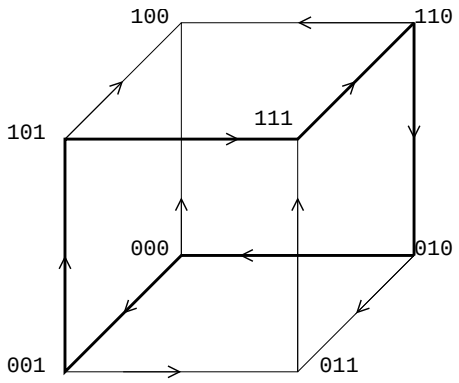

Figure 3.1: Digraph on the 3-cube.

It may be the case that not all the cycles on the n-cube really have trajectories passing through the corresponding orthants in phase space since the returning cone of the corresponding cycle on the n-cube may be empty. As a beginning of the discussion about structural principles, we show that for a given structure there can exist trajectories that follow a simple cycle for some sets of focal points. Furthermore, periodic orbits can exist for some sets of focal points.

In the proof of the existence of periodic orbits, the construction idea is that we will define the focal points for each orthant such that they are consistent with the directed graph on the hypercube (i.e. the unique directed n-cube graph of the network derived from the defined focal points is the same as the one we are given) such that there exist trajectories which follow the corresponding orthants of the simple cycle. In order to get a fixed point for the cycle map (which gives a periodic orbit), we need to consider the focal point of the orthant corresponding to one of the critical vertices (hereafter called **critical orthant**) particularly. The stability of the periodic cycle also depends on the focal point of the critical orthant. In the proof, we will choose one of the critical orthants as the last orthant being entered, so the initial point for the cycle is on the exiting boundary of the critical orthant. Before starting the main results of this section, we give a lemma first which shows that although different critical orthants may have different alternate exit variables, we can use any one of them as the last orthant in the construction.

Lemma 3.0.1. *Given an n-cube graph and a cycle on that graph, if every alternate exit variable in a critical orthant is an entry variable at least once on the cycle, then all alternate exit variables of other critical orthants are entry variables at least once on the cycle.*

Proof. In a critical orthant, if every $i \in A^u$ is an entry variable somewhere, then all the variables are entry variables somewhere on the cycle since by definition, s_{k-1} and $i \in A^s$ are entry variables at this critical orthant and s_k is an entry variable at the following orthant on the cycle. Therefore every alternate exit variable of any critical orthant is an entry variable somewhere on the cycle.

3.1 Simple Cycles With a Non-Branching Vertex

Theorem 3.1.1. *Given an n-cube graph and a simple cycle on that graph, if critical vertices on the cycle are non-branching vertices, then there exist focal points consistent with the digraph, such that the cycle has a periodic orbit.*

Proof. First, we will prove that it is possible to go around the cycle once. We choose as the starting boundary the exit wall of a critical orthant, so that we always enter this critical orthant at the last step. Let $f^{(k)}$ be the focal point associated with the $(k+1)$th orthant being entered and $y^{(k+1)}$ be the $(k+1)$th orthant boundary crossing on a trajectory which is the boundary on leaving the $(k+1)$th orthant.

Without loss of generality with regard to the signs and scaling of the variables, suppose $y_n^{(0)} = 0$ on the starting boundary and choose $y^{(0)}$, where $y_i^{(0)} = 1, i =$

$1, 2, \ldots, n-1$ and $y_n^{(0)} = 0$ as the initial point. We prove that for any cycle starting from $y^{(0)}$ with N steps in total, there exist focal points $f^{(k)}(\varepsilon)$, $k = 0, \ldots, N-1$, where ε is a positive number satisfying $\varepsilon \ll 1$ and

$$(1-\varepsilon)^{N-1} - \varepsilon > 0 \tag{3.1}$$

such that the orbit from $y^{(0)}$ follows the cycle and $(1-\varepsilon)^k - \varepsilon \leq |y_{i \neq s_k}^{(k)}| \leq 1$, for $k = 1, \ldots, N-1$. In other words, we keep the magnitude of the non-switching variables close to 1 (see Figure 3.2 for illustration).

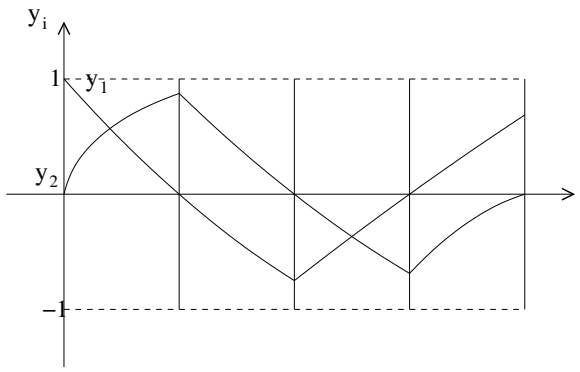

Figure 3.2: Evolution of 2 variables over time.

In the kth orthant being entered, where $k \leq N-1$, we define $f^{(k-1)}$ by the following rules depending on the given digraph on the n-cube. For $i = 1, 2, \ldots, n$,

1. if $i \in A_k^s$, then $|f_i^{(k-1)}| = 1$;
2. if $i \in A_k^u$, then $|f_i^{(k-1)}| = \varepsilon$;
3. if $i = s_k$, then $|f_i^{(k-1)}| = \gamma = 1/\varepsilon$;
4. if $i = s_{k-1}$, then $|f_i^{(k-1)}| = \gamma = 1/\varepsilon$.

We will prove the theorem by mathematical induction for the first $N-1$ steps. At the first step, suppose $y_n^{(1)} < 0$, where $y_n^{(1)} > 0$ will be done similarly. Following the rules above, we define the focal point $f^{(0)}$ by:

1. if $i \in A_1^s$, then $f_i^{(0)} = 1$;
2. if $i \in A_1^u$, then $f_i^{(0)} = -\varepsilon$;
3. $f_n^{(0)} = -\gamma$; $f_{s_1}^{(0)} = -\gamma$.

Then we get $y^{(1)}$ easily by Eq. (2.3):

1. if $i \in A_1^s$, $y_i^{(1)} = 1$;

2. if $i \in A_1^u$, then

$$y_i^{(1)} = \frac{f_i^{(0)} y_{s_1}^{(0)} - f_{s_1}^{(0)} y_i^{(0)}}{y_{s_1}^{(0)} - f_{s_1}^{(0)}} = \frac{(-\varepsilon) - (-\gamma)}{1 - (-\gamma)} = \frac{(-\varepsilon) + \gamma}{1 + \gamma} = \frac{1 - \varepsilon^2}{1 + \varepsilon} = 1 - \varepsilon$$

since $y_{s_1}^{(0)} = 1$. Then

$$y_i^{(1)} - [(1-\varepsilon)^1 - \varepsilon] = 1 - \varepsilon - (1-\varepsilon)^1 + \varepsilon = \varepsilon > 0.$$

3.
$$y_n^{(1)} = \frac{f_n^{(0)} y_{s_1}^{(0)} - f_{s_1}^{(0)} y_n^{(0)}}{y_{s_1}^{(0)} - f_{s_1}^{(0)}} = \frac{-\gamma}{1 + \gamma} = \frac{1}{1 + \varepsilon}.$$

Then

$$|y_n^{(1)}| - [(1-\varepsilon)^1 - \varepsilon] = \frac{1}{1+\varepsilon} - (1-\varepsilon)^1 + \varepsilon > 1 - \varepsilon - (1-\varepsilon)^1 + \varepsilon = \varepsilon > 0.$$

Hence, it is clear that

$$(1-\varepsilon)^1 - \varepsilon \leq |y_{i \neq s_1}^{(1)}| \leq 1.$$

Now, suppose in the first k steps where $k < N - 1$, we have

$$(1-\varepsilon)^k - \varepsilon \leq |y_{i \neq s_k}^{(k)}| \leq 1,$$

where $i = 1, \ldots, n$, except the switching variable at that step.

In the $(k+1)$th step, we will only discuss the case where $y_{i \neq s_k}^{(k)} > 0$ and $y_{s_k}^{(k+1)} > 0$; other cases are similar by geometric symmetry. Then we define $f^{(k)}$ by the above rules. For $i = 1, 2, \ldots, n$,

1. if $i \in A_{k+1}^s$, then $f_i^{(k)} = 1$;

2. if $i \in A_{k+1}^u$, then $f_i^{(k)} = -\varepsilon$;

3. $f_{s_k}^{(k)} = \gamma$; $f_{s_{k+1}}^{(k)} = -\gamma$.

Since $y_{s_{k+1}}$ will switch in the $(k+1)$th step, the passage time is

$$t = \log\left(1 - \frac{y_{s_{k+1}}^{(k)}}{f_{s_{k+1}}^{(k)}}\right).$$

Note that $(1-\varepsilon)^k - \varepsilon \leq |y^{(k)}_{i\neq s_k}| \leq 1$. We will get the longest possible switching time t^+ when $y^{(k)}_{s_{k+1}} = 1$ and we will get the shortest possible switching time t^- when $y^{(k)}_{s_{k+1}} = (1-\varepsilon)^k - \varepsilon$.

We now prove the following two claims:

1. In the longest time period t^+, $y^{(k+1)}_{s_k} \leq 1$ and for any $i \in A^u_{k+1}$ with $y^{(k)}_i = (1-\varepsilon)^k - \varepsilon$, we have $y^{(k+1)}_i \geq (1-\varepsilon)^{k+1} - \varepsilon$.

2. In the shortest time period t^-, $y^{(k+1)}_{s_k} \geq (1-\varepsilon)^{k+1} - \varepsilon$.

Note that in the second claim, we don't need to consider elements $y^{(k)}_i = (1-\varepsilon)^k - \varepsilon$ where $i \in A^u_{k+1}$ since if for any $i \in A^u_{k+1}$, $y^{(k+1)}_i \geq (1-\varepsilon)^{k+1} - \varepsilon$ is true in claim 1, then it is true in claim 2 in a shorter decreasing time. For $i \in A^s_{k+1}$, it is obvious that $y^{(k+1)}_i$ remains in the desired interval, since it approaches 1.

With the above two claims, we will have

$$(1-\varepsilon)^{k+1} - \varepsilon \leq |y^{(k+1)}_{i\neq s_{k+1}}| \leq 1$$

and this will complete the mathematical induction for the first $N-1$ steps.

From Eq. (2.11),

$$t^+ = \log \frac{\gamma+1}{\gamma}, \tag{3.2}$$

we obtain

$$\begin{aligned} y^{(k+1)}_{s_k} &= f^{(k)}_{s_k} + (y^{(k)}_{s_k} - f^{(k)}_{s_k})e^{-t^+} \\ &= \gamma - \gamma\left(\frac{\gamma}{\gamma+1}\right) \\ &= \frac{\gamma(\gamma+1) - \gamma^2}{\gamma+1} \\ &= \frac{\gamma}{\gamma+1} < 1 \end{aligned}$$

and if for some $i \in A^u_{k+1}$, $y_i^{(k)} = (1-\varepsilon)^k - \varepsilon$, then

$$\begin{aligned} y_i^{(k+1)} &= f_i^{(k)} + (y_i^{(k)} - f_i^{(k)})e^{-t^+} \\ &= -\varepsilon + [(1-\varepsilon)^k - \varepsilon + \varepsilon]\left(\frac{\gamma}{\gamma+1}\right) \\ &= -\varepsilon + (1-\varepsilon)^k\left(\frac{1}{1+\varepsilon}\right) \\ &\geq -\varepsilon + (1-\varepsilon)^k(1-\varepsilon) \\ &= -\varepsilon + (1-\varepsilon)^{k+1}. \end{aligned}$$

This completes the proof of the first claim.

For the second claim,

$$y_{s_k}^{(k+1)} = \frac{f_{s_k}^{(k)} y_{s_{k+1}}^{(k)} - f_{s_{k+1}}^{(k)} y_{s_k}^{(k)}}{y_{s_{k+1}}^{(k)} - f_{s_{k+1}}^{(k)}} = \frac{\gamma[(1-\varepsilon)^k - \varepsilon]}{[(1-\varepsilon)^k - \varepsilon] + \gamma},$$

and then

$$\begin{aligned} & y_{s_k}^{(k+1)} - [(1-\varepsilon)^{k+1} - \varepsilon] \\ = \; & \frac{\gamma[(1-\varepsilon)^k - \varepsilon] - [(1-\varepsilon)^{k+1} - \varepsilon][(1-\varepsilon)^k - \varepsilon + \gamma]}{(1-\varepsilon)^k - \varepsilon + \gamma}. \end{aligned}$$

Since $0 < (1-\varepsilon)^k - \varepsilon < 1$, it is clear that

$$[(1-\varepsilon)^k - \varepsilon] + \gamma > 0$$

and

$$\begin{aligned} & \gamma[(1-\varepsilon)^k - \varepsilon] - [(1-\varepsilon)^{k+1} - \varepsilon][(1-\varepsilon)^k - \varepsilon + \gamma] \\ = \; & \gamma(1-\varepsilon)^k - 1 - (1-\varepsilon)^{2k+1} + \varepsilon(1-\varepsilon)^{k+1} - \gamma(1-\varepsilon)^{k+1} + (1-\varepsilon)^k\varepsilon - \varepsilon^2 + 1 \\ > \; & \gamma(1-\varepsilon)^k - (1-\varepsilon)^{2k+1} - \gamma(1-\varepsilon)^{k+1} + \varepsilon(1-\varepsilon)^{k+1} \\ = \; & \gamma(1-\varepsilon)^k[1-(1-\varepsilon)] + (1-\varepsilon)^{k+1}[\varepsilon - (1-\varepsilon)^k] \\ = \; & (1-\varepsilon)^k - (1-\varepsilon)^{k+1}[(1-\varepsilon)^k - \varepsilon] \\ = \; & (1-\varepsilon)^k[1-(1-\varepsilon)((1-\varepsilon)^k - \varepsilon)] \\ > \; & 0. \end{aligned}$$

Therefore

$$y_{s_k}^{(k+1)} - [(1-\varepsilon)^{k+1} + \varepsilon] > 0.$$

This completes the proof of the second claim.

Now, the Nth orthant, i.e. the critical orthant chosen at the beginning of the construction, has focal point with the same sign as $y^{(N)}$ for each variable except the one that will be switching in this step, so the focal point of the Nth orthant is in the adjacent orthant, i.e. the first orthant on the cycle and we must leave the Nth orthant on the starting boundary. Thus, we have focal points for which it is possible to go around the cycle once. Now we choose the focal point for the Nth orthant so that our constructed orbit is periodic. We just draw a line passing through $y^{(N-1)}$ and $y^{(0)}$ then choose any point on the extension of this line which lies in the first orthant of this cycle as the focal point of the Nth orthant. That is, define

$$f^{(N-1)} = y^{(N-1)} + (1+\alpha)(y^{(0)} - y^{(N-1)}), \text{ where } \alpha > 0. \tag{3.3}$$

Then from Eq. (2.2)

$$y^{(N)} \;=\; y^{(N-1)} + (1-e^{-t})(1+\alpha)(y^{(0)} - y^{(N-1)}),$$

and $y^{(N)} = y^{(0)}$ is obtained when $1 - e^{-t} = \frac{1}{1+\alpha}$, that is $t = \ln(1+\frac{1}{\alpha})$. Therefore, the trajectory starting from point $y^{(N-1)}$ will approach $f^{(N-1)}$ in a straight line in the critical orthant and reach point $y^{(0)}$ at time $t = \ln(1+\frac{1}{\alpha})$. This focal point makes $y^{(0)}$ a fixed point of the return map, and we get a periodic orbit for the given cycle.

In the following discussion of stability, we will find out that although any focal point on the extension of the line passing through $y^{(N-1)}$ and $y^{(0)}$ which lies in the first orthant makes $y^{(0)}$ a fixed point of the return map, not all such focal points make this periodic orbit stable, and we have the following Theorem.

Theorem 3.1.2. *Given an n-cube graph and a simple cycle on that graph, if the critical vertices on the cycle are non-branching vertices, then there exist focal points consistent with the digraph, such that the cycle has a Poincaré stable periodic orbit.*

We will prove that for a suitable focal point of the Nth orthant, the periodic cycle constructed above is Poincaré stable.

First, we need to define the distance between two points x and y in $\mathbb{R}^n$ by the

usual Euclidean distance:

$$\text{dist}(x, y) = |x - y| = \sqrt{(x_1 - y_1)^2 + \cdots + (x_n - y_n)^2}.$$

Definition [32]: Let $\mathcal{H}^*$ be the half-path for the solution $x^*(t)$ of $\dot{x} = X(x)$ which starts at a^* at $t = t_0$. Suppose that for every $\epsilon > 0$ there exists $\delta(\epsilon) > 0$ such that if $\mathcal{H}$ is the half-path starting at a,

$$|a - a^*| < \delta \Rightarrow \sup_{x \in \mathcal{H}} \mathbf{dist}(x, \mathcal{H}^*) < \epsilon.$$

Then $\mathcal{H}^*$ (or the corresponding solution) is said to be Poincaré stable. Otherwise $\mathcal{H}^*$ is unstable.

Here, the distance from a point x to a curve ℓ (including endpoints) is defined by

$$\text{dist}(x, \ell) = \min_{y \in \ell}(\text{dist}(x, y)).$$

Let M_i be the network's mapping from the ith step to the $(i + 1)$th step defined by Eq. (2.4) and Eq. (2.5), where $i = 0, 1, \ldots, N - 2$, that is

$$y^{(i+1)} = M^{(i)} y^{(i)}, \quad i = 0, 1, \ldots, N - 2.$$

Since these mappings $M^{(i)}$ are continuous, the composition $M^{(i)} \cdots M^{(0)} y^{(0)}$ is also continuous for every $i = 0, 1, \ldots, N - 2$.

From the definition of continuity, we know that, given $\delta^\star$, there exist $\delta_i > 0$,$i = 0, 1, \ldots, N - 2$, such that

$$|M^{(i)} \cdots M^{(0)} y^{(0)} - M^{(i)} \cdots M^{(0)} x^{(0)}| < \delta^\star, \text{ when } |y^{(0)} - x^{(0)}| < \delta_i.$$

We may take each $\delta_i < \delta^\star$. Let $\delta = \min_{0 \le i \le N-2} \delta_i$, then

$$|y^{(i)} - x^{(i)}| < \delta^\star \text{ when } |y^{(0)} - x^{(0)}| < \delta, \text{ for } i = 0, 1, \ldots, N - 2, \tag{3.4}$$

and we will assume $\delta^\star > \delta$ in the following discussion.

Notice that from the point of view of continuity of the map in $\mathbb{R}^n$, the above is true, but the map is actually only defined on the returning cone for the cycle. If we regard $x^{(0)}$ as another new initial point, then for these two orbits to stay close in the first $N - 1$ steps, we still need to check that $x^{(0)}$ follows the same cycle as $y^{(0)}$ does.

We will prove in the following lemma that all the points in some neighborhood of $y^{(0)}$ will follow the same cycle as $y^{(0)}$ in the first $N-1$ steps.

Lemma 3.1.1. *Let $\delta^\star$, chosen above, satisfy $\delta^\star < \frac{-\varepsilon+\gamma(1-\varepsilon)^{N-2}-1}{\varepsilon+\gamma}$. Then for any $|y^{(0)} - x^{(0)}| < \delta$, $x^{(0)}$ will follow the same cycle as $y^{(0)}$ in the first $N-1$ steps.*

Before we start the proof of this lemma, we will prove $-\varepsilon + \gamma(1-\varepsilon)^{N-2} - 1 > 0$ to ensure that $\delta^\star$ chosen in the lemma exists. From the chosen of ε by Eq. (3.1), we have

$$(1-\varepsilon)^{N-2} > \frac{\varepsilon}{1-\varepsilon}.$$

Then

$$\begin{aligned} -\varepsilon + \gamma(1-\varepsilon)^{N-2} - 1 &= -\varepsilon + \frac{1}{\varepsilon}(1-\varepsilon)^{N-2} - 1 \\ &= \frac{-\varepsilon^2 + (1-\varepsilon)^{N-2} - \varepsilon}{\varepsilon} \\ &> \frac{-\varepsilon^2 + \frac{\varepsilon}{1-\varepsilon} - \varepsilon}{\varepsilon} \\ &= -\varepsilon + \frac{1}{1-\varepsilon} - 1 \\ &> -\varepsilon + (1+\varepsilon) - 1 \\ &= 0. \end{aligned}$$

Proof. Let $t_{x_i}^{(k)} = \log(1 - \frac{x_i^{(k-1)}}{f_i^{(k-1)}})$, i.e. $t_{x_i}^{(k)}$ is the alternate switching time for $i \in A_k^u$. We will proceed using induction. Assume y_s switches in the first step for point $y^{(0)}$. We need to prove that for any point $x^{(0)}$ satisfying $|y^{(0)} - x^{(0)}| < \delta$, all the elements x_i of $x^{(0)}$ where $i \in A_1^u$ satisfy $t_{x_s}^{(1)} < t_{x_i}^{(1)}$, i.e.

$$\log(1 - \frac{x_s^{(0)}}{f_s^{(0)}}) < \log(1 - \frac{x_i^{(0)}}{f_i^{(0)}}),$$

which is

$$\frac{x_s^{(0)}}{f_s^{(0)}} > \frac{x_i^{(0)}}{f_i^{(0)}}.$$

Recalling that $y_i^{(0)} = 1$ and $|x_i^{(0)} - y_i^{(0)}| \le |x^{(0)} - y^{(0)}| < \delta$ for $i = 1, 2, \ldots, n-1$, we have

$$1 - \delta^\star < 1 - \delta < x_i^{(0)} < 1 + \delta < 1 + \delta^\star, \quad \forall\, i \neq n.$$

Therefore, for those variables for which $f_i^{(0)} < 0$,

$$\frac{x_s^{(0)}}{f_s^{(0)}} - \frac{x_i^{(0)}}{f_i^{(0)}} > \frac{1+\delta^\star}{-\gamma} - \frac{1-\delta^\star}{-\varepsilon} = -\varepsilon - \varepsilon\delta^\star + \frac{1-\delta^\star}{\varepsilon} = \frac{-\varepsilon^2 - \varepsilon^2\delta^\star + 1 - \delta^\star}{\varepsilon} \geq 0,$$

since $\delta^\star < \frac{-\varepsilon+\gamma(1-\varepsilon)^{N-2}-1}{\varepsilon+\gamma} = \frac{-\varepsilon^2+(1-\varepsilon)^{N-2}-\varepsilon}{\varepsilon^2+1}$, and then

$$-\varepsilon^2 - \varepsilon^2\delta^\star + 1 - \delta^\star \geq \frac{1+\varepsilon+\varepsilon^2+\varepsilon^3}{1+\varepsilon^2} - (1-\varepsilon)^{N-2} \geq 1 - (1-\varepsilon)^{N-2} > 0$$

Now assume that in the first k steps the new initial point $x^{(0)}$ follows the cycle, where $k \leq N-2$. Using the result of continuity above, we also have

$$|x^{(i)} - y^{(i)}| < \delta^\star, \quad \forall i = 1, 2, \ldots, k,$$

since $|x^{(0)} - y^{(0)}| < \delta$.

Now, we will prove that in the $(k+1)$th step , the new initial point $x^{(0)}$ also follows the cycle.

Suppose y_p switches in the kth step and y_q switches in the $(k+1)$th step. By geometrical symmetry, we only need to consider the case where $y_{i\neq p}^{(k)} > 0$, and then we have the corresponding focal points $f_q^{(k)} = -\gamma$, $f_i^{(k)} = -\varepsilon$, for all $i \in A_{k+1}^u$. Since the qth variable will be switching for point $y^{(0)}$ at the $(k+1)$th step, i.e., $t_q^{(k+1)} < t_i^{(k+1)}$ for all $i \in A_{k+1}^u$, we have

$$\varepsilon y_q^{(k)} - \gamma y_i^{(k)} < 0, \ \forall i \in A_{k+1}^u.$$

As for $x^{(0)}$, if we want x_q to switch first in the $(k+1)$th step, we just need to show

$$\varepsilon x_q^{(k)} - \gamma x_i^{(k)} < 0, \ \forall i \in A_{k+1}^u.$$

When $\delta^\star < \frac{-\varepsilon+\gamma(1-\varepsilon)^{N-2}-1}{\varepsilon+\gamma}$, the above inequality is true since

$$\begin{aligned}
\varepsilon x_q^{(k)} - \gamma x_i^{(k)} &\leq \varepsilon(y_q^{(k)} + \delta^\star) - \gamma(y_i^{(k)} - \delta^\star) \\
&= (\varepsilon y_q^{(k)} - \gamma y_i^{(k)}) + \delta^\star(\varepsilon + \gamma) \\
&< \varepsilon - \gamma[(1-\varepsilon)^k - \varepsilon] + \frac{-\varepsilon + \gamma(1-\varepsilon)^{N-2} - 1}{\varepsilon + \gamma}(\varepsilon + \gamma) \\
&= \varepsilon - \gamma(1-\varepsilon)^k + 1 - \varepsilon + \gamma(1-\varepsilon)^{N-2} - 1 \\
&= -\gamma[(1-\varepsilon)^k - (1-\varepsilon)^{N-2}] \\
&\leq 0, \qquad\qquad \forall i \in A_{k+1}^u.
\end{aligned}$$

This proves our claim.

Now, we will prove Theorem 3.1.2.

Proof. The lemma above establishes that for the first $N-1$ steps, trajectories from initial points near $y^{(0)}$ follow the same sequence of orthants. We will focus on the Nth step. We already defined the focal point in this step by

$$f^{(N-1)} = y^{(N-1)} + (1+\alpha)(y^{(0)} - y^{(N-1)}),$$

where α is a positive number such that $f^{(N-1)}$ is in the first orthant on the cycle since the critical orthant is a non-branching orthant. Note that $f^{(N-1)} \to y^{(0)}$ when $\alpha \to 0$. Therefore α can be a small positive number. Hence, we can consider $\alpha \to 0$ in the following calculation.

We want to prove that for a suitable $f^{(N-1)}$, we have

$$|x^{(N)} - y^{(0)}| \leq \delta,$$

that is, $x^{(N)}$ returns to a δ neighborhood of $y^{(0)}$, and this will complete the proof. From the definition of $f^{(N-1)}$, for all $i \neq s_N$, where $s_N = n$ in this case, we have

$$
\begin{aligned}
& \lim_{\alpha\to 0} |x_i^{(N)} - y_i^{(0)}| \\
= & \lim_{\alpha\to 0} |x_i^{(N)} - 1| \\
= & \lim_{\alpha\to 0} \left| \frac{f_i^{(N-1)} x_n^{(N-1)} - f_n^{(N-1)} x_i^{(N-1)}}{x_n^{(N-1)} - f_n^{(N-1)}} - 1 \right| \\
= & \lim_{\alpha\to 0} \left| \frac{[y_i^{(N-1)} + (1+\alpha)(1 - y_i^{(N-1)})] x_n^{(N-1)} - [y_n^{(N-1)} + (1+\alpha)(-y_n^{(N-1)})] x_i^{(N-1)}}{x_n^{(N-1)} - [y_n^{(N-1)} + (1+\alpha)(-y_n^{(N-1)})]} - 1 \right| \\
= & \lim_{\alpha\to 0} \left| \frac{\alpha x_i^{(N-1)} y_n^{(N-1)} + x_n^{(N-1)} + \alpha x_n^{(N-1)} - \alpha y_i^{(N-1)} x_n^{(N-1)}}{\alpha y_n^{(N-1)} + x_n^{(N-1)}} - 1 \right| \\
= & |x_n^{(N-1)} / x_n^{(N-1)} - 1| \\
= & 0.
\end{aligned}
$$

Hence, choosing α small enough, there exists $k < 1$, such that

$$
|x_i^{(N)} - y_i^{(0)}| \leq \frac{k}{\sqrt{n-1}} |x^{(0)} - y^{(0)}|, \quad \forall i = 1, 2, \ldots n-1.
$$

Therefore

$$
\begin{aligned}
|x^{(N)} - y^{(0)}| &= \sqrt{(x_1^{(N)} - y_1^{(0)})^2 + (x_2^{(N)} - y_2^{(0)})^2 + \cdots + (x_n^{(N)} - y_n^{(0)})^2} \\
&\leq \sqrt{(n-1) \cdot \frac{k^2}{n-1} (x^{(0)} - y^{(0)})^2} \\
&= k |x^{(0)} - y^{(0)}|, \qquad (3.5)
\end{aligned}
$$

since $x_n^{(N)} = 0$ and $y_n^{(0)} = 0$.

Using the continuity of the map (Eq. (3.4)), Lemma 3.1.1 and Eq. (3.5), we know that for any $0 < \delta^\star < \frac{-\varepsilon+\gamma(1-\varepsilon)^{N-2}-1}{\varepsilon+\gamma}$, there exists $\delta > 0$ (which is the minimum of δ_i corresponding to $\delta^\star$), such that for any $x^{(0)}$ satisfying $|y^{(0)} - x^{(0)}| < \delta$, we have $|y^{(k)} - x^{(k)}| < \delta^\star$ for all $k = 1, \ldots, N$. Note that these $y^{(k)}$ and $x^{(k)}$ are only images on the orthant boundary, not for all the points on the trajectory. Using the definition of the distance from a point to a curve defined above and noticing that the trajectory between two orthant boundaries is a straight line, it is clear that the distance between these two orbits will always less that $\delta^\star$. Therefore $\sup_{x\in\mathcal{H}} \mathbf{dist}(x, \mathcal{H}^*) < \delta^\star$ and this orbit is Poincaré stable in a neighborhood of $y^{(0)}$.

3.2 Simple Cycles With No Non-Branching Vertex

In Theorem 3.1.1 and Theorem 3.1.2, we get the existence and stability of a periodic orbit for a simple cycle on the n-cube when critical vertices are non-branching vertex. Using the same idea as in Theorem 3.1.1, we obtain the existence of a periodic orbit for a simple cycle when critical vertices on the cycle have two outgoing arrows each. The basic idea is the same, but we need to deal with the alternate exit variable in any one of the critical orthants carefully.

Theorem 3.2.1. *Given an n-cube graph and a simple cycle on that graph. If a critical orthant on the cycle has only one alternate exit variable, say i_0, and $i_0 \in A^s$ somewhere on the cycle, then there exist focal points consistent with the digraph, such that the cycle has a periodic orbit.*

Proof. We will use the same notation as in Theorem 3.1.1, i.e. let $f^{(k-1)}$ be the focal point associated with the kth orthant being entered and $y^{(k)}$ be the kth orthant boundary crossing on a trajectory.

Using the same idea as in Theorem 3.1.1, for any cycle on the graph, we choose the starting boundary so that the orthant with two exit variables is the last one on the cycle and use $y^{(0)}$, where $y_i^{(0)} = 1, i = 1, 2, \ldots, n-1$ and $y_n^{(0)} = 0$ as the initial point without loss of generality. We prove that for any cycle starting from $y^{(0)}$ with N steps in total, there exist focal points $f^{(k)}$, $k = 0, \ldots, N-1$, such that the cycle has a periodic orbit.

Let the last time the i_0th arrow points inward to a vertex on the cycle be at the Ith vertex where $1 \leq I \leq N-1$. Then $\text{sign}(y_{i_0}^{(I)}) = \text{sign}(y_{i_0}^{(N)})$ since the i_0th coordinate will not switch in steps from I to N. They are both positive by our choice of $y^{(0)}$.

Using the same idea as in Theorem 3.1.1, in the kth orthant being entered, we define $f_i^{(k-1)}$ for all $k \leq N-1$ when $i \neq i_0$ and define $f_{i_0}^{(k-1)}$ for all $k \leq (I-1)$ by the following rules:

1. if $i \in A_k^s$, then $|f_i^{(k-1)}| = 1$;
2. if $i \in A_k^u$, then $|f_i^{(k-1)}| = \varepsilon$;
3. if $i = s_k$, then $|f_i^{(k-1)}| = \gamma = 1/\varepsilon$;
4. if $i = s_{k-1}$, then $|f_i^{(k-1)}| = \gamma = 1/\varepsilon$.

For the focal points $f_{i_0}^{(k-1)}$, $k \in [I, N-1]$, note that since the Ith step is the last step that the i_0th arrow points inward, the i_0th variable will keep the same sign for $k \in [I, N-1]$. From our assumption, $y_{i_0}^{(0)} = 1 > 0$, we know that $y_{i_0}^{(k)} > 0$ for all $k \in [I, N-1]$. Define $f_{i_0}^{(I-1)} = \beta_0$ and $f_{i_0}^{(k)} = -\varepsilon$ for all $k \in [I, N-2]$, where β_0 is a large constant such that $y_{i_0}^{(k)} > 1$ for all $k \in [I, N-1]$. We will find the suitable β_0 in the following construction.

Comparing the focal points in Theorem 3.1.1 with Theorem 3.2.1, we can see that as long as $(1-\varepsilon)^{N-1} - \varepsilon > 0$, we still have $(1-\varepsilon)^k - \varepsilon \leq |y_{i \neq s_k}^{(k)}|$ and the first conclusion in the proof of Theorem 3.1.1, i.e. it is possible to go around the cycle once, is still true. This is because we only change the focal points of the i_0th component from the Ith step and this variable does not switch in steps $I+1, \ldots, N-1$. Other variables will keep the same value as in Theorem 3.1.1 since the switching variables and the switching times are still the same from the first step to the $(N-1)$th step.

The difficulty of this construction is how to make $y^{(0)}$ a fixed point. Note that since the i_0th arrow is an outgoing arrow, $y_{i_0}^{(N-1)}$ must decrease in the last orthant, i.e. the critical orthant under consideration, by Eq. (2.2). In order to have $y_{i_0}^{(N)} = y_{i_0}^{(0)} = 1$, we need to have $y_{i_0}^{(N-1)} > 1$. We will prove in the following that there exists β_0, such that $y_{i_0}^{(N-1)} > 1$.

Before the calculation of β_0, we narrow the cases here. First, since β_0 and $y_{i_0}^{(I-1)}$ are negatively correlated, i.e. the larger $y_{i_0}^{(I-1)}$ is, the smaller β_0 will be required, we will assume $y_{i_0}^{(I-1)} = 0$. Second, we will assume that the switching time at the Ith step, when y_{i_0} is increasing, is the shortest one among all the possibilities, that is $|y_{s_I}^{(I-1)}| = (1-\varepsilon)^{I-1} - \varepsilon$. Third, we will assume that the switching time from the $(I+1)$ step to the $(N-1)$ step are the longest ones among all the possibilities, when y_{i_0} is decreasing, that is $|y_{s_k}^{(I-1)}| = 1$ for all $k \in [I+1, N-1]$. The β_0 obtained under these assumptions will be suitable for all cases.

Now, we calculate β_0 under the above assumption. From the first two assumptions, we have $y_{s_I}^{(I-1)} = \pm[(1-\varepsilon)^{I-1} - \varepsilon]$, $f_{s_I}^{(I-1)} = \mp\gamma$, $y_{i_0}^{(I-1)} = 0$ and $f_{i_0}^{(I-1)} = \beta_0$. Hence

$$y_{i_0}^{(I)} = \frac{f_{i_0}^{(I-1)} y_{s_I}^{(I-1)} - f_{s_I}^{(I-1)} y_{i_0}^{(I-1)}}{y_{s_I}^{(I-1)} - f_{s_I}^{(I-1)}} = \frac{\beta_0[(1-\varepsilon)^{(I-1)} - \varepsilon]}{[(1-\varepsilon)^{(I-1)} - \varepsilon] + \gamma}. \tag{3.6}$$

From the third assumption, we have $y_{s_{(I+1)}}^{(I)} = \pm 1$, $f_{s_{(I+1)}}^{(I)} = \mp\gamma$ and $f_{i_0}^{(I)} = -\varepsilon$. By Eq. (2.11), we know that the longest time is

$$t^+ = \log \frac{\gamma + 1}{\gamma}.$$

Therefore

$$y_{i_0}^{(I+1)} = f_{i_0}^{(I)} + (y_{i_0}^{(I)} - f_{i_0}^{(I)})\frac{\gamma}{\gamma+1} = -\varepsilon + (y_{i_0}^{(I)} + \varepsilon)\frac{\gamma}{\gamma+1}.$$

Similarly, we have

$$y_{i_0}^{(I+2)} \geq -\varepsilon + (y_{i_0}^{(I+1)} + \varepsilon)\frac{\gamma}{\gamma+1}.$$

Hence

$$y_{i_0}^{(I+2)} \geq -\varepsilon + (y_{i_0}^{(I)} + \varepsilon)(\frac{\gamma}{\gamma+1})^2$$

and

$$y_{i_0}^{(N-1)} \geq -\varepsilon + (y_{i_0}^{(I)} + \varepsilon)(\frac{\gamma}{\gamma+1})^{N-I-1}.$$

Now if we want $y_{i_0}^{(N-1)} > 1$, let

$$-\varepsilon + (y_{i_0}^{(I)} + \varepsilon)(\frac{\gamma}{\gamma+1})^{N-I-1} > 1,$$

therefore

$$y_{i_0}^{(I)} > (1+\varepsilon)(\frac{\gamma}{\gamma+1})^{I-N+1} - \varepsilon,$$

i.e

$$\frac{\beta_0[(1-\varepsilon)^{(I-1)} - \varepsilon]}{[(1-\varepsilon)^{(I-1)} - \varepsilon] + \gamma} > (1+\varepsilon)(\frac{\gamma}{\gamma+1})^{I-N+1} - \varepsilon$$

by Eq. 3.6.

Now, we obtain β_0 from the above inequality

$$\beta_0 > \frac{[(1-\varepsilon)^{(I-1)} - \varepsilon] + \gamma}{[(1-\varepsilon)^{(I-1)} - \varepsilon]}[(1+\varepsilon)(\frac{\gamma}{\gamma+1})^{I-N+1} - \varepsilon]. \tag{3.7}$$

Clearly, $\beta_0 > 0$, and β_0 and γ have the same order.

In order to make $y^{(0)}$ a fixed point, let the focal point $f^{(N-1)}$ of the Nth orthant be on the extension of the line passing through $y^{(N-1)}$ and $y^{(0)}$, i.e.

$$f^{(N-1)} = y^{(N-1)} + (1+\alpha)(y^{(0)} - y^{(N-1)}), \text{ where } \alpha > 0. \tag{3.8}$$

Note that not all the $\alpha > 0$ give us a focal point in the Nth orthant. We need to find the restriction on α such that $f^{(N-1)}$ is in the right orthant.

1. Since $y_{i_0}^{(N-1)} > 1 > 0$, we know that $f_{i_0}^{(N-1)} < 0$, i.e.

$$y_{i_0}^{(N-1)} + (1+\alpha)(y_{i_0}^{(0)} - y_{i_0}^{(N-1)}) < 0,$$

where $y_{i_0}^{(0)} = 1$. Therefore, we need

$$\alpha > \frac{1}{y_{i_0}^{(N-1)} - 1}.$$

2. For the nth variable, since the nth element switches at step N, we need

$$\text{sign } (y_n^{(N-1)}) = -\text{sign } (f_n^{(N-1)}).$$

All $\alpha > 0$ will work since

$$f_n^{(N-1)} = y_n^{(N-1)} + (1+\alpha)(0 - y_n^{(N-1)}) = -\alpha y_n^{(N-1)}.$$

3. For other variables, since $0 < y_i^{(N-1)} \leq 1$ and $y_i^{(0)} = 1$, we need $f_i^{(N-1)} > 0$. All $\alpha > 0$ will do since

$$\begin{aligned} f_i^{(N-1)} &= y_i^{(N-1)} + (1+\alpha)(y_i^{(0)} - y_i^{(N-1)}) \\ &= y_i^{(N-1)} + (1+\alpha)(1 - y_i^{(N-1)}) \\ &> 0. \end{aligned}$$

Choosing α such that

$$\alpha > \frac{1}{y_{i_0}^{(N-1)} - 1}, \tag{3.9}$$

where $y_{i_0}^{(N-1)}$ can be obtained by Eq. (2.4) and Eq. (2.5) after the choosing of β_0 by Eq. (3.7).

Now, we have the focal points of all the orthants on the cycle. For the last orthant, i.e. the critical orthant, we will show that given focal point $f^{(N-1)}$, the nth variable will switch before the i_0th variable. This can be done by showing that the switching time $t_n^{(N)}$ of the nth variable is shorter than the switching time $t_{i_0}^{(N)}$ of the i_0th variable. From Eq. (2.11), we know that

$$t_n^{(N)} = \log\left(1 - \frac{y_n^{(N-1)}}{f_n^{(N-1)}}\right) \text{ and } t_{i_0}^{(N)} = \log\left(1 - \frac{y_{i_0}^{(N-1)}}{f_{i_0}^{(N-1)}}\right).$$

In order to prove $t_n^{(N)} < t_{i_0}^{(N)}$, we prove $\frac{y_n^{(N-1)}}{f_n^{(N-1)}} - \frac{y_{i_0}^{(N-1)}}{f_{i_0}^{(N-1)}} > 0$ instead.

Note that $y_{i_0}^{(0)} = 1$, $y_n^{(0)} = 0$, $|y_n^{(N-1)}| \leq 1 < y_{i_0}^{(N-1)}$ and $f_{i_0}^{(N-1)} < 0$ since $y_{i_0}^{(N-1)} > 0$. From Eq. (3.8), we get

$$f_n^{(N-1)} = y_n^{(N-1)} + (1+\alpha)(-y_n^{(N-1)}) = -\alpha y_n^{(N-1)}$$

and

$$f_{i_0}^{(N-1)} = y_{i_0}^{(N-1)} + (1+\alpha)(1-y_{i_0}^{(N-1)}) = 1+\alpha-\alpha y_{i_0}^{(N-1)}$$

1. if $y_n^{(N-1)} > 0$, we have $f_n^{(N-1)} < 0$, then

$$\begin{aligned}
\frac{y_n^{(N-1)}}{f_n^{(N-1)}} - \frac{y_{i_0}^{(N-1)}}{f_{i_0}^{(N-1)}} &= \frac{y_n^{(N-1)} f_{i_0}^{(N-1)} - y_{i_0}^{(N-1)} f_n^{(N-1)}}{f_{i_0}^{(N-1)} f_n^{(N-1)}} \\
&= \frac{y_n^{(N-1)}(1+\alpha-\alpha y_{i_0}^{(N-1)}) + y_{i_0}^{(N-1)} \alpha y_n^{(N-1)}}{f_{i_0}^{(N-1)} f_n^{(N-1)}} \\
&= \frac{(1+\alpha) y_n^{(N-1)}}{f_{i_0}^{(N-1)} f_n^{(N-1)}} > 0
\end{aligned}$$

2. if $y_n^{(N-1)} < 0$, we have $f_n^{(N-1)} > 0$, then $\frac{y_n^{(N-1)}}{f_n^{(N-1)}} - \frac{y_{i_0}^{(N-1)}}{f_{i_0}^{(N-1)}} > 0$, since both terms in the subtraction are the same as in case 1.

Therefore $t_n^{(N)} < t_{i_0}^{(N)}$ and the nth variable will switch before the i_0th variable in the Nth orthant.

Using the $f^{(N-1)}$ defined above, point $y^{(N-1)}$ will approach $y^{(0)}$ in a straight line which makes $y^{(N)} = y^{(0)}$ and the trajectory leaves the Nth orthant on the starting boundary.

Then

$$y^{(N)} = y^{(N-1)} + (1-e^{-t})(1+\alpha)(y^{(0)} - y^{(N-1)}) = y^{(0)}$$

is obtained when $1 - e^{-t} = \frac{1}{1+\alpha}$, that is $t = \ln(1+\frac{1}{\alpha})$. Therefore, trajectory starting from point $y^{(N-1)}$ will approach $f^{(N-1)}$ in a straight line in the critical orthant and reach point $y^{(0)}$ at time $t = \ln(1+\frac{1}{\alpha})$. This focal point makes $y^{(0)}$ a fixed point of the return map, and we get a periodic orbit for the given cycle. This completes our proof.

From the proof of Theorem 3.2.1, we get a more general result.

Theorem 3.2.2. *Given an n-cube graph and a simple cycle on that graph. If all alternate exit variables in a critical orthant point inward at least once on the cycle, then there exist focal points consistent with the digraph, such that the cycle has a periodic orbit.*

Proof. Choose the exit boundary of the critical orthant as the starting boundary. Then for each exit variable, we find the corresponding β_0 and α as in the proof of Thm. 3.2.1. Defining the focal point of the last orthant by the maximum of these α's, we get a fixed point of the cycle map and thus the periodic orbit.

3.3 Examples

Example 3.3.1. We will use Fig. 3.1 to illustrate the construction idea in Theorem 3.1.1. Orthant 111 is a critical orthant with only one outgoing arrow on the cycle in bold in Fig. 3.1. Choosing the boundary between orthant 111 and 110 as the starting boundary. From the general rule stated in the proof of Theorem 3.1.1, we get the focal point structure of this state transition digraph (Table 3.1 (a)).

Table 3.1

(a) Focal points of Fig. 3.1 defined by the rules in the proof of Theorem 3.1.1.

Orthant ($\tilde{x_i}$)			Focal points (F_i)		
0	0	0	ε	-γ	γ
0	0	1	γ	ε	γ
0	1	0	-γ	-γ	ε
0	1	1	ε	1	1
1	0	0	1	-1	-1
1	0	1	γ	γ	-ε
1	1	0	-γ	-ε	-γ
1	1	1	$f_1^{(N-1)}$	$f_2^{(N-1)}$	$f_3^{(N-1)}$

(b) Let $\varepsilon = 0.1$, and then calculate $f^{(N)}$ by Eq. (3.3).

Orthant ($\tilde{x_i}$)			Focal points (F_i)		
0	0	0	0.1	-10	10
0	0	1	10	0.1	10
0	1	0	-10	-10	0.1
0	1	1	0.1	1	1
1	0	0	1	-1	-1
1	0	1	10	10	-0.1
1	1	0	-10	-0.1	-10
1	1	1	1.3439	2	-0.6494

Note that orthants 011 and 100 are not on the cycle, so their focal points do not affect the existence of the periodic orbit in the phase space corresponding to the cycle in bold. We can use any value as long as the sign is right. Here we still use the rules to define them. To choose the suitable ε we need ε to satisfy $(1-\varepsilon)^5 - \varepsilon > 0$ since $N = 6$ in this case. That is, ε must satisfy $0 < \varepsilon < 0.245$. Let $\varepsilon = 0.1$, then $\gamma = 1/\varepsilon = 10$. Let $y^{(0)} = [1\ 1\ 0]^T$ be the initial point. We calculate the mapping from boundary to boundary by Eq. (2.4) and Eq. (2.5). The value of each $y^{(k)}$, $k = 0, 1, \ldots, 5$ is

$$y^{(0)} = [1\ \ 1\ \ 0]^T, \quad y^{(1)} = [0\ \ 0.9\ \ -0.9091]^T, \quad y^{(2)} = [-0.8257\ \ 0\ \ -0.8258]^T,$$
$$y^{(3)} = [-0.7551\ \ -0.7628\ \ 0]^T, \; y^{(4)} = [0\ \ -0.7022\ \ 0.7021]^T,$$
$$y^{(5)} = [0.6561\ \ 0\ \ 0.6494]^T.$$

Now, for the last step in order to make $y^{(0)}$ a fixed point, we define the focal point

of orthant 111 by Eq. (3.3), i.e.

$$f^{(5)} = y^{(5)} + (1+\alpha)(y^{(0)} - y^{(5)}). \text{ where } \alpha > 0.$$

Since any $\alpha > 0$ will do, we use $\alpha = 1$ here. By simple calculation, we get

$$f^{(5)} = [1.3439 \quad 2 \quad -0.6494]^T.$$

By now, the construction is done (Table 3.1 (b)). We can check if these focal point make $y^{(0)}$ a fixed point by calculating $y^{(6)}$. By Eq. (2.4) and Eq. (2.5), we get $y^{(6)} = [1 \quad 1 \quad 0]^T = y^{(0)}$. The trajectory starting from $y^{(0)}$ will be a periodic orbit. This completes the construction.

From Eq. (2.6), (2.7) and (2.14), we get

$$A = \begin{pmatrix} 0.9382 & 2.0501 \\ -0.0924 & 3.0807 \end{pmatrix}, \quad \phi = \begin{pmatrix} 0.2508 \\ 1.7374 \end{pmatrix}.$$

The eigenvalues λ_i, $i = 1, 2$ and their corresponding eigenvectors v_i, $i = 1, 2$ are

$$l_1 \approx 1.0306, \quad l_2 \approx 2.9883,$$

$$v_1 \approx \begin{pmatrix} -0.9990 \\ -0.0450 \end{pmatrix}, \quad v_2 \approx \begin{pmatrix} -0.7071 \\ -0.7071 \end{pmatrix}.$$

From Proposition 2.3.4 and 2.3.6, we know that this system has two fixed points $y_1^* = [0.093 \quad 0.0042 \quad 0]^T$ and $y_2^* = y^{(0)} = [1 \quad 1 \quad 0]^T$. By Proposition 2.3.7, $y^{(0)}$ is stable because $y^{(0)}$ is on the span of v_2 which is the corresponding eigenvector of the dominant eigenvalue l_2. But the periodic cycle passing through $y^{(0)}$ is just Poincaré stable in a neighborhood of $y^{(0)}$ since there exist another fixed point y_1^*. Note that since the α used here already makes the periodic cycle passing through $y^{(0)}$ Poincaré stable, we don't need to use a smaller α for the Poincaré stable in this case.

Example 3.3.2. We will use Fig. 3.3 to illustrate the construction idea in Theorem 3.2.1. In this case, all the vertices on the simple cycle have two outgoing arrows. We choose orthant 111 as the critical orthant under consideration. Choosing the boundary between orthant 111 and 110 as the starting boundary. Then $N = 6$, $i_0 = 1$ and $I = 5$. Therefore we need to define $f_1^{(4)} = \beta_0$ which is the first element of the focal point of orthant 101. From the general rule stated in the proof of Theo-

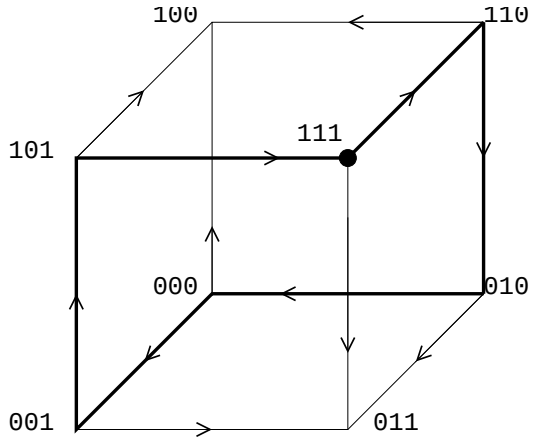

Figure 3.3: Digraph on the 3-cube in Example 3.3.2.

rem 3.2.1, we get the focal point structure of this state transition digraph (Table 3.2 (a)).

Table 3.2

(a) Focal points of Fig. 3.3 defined by the rules in the proof of Theorem 3.2.1.

Orthant ($\tilde{x}_i$)			Focal points (F_i)		
0	0	0	ε	-γ	γ
0	0	1	γ	ε	γ
0	1	0	-γ	-γ	ε
0	1	1	-1	1	1
1	0	0	1	-1	-1
1	0	1	β_0	γ	-ε
1	1	0	-γ	-ε	-γ
1	1	1	$f_1^{(N-1)}$	$f_2^{(N-1)}$	$f_3^{(N-1)}$

(b) Let $\varepsilon = 0.1$, choose β_0 by Eq. (3.7) and α by Eq. (3.9), then calculate $f^{(N-1)}$ by Eq. (3.8).

Orthant ($\tilde{x}_i$)			Focal points (F_i)		
0	0	0	0.1	-10	10
0	0	1	10	0.1	10
0	1	0	-10	-10	0.1
0	1	1	-1	1	1
1	0	0	1	-1	-1
1	0	1	20	10	-0.1
1	1	0	-10	-0.1	-10
1	1	1	-0.5615	6	-3.247

This digraph is just slightly different from the digraph in the example for Thm. 3.1.1. Similarly, we have the following remark. Orthants 011 and 100 are not on the cycle, so their focal points do not affect the existence of the periodic orbit in the phase space corresponding to the cycle in bold. We can use any value as long as the sign is right. Here we still use the rules to define them. To choose the suitable ε we need ε satisfy $(1-\varepsilon)^5 - \varepsilon > 0$ since $N = 6$ in this case. That is, ε must satisfy $0 < \varepsilon < 0.245$. Let $\varepsilon = 0.1$, then $\gamma = 1/\varepsilon = 10$. Let $y^{(0)} = [1\ 1\ 0]^T$ be the initial point. We calculated the mapping from boundary to boundary by Eq. (2.4) and Eq. (2.5). The value of each $y^{(k)}$, $k = 0, 1, \ldots, 4$ is

$$y^{(0)} = [1\ \ 1\ \ 0]^T, \quad y^{(1)} = [0\ \ 0.9\ \ -0.9091]^T, \quad y^{(2)} = [-0.8257\ \ 0\ \ -0.8258]^T,$$
$$y^{(3)} = [-0.7551\ \ -0.7628\ \ 0]^T,\ y^{(4)} = [0\ \ -0.7022\ \ 0.7021]^T.$$

First, from Eq. (3.7)

$$\begin{aligned}\beta_0 &> \frac{[(1-\varepsilon)^{(I-1)}-\varepsilon]+\gamma}{[(1-\varepsilon)^{(I-1)}-\varepsilon]}[(1+\varepsilon)(\frac{\gamma}{\gamma+1})^{I-N+1}-\varepsilon] \\ &= \frac{0.9^4-0.1+10}{0.9^4-0.1}[1.1\times(\frac{10}{10.1})^{5-6+1}-0.1] \\ &= 18.9824,\end{aligned}$$

choosing $\beta_0 = 20$, we get $y^{(5)}$ by Eq. (2.4) and Eq. (2.5)

$$y^{(N-1)} = y^{(5)} = [1.3123 \;\; 0 \;\; 0.6494]^T.$$

Second, from Eq. (3.9)

$$\alpha > \frac{1}{y_{i_0}^{(N-1)}-1} = \frac{1}{1.3123-1} = 3.202,$$

choosing $\alpha = 5$, we get $f^{(N-1)}$ by Eq. (3.8)

$$\begin{aligned}f^{(N-1)} &= y^{(N-1)} + (1+\alpha)(y^{(0)} - y^{(N-1)}) \\ &= [1.3123 \;\; 0 \;\; 0.6494]^T + (1+5)([1 \;\; 1 \;\; 0]^T - [1.3123 \;\; 0 \;\; 0.6494]^T) \\ &= [-0.5615 \;\; 6 \;\; -3.247]^T.\end{aligned}$$

By Eq. (2.4) and Eq. (2.5), we get $y^{(6)} = [1 \;\; 1 \;\; 0]^T = y^{(0)}$. We get a periodic orbit following the simple cycle in the corresponding orthants. This completes the construction.

To complete the example, we will show that this periodic orbit is unstable. From Eq. (2.6), (2.7) and (2.14), we get

$$A = \begin{pmatrix} 2.0058 & -0.2130 \\ -0.0554 & 1.8484 \end{pmatrix}, \quad \phi = \begin{pmatrix} 0.2878 \\ 0.5051 \end{pmatrix}.$$

The eigenvalues λ_i, $i = 1, 2$ and their corresponding eigenvectors v_i, $i = 1, 2$ are

$$l_1 \approx 2.0613, \quad l_2 \approx 1.7929,$$

$$v_1 \approx \begin{pmatrix} 0.9677 \\ -0.2521 \end{pmatrix}, \quad v_2 \approx \begin{pmatrix} 0.707 \\ 0.707 \end{pmatrix}.$$

From Proposition 2.3.4 and 2.3.6, we know that $y^{(0)} = [1 \quad 1 \quad 0]^T$ is the only fixed point on this boundary. By Proposition 2.3.7, the periodic orbit passing through $y^{(0)}$ is unstable since $y^{(0)}$ is on the span of v_2 which is the corresponding eigenvector of the non-dominant eigenvalue l_2.

Chapter 4

Existence and Stability of Periodic Orbits on Simple Figure-8 Cycles

4.1 Simple Figure-8 Cycles With Non-branching Vertex

In Chapter 3, we already have construction for existence and stability of a periodic orbit for simple cycles where at least 1 vertex has no alternate exit variables. In this chapter, we will get the existence and stability of periodic orbits for a more complicated cycle on the n-cube based on the focal points construction rules (called general rules hereafter) in the proof of Theorem 3.1.1, i.e., in the kth orthant being entered, we define $f^{(k-1)}$ by the following rules depending on the given digraph on the n-cube if we don't define $f^{(k-1)}$ particularly:

for $i = 1, 2, \ldots, n$,

1. if $i \in A_k^s$, then $|f_i^{(k-1)}| = 1$;
2. if $i \in A_k^u$, then $|f_i^{(k-1)}| = \varepsilon$;
3. if $i = s_k$, then $|f_i^{(k-1)}| = \gamma = 1/\varepsilon$;
4. if $i = s_{k-1}$, then $|f_i^{(k-1)}| = \gamma = 1/\varepsilon$.

Given a digraph on the n-cube, if the periodic sequence of vertices of a cycle contains exactly one of the vertices twice in one period and no vertex more than twice in one period, then we call the cycle a **simple figure-8 cycle** (see Fig. 4.1 for illustration).

Theorem 4.1.1. *Given an n-cube graph and a simple figure-8 cycle on that graph. If there is a non-branching vertex on the cycle, then there exist focal points consistent*

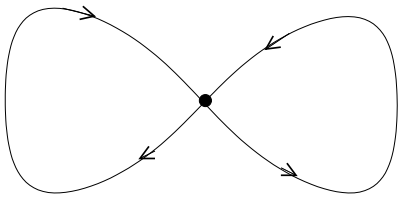

Figure 4.1: Simple figure-8 cycle.

with the digraph, such that the simple figure-8 cycle has a Poincaré stable periodic orbit.

Proof. Let the cycle pass through M orthants in total, where we count the common orthant twice. Choose a point $y^{(0)}$ on the exit boundary of the critical orthant corresponding to the non-branching vertex to start the trajectory and count the orthants starting with the first orthant following the critical orthant on the cycle. Assume the common orthant is the vth and the wth orthant on the cycle where $v < w$. Then the s_vth variable switches when the common orthant is the vth orthant and the s_wth variable switches when the common orthant is the wth orthant. Note that $s_v \neq s_w$.

Let $f^{(k-1)}$ be the focal point associated with the kth orthant on the cycle and $y^{(k)}$ be the point on the kth orthant boundary where the trajectory leaves this orthant. We will define first the focal point of the common orthant by

$$|f_{s_v}^{(v-1)}| = |f_{s_w}^{(v-1)}| = \gamma \tag{4.1}$$

and other components of $f^{(v-1)}$ will be defined by the general rules. Now, we will separate our construction into two cases for the first $v-1$ orthants:

1. If variable $s_w \in A_k^s$ at least once for $k \in \{1, 2, \ldots, v-1\}$ and the last such k is I_w, choose the point $y_i^{(0)} = \pm 1$ for all $i = 1, \ldots, n$ except one variable which is supposed to be zero on the exit boundary of the critical orthant as the starting point.

   Define the focal points of the orthant(s) from the first orthant to the $(I_w - 1)$th orthant by the general rules. The trajectory will follow the cycle in these steps and we have $(1-\varepsilon)^{(k)} - \varepsilon \leq |y_{i \neq s_k}^{(k)}| \leq 1$ for all $k = \{1, \ldots, I_w - 1\}$.

   For the focal point of the I_wth orthant, define $f_{i \neq s_w}^{(I_w-1)}$ by the general rules. For $f_{s_w}^{(I_w-1)}$, in order to let the s_vth variable switch in the vth orthant and let the s_wth variable stay away from zero after the decreasing in orthant v, we will

make the absolute value of the s_wth variable very large in the I_wth orthant such that $|y_{s_w}^{(v)}| \geq 1$.

Because of symmetry, we assume $y_{s_w}^{(v)} > 0$. The case $y_{s_w}^{(v)} < 0$ is handled similarly. Using the same idea as in the proof of Theorem 3.2.1, we get a β_w such that $y_{s_w}^{(v)} \geq 1$ whenever $f_{s_w}^{(I_w-1)} \geq \beta_w$. The worst case occurs when $y_{s_w}^{(I_w-1)} = 0$ and $y_{s_{I_w}}^{(I_w-1)} = \pm[(1-\varepsilon)^{I_w-1} - \varepsilon]$ switches in the I_wth orthant. If $y_{s_w}^{(I_w-1)} > 0$ and $|y_{s_{I_w}}^{(I_w-1)}| > [(1-\varepsilon)^{I_w-1} - \varepsilon]$, then the β_w we find here will certainly suffice. Using $f_{s_{I_w}}^{(I_w-1)} = \mp\gamma$ and $f_{s_w}^{(I_w-1)} = \beta_w > 0$, we have

$$y_{s_w}^{(I_w)} = \frac{f_{s_w}^{(I_w-1)} y_{s_{I_w}}^{(I_w-1)} - f_{s_{I_w}}^{(I_w-1)} y_{s_w}^{(I_w-1)}}{y_{s_{I_w}}^{(I_w-1)} - f_{s_{I_w}}^{(I_w-1)}} = \frac{\beta_w[(1-\varepsilon)^{I_w-1} - \varepsilon]}{[(1-\varepsilon)^{I_w-1} - \varepsilon] + \gamma}. \tag{4.2}$$

Define the focal points of the orthant(s) from $I_w + 1$ to $v - 1$ by the general rules. Let $y_{s_{I_w+1}}^{(I_w)}$ switch in the $(I_w + 1)$th orthant, then we have $f_{s_{I_w+1}}^{(I_w)} = \mp\gamma$ and $f_{s_w}^{(I_w)} = -\varepsilon$. Again, the worst case occurs when $y_{s_{I_w+1}}^{(I_w)} = \pm 1$. If $|y_{s_{I_w+1}}^{(I_w)}| < 1$, then the I_wth variable will be even less likely to switch in the vth orthant. We know from the proof of Theorem 3.1.1 that the longest possible switching time is $t^+ = \log \frac{\gamma+1}{\gamma}$. Therefore,

$$y_{s_w}^{(I_w+1)} \geq f_{s_w}^{(I_w)} + (y_{s_w}^{(I_w)} - f_{s_w}^{(I_w)}) \frac{\gamma}{\gamma+1} = -\varepsilon + (y_{s_w}^{(I_w)} + \varepsilon) \frac{\gamma}{\gamma+1}.$$

Similarly, we have

$$y_{s_w}^{(I_w+2)} \geq -\varepsilon + (y_{s_w}^{(I_w+1)} + \varepsilon) \frac{\gamma}{\gamma+1},$$

hence

$$y_{s_w}^{(I_w+2)} \geq -\varepsilon + (y_{s_w}^{(I_w)} + \varepsilon) (\frac{\gamma}{\gamma+1})^2.$$

Following the idea above,

$$y_{s_w}^{(v-1)} \geq -\varepsilon + (y_{s_w}^{(I_w)} + \varepsilon) (\frac{\gamma}{\gamma+1})^{v-1-I_w}.$$

Again taking the worst case, assume the value of the switching variable on entering the vth orthant is $y_{s_v}^{(v-1)} = \pm 1$, and remember we already defined

$|f_{s_v}^{(v-1)}| = |f_{s_w}^{(v-1)}| = \gamma$ in Eq. (4.1). Then we get

$$\begin{aligned} y_{s_w}^{(v)} &= \frac{f_{s_w}^{(v-1)} y_{s_v}^{(v-1)} - f_{s_v}^{(v-1)} y_{s_w}^{(v-1)}}{y_{s_v}^{(v-1)} - f_{s_v}^{(v-1)}} = \frac{-\gamma + \gamma y_{s_w}^{(v-1)}}{1+\gamma} \\ &\geq \frac{-\gamma + \gamma(-\varepsilon + (y_{s_w}^{(I_w)} + \varepsilon)(\frac{\gamma}{\gamma+1})^{v-1-I_w})}{1+\gamma}, \end{aligned}$$

that is

$$y_{s_w}^{(v)} \geq -1 + \frac{\gamma y_{s_w}^{(I_w)} (\frac{\gamma}{\gamma+1})^{v-1-I_w} + (\frac{\gamma}{\gamma+1})^{v-1-I_w}}{1+\gamma}.$$

Now, we will solve the inequality below to get β_w

$$-1 + \frac{\gamma y_{s_w}^{(I_w)} (\frac{\gamma}{\gamma+1})^{v-1-I_w} + (\frac{\gamma}{\gamma+1})^{v-1-I_w}}{1+\gamma} \geq 1.$$

Let $\varepsilon^* = (1-\varepsilon)^{I_w - 1} - \varepsilon$, we know from Eq. (4.2) that

$$y_{s_w}^{(I_w)} = \frac{\beta_w[(1-\varepsilon)^{I_w-1} - \varepsilon]}{[(1-\varepsilon)^{I_w-1} - \varepsilon] + \gamma} = \frac{\beta_w \varepsilon^*}{\varepsilon^* + \gamma},$$

This gives

$$\beta_w \geq \frac{2(\frac{\gamma}{\gamma+1})^{I_w - v+1}(1+\gamma)(\varepsilon^* + \gamma)}{\gamma \varepsilon^*} - \frac{\varepsilon^* + \gamma}{\gamma \varepsilon^*}.$$

2. If the s_wth variable never points inward in the first $v-1$ orthants, i.e., $s_w \notin A_k^s$, $k = \{1, \ldots, v-1\}$, we cannot use an initial point with value ± 1 to complete the construction, but we can define $|y_{s_w}^{(0)}| = \beta_0$ and $y_i^{(0)} = \pm 1$ for all $i = 1, \ldots, n$ except s_w and the one variable which is zero on the starting boundary, where β_0 is very large such that $|y_{s_w}^{(v)}| \geq 1$. In the following, we will get the requirement for β_0.

   Because of symmetry, we assume $y_{s_w}^{(v)} > 0$, then $y_{s_w}^{(0)} = \beta_0 > 0$. Using the same idea as above, since the longest switching time is $t^+ = \log \frac{\gamma+1}{\gamma}$, we have

$$y_{s_w}^{(v-1)} \geq -\varepsilon + (y_{s_w}^{(0)} + \varepsilon)(\frac{\gamma}{\gamma+1})^{v-1}.$$

   Assume the value of the switching variable in the vth orthant is $y_{s_v}^{(v-1)} = \pm 1$, and use the definition of the focal point of the vth orthant above Eq. (4.1).

Then we get

$$\begin{aligned} y_{s_w}^{(v)} &= \frac{f_{s_w}^{(v-1)} y_{s_v}^{(v-1)} - f_{s_v}^{(v-1)} y_{s_w}^{(v-1)}}{y_{s_v}^{(v-1)} - f_{s_v}^{(v-1)}} = \frac{-\gamma + \gamma y_{s_w}^{(v-1)}}{1+\gamma} \\ &\geq \frac{-\gamma + \gamma(-\varepsilon + (y_{s_w}^{(0)} + \varepsilon)(\frac{\gamma}{\gamma+1})^{v-1})}{1+\gamma}, \end{aligned}$$

that is

$$y_{s_w}^{(v)} \geq -1 + \frac{\gamma y_{s_w}^{(0)} (\frac{\gamma}{\gamma+1})^{v-1} + (\frac{\gamma}{\gamma+1})^{v-1}}{1+\gamma}.$$

Now, we will solve the inequality below to get β_0:

$$-1 + \frac{\gamma y_{s_w}^{(0)} (\frac{\gamma}{\gamma+1})^{v-1} + (\frac{\gamma}{\gamma+1})^{v-1}}{1+\gamma} \geq 1,$$

where

$$y_{s_w}^{(0)} = \beta_0.$$

Solving the inequality above we get

$$\beta_0 \geq \frac{2(\frac{\gamma}{\gamma+1})^{1-v}(1+\gamma)}{\gamma} - \frac{1}{\gamma}. \tag{4.3}$$

Note that when $v = 1$, it belongs to the second case. In order to define $|y_{s_w}^{(0)}| = \beta_0$ such that $|y_{s_w}^{(v)}| = |y_{s_w}^{(1)}| \geq 1$, we only need to calculate one step. That is

$$\begin{aligned} y_{s_w}^{(v)} &= \frac{f_{s_w}^{(v-1)} y_{s_v}^{(v-1)} - f_{s_v}^{(v-1)} y_{s_w}^{(v-1)}}{y_{s_v}^{(v-1)} - f_{s_v}^{(v-1)}} \\ &= \frac{-\gamma + \gamma y_{s_w}^{(v-1)}}{1+\gamma} = \frac{-\gamma + \gamma\beta_0}{1+\gamma}. \end{aligned}$$

Then solve the inequality

$$\frac{-\gamma + \gamma\beta_0}{1+\gamma} \geq 1,$$

we get $\beta_0 \geq \frac{1+2\gamma}{\gamma}$ which is consistent with Eq. (4.3).

Now for the focal point of the $(v+1)$th orthant, if the s_wth variable will switch, define the focal point $f_{s_w}^{(v)} = -\gamma y_{s_w}^{(v)}$. Then since the switching time is the same as the switching time when $y_{s_w}^{(v)} = 1$ and $f_{s_w}^{(v)} = -\gamma$ by general rules, other variables still satisfy $(1-\varepsilon)^{(v+1)} - \varepsilon \leq y_i^{(v+1)}$. If the s_wth variable points inward or points outward

without switching, we use

$$y_{s_w}^{(v+1)} = \frac{f_{s_w}^{(v)} y_{s_{v+1}}^{(v)} - f_{s_{v+1}}^{(v)} y_{s_w}^{(v)}}{y_{s_{v+1}}^{(v)} - f_{s_{v+1}}^{(v)}},$$

to find the focal point $f_{s_w}^{(v)}$ such that $y_{s_w}^{(v+1)} = 1$, then $(1-\varepsilon)^{(v+1)} - \varepsilon \leq |y_{i \neq s_{v+1}}^{(v+1)}| \leq 1$. All the variables are back in control again.

From the $(v+1)$th orthant to the wth orthant, note that the s_vth variable will point inward at least once, since $s_v \in A_{v+1}^s$. This time, we are going to find the β_v at the last step when the s_vth variable pointing inward to make the s_vth variable very large such that the s_wth variable will switch at the wth orthant on the cycle and $|y_{s_v}^{(w)}| \geq 1$. We can use the same idea as in case 1 above and since the method is similar, we don't solve β_v step by step here. But if we assume that the last orthant for the s_vth variable pointing in is in the I_vth orthant, and $f_{s_v}^{(I_v-1)} = \beta_v$, then we just need to require

$$\beta_v \geq \frac{2(\frac{\gamma}{\gamma+1})^{I_v-w+1}(1+\gamma)(\varepsilon^*+\gamma)}{\gamma\varepsilon^*} - \frac{\varepsilon^*+\gamma}{\gamma\varepsilon^*},$$

where $\varepsilon^* = (1-\varepsilon)^{I_v-1} - \varepsilon$.

Now it is time to use the critical orthant to make the initial point a fixed point, note that if the wth orthant is followed by the critical orthant, in order to make the initial point a fixed point, let the focal point $f^{(N-1)}$ of the critical orthant on the extension of the line passing through $y^{(N-1)}$ and $y^{(0)}$, i.e.

$$f^{(N-1)} = y^{(N-1)} + (1+\alpha)(y^{(0)} - y^{(N-1)}), \text{ for any } \alpha > 0.$$

If the $(w+1)$th orthant is not the critical orthant, using the same idea as we did in the $(v+1)$th orthant for the s_wth variable, we get $(1-\varepsilon)^{(w+1)} - \varepsilon \leq |y_{i \neq s_{w+1}}^{(w+1)}| \leq 1$, and define the focal points of orthant(s) between the $(w+1)$th orthant and the Nth orthant, i.e. the critical orthant, by the general rules, then define the focal point of the critical orthant by the above method again, i.e. let the focal point $f^{(N-1)}$ of the critical orthant on the extension of the line passing through point $y^{(N-1)}$ and $y^{(0)}$.

By now, we get the focal points of orthants on the cycle, and these focal points make $y^{(0)}$ a fixed point, this complete the construction. In order to get the stability of the periodic cycle, we need to use the continuity of the trajectory and the existence of the critical orthant such that we can make $\alpha \to 0$ if we want. The method of Theorem 3.2.1 will prove the stability, and this completes the proof.

4.2 Generalized Simple Figure-8 Cycles

In the above theorem, we get the existence and stability of a simple figure-8 cycle with only one common orthant. Now we will use the same idea to get a more general result. We call the cycle as shown in Fig. 4.2, where trajectory passes through some orthants twice and no such orthants are adjacent, a **generalized simple figure-8 cycle**.

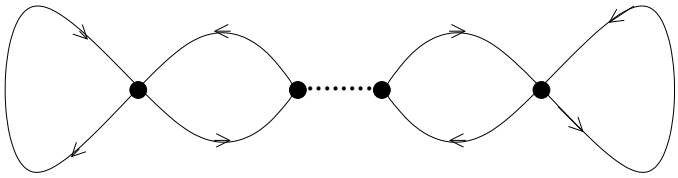

Figure 4.2: Generalized simple figure-8 cycle.

Theorem 4.2.1. *Given an n-cube graph and a generalized simple figure-8 cycle on that graph. If there is a non-branching vertex on the cycle, then there exist focal points consistent with the digraph, such that the simple figure-8 cycle has a Poincaré stable periodic orbit.*

Proof. Assume there are N steps on the cycle and M common orthants in total. Choose a point $y^{(0)}$ on the exiting boundary of the critical orthant corresponding to the non-branching vertex to start the trajectoty and count the orthants starting from the first orthant following the critical orthant on the cycle. We label the common orthants according to the order passed through by the trajectory, and we call them common orthant i, where $i = 1, \ldots, M$. Let common orthant i be the v_ith orthant and the w_ith orthant on the cycle where $v_i < w_i$. Then variable s_{v_i} switches in the v_ith orthant and variable s_{w_i} switches in the w_ith orthant.

In the following discussion, we will find the suitable position of $y^{(0)}$ and construct focal points for each orthant to get a periodic orbit of the given cycle. The idea is exactly the same as Theorem 4.1.1 except that we need to do the calculation M times since we have M common orthants here, so we will not show the calculation in detail.

Let $f^{(k-1)}$ be the focal point associated with the kth orthant on the cycle and $y^{(k)}$ be the point on the kth orthant boundary where the trajectory leaves this orthant. For $\forall i$ where $i = 1, \ldots, M$, we define $|f^{(v_i-1)}_{s_{w_i}}| = |f^{(v_i-1)}_{s_{v_i}}| = \gamma$. Since s_{v_i} switches first when the trajectory passes through this orthant, we need to make variable s_{w_i} large before the trajectory enters this orthant. For the first v_i orthants, we separate the construction into two cases:

1. If variable $s_{w_i} \in A_k^s$ at least once for $k \in \{1, 2, \ldots, v_i - 1\}$ and the last such k is I_{w_i}, we want to make variable s_{w_i} very large in this orthant such that the s_{v_i}th variable switch in the v_ith orthant and $|y_{s_{w_i}}^{(v_i)}| \geq 1$. Without loss of generality, we assume $y_{s_{w_i}}^{(v_i)} > 0$, let $f_{s_{w_i}}^{(I_{w_i}-1)} = \beta_{w_i}$. Using the same idea as in the proof of Theorem 4.1.1, we get

$$\beta_{w_i} \geq \frac{2(\frac{\gamma}{\gamma+1})^{I_{w_i}-v_i+1}(1+\gamma)(\varepsilon^*+\gamma)}{\gamma\varepsilon^*} - \frac{\varepsilon^*+\gamma}{\gamma\varepsilon^*},$$

where $\varepsilon^* = (1-\varepsilon)^{I_{w_i}-1} - \varepsilon$.

2. If the s_{w_i}th variable never points inward in the first $v_i - 1$ orthants, i.e., $s_{w_i} \notin A_k^s$, $k = \{1, \ldots, v_i - 1\}$, let $|y_{s_{w_i}}^{(0)}| = \beta_i$ where β_i is very large such that when we first come to the common orthant, the s_{w_i}th variable can be very large and $|y_{s_{w_i}}^{(v_i)}| \geq 1$. For the sake of symmetry, we assume $y_{s_{w_i}}^{(v_i)} > 0$, then $y_{s_{w_i}}^{(0)} = \beta_i > 0$. Using the same idea as in the proof of Theorem 3.1, we get

$$\beta_i \geq \frac{2(\frac{\gamma}{\gamma+1})^{1-v_i}(1+\gamma)}{\gamma} - \frac{1}{\gamma}.$$

Now for the focal point of the (v_i+1)th orthant, if the s_{w_i}th variable will switch, define the focal point $f_{s_{w_i}}^{(v_i)} = -\gamma y_{s_{w_i}}^{(v_i)}$. Then since the switching time is the same as the switching time when $y_{s_{w_i}}^{(v_i)} = 1$, other variables still satisfying $(1-\varepsilon)^{(v_i+1)} - \varepsilon \leq |y_i^{(v_i+1)}|$. if the s_{w_i}th variable points in or points out without switching, we use Eq. (2.3)

$$y_{s_{w_i}}^{(v_i+1)} = \frac{f_{s_{w_i}}^{(v_i)} y_{j_i}^{(v_i)} - f_{j_i}^{(v_i)} y_{s_{w_i}}^{(v_i)}}{y_{j_i}^{(v_i)} - f_{j_i}^{(v_i)}}$$

to find the focal point $f_{s_{w_i}}^{(v_i)}$ such that $y_{s_{w_i}}^{(v_i+1)} = 1$, where j_i is the switching variable at step $v_i + 1$.

From the (v_i+1)th step to the next time the trajectory pass through the same orthant again, variable $s_{v_i} \in A_k^s$ at least once for $k \in \{v_i + 1, \ldots, w_i - 1\}$, since it is true in the (v_i+1)th orthant. Assume the last orthant where the s_{v_i}th variable pointing inward is in the I_{v_i}th orthant. This time, we are going to find β_{v_i} to make the s_{v_i}th variable very large such that the s_{w_i}th variable will switch and the required β_{v_i} is

$$\beta_{v_i} \geq \frac{2(\frac{\gamma}{\gamma+1})^{I_{v_i}-w_i+1}(1+\gamma)(\varepsilon^*+\gamma)}{\gamma\varepsilon^*} - \frac{\varepsilon^*+\gamma}{\gamma\varepsilon^*},$$

where $\varepsilon^* = (1-\varepsilon)^{I_{v_i}-1} - \varepsilon$.

By now in order to let the trajectory follow the cycle and return to the critical orthant, we define some elements of the focal points particularly by the required values β_{w_i} and β_{v_i}. Other focal points for the orthant on the cycle will be defined by the general rules, and the elements of the initial points which are not defined particularly by β_i will be use ± 1 .

Now it is time to use the critical orthant to make the initial point a fixed point. and we only need to let the focal point $f^{(N-1)}$ of the critical orthant on the extension of the line passing through the point $y^{(N-1)}$ and $y^{(0)}$, i.e.

$$f^{(N-1)} = y^{(N-1)} + (1+\alpha)(y^{(0)} - y^{(N-1)}), \text{ for any } \alpha > 0.$$

By now, we get the focal points of orthants on the cycle, and these focal points make $y^{(0)}$ a fixed point. This completes the construction. In order to get the stability of the periodic cycle, we need to use the continuity of the trajectory and the existence of the non-bracnching vertex such that we can make $\alpha \to 0$ if we want. Theorem 3.1.2 will prove the stability , and this complete the proof.

Chapter 5

More Results About Figure-8 Patterns

5.1 Lemmas

In Chapter 4, we considered simple figure-8 cycles and cycles with more than one common orthant but only when not adjacent to each other. In this chapter, we consider figure-8 "patterns" with adjacent common orthants. In this case, we can choose a starting boundary between adjacent common orthants. Then we can deal with multiple cycles by their returning cones on a single starting boundary (Poincaré section) and the images of these returning cones under their respective cycle mappings.

We assume that there are only two cycles on the n-cube ($n \geq 4$), cycle A and cycle B, and they compose one figure-8 pattern with more than one common orthant. To simplify the problem, we assume that other directed edges which are not on the figure-8 pattern but adjacent to it are all pointing inward towards the figure-8 pattern. This means that we no longer assume Condition 2.1.2 in this chapter and some edges on the n-cube may have two different directions corresponding to a white wall, when two vertices of the cycle are joined by an edge (called a 'chord' in [7]) that is not part of the cycle (see discussion following Condition 2.1.2 in Section 2.1). We assume that the figure-8 pattern does not encounter a black wall so the boundary transitions for any point starting from C_A or C_B are unambiguous.

We call the first common orthant on the figure-8 pattern orthant Q_1 and the last common orthant on the figure-8 pattern orthant Q_2. Let M and N be the number of non-common orthants on cycles A and B respectively. On cycle A, let a be the index of the variable that switches when entering orthant Q_1 and let c be the index of the variable that switches when leaving orthant Q_2. Similarly, on cycle B, let b be the index of the variable that switches when entering orthant Q_1 and d be the index of the variable that switches when leaving orthant Q_2. For later reference, let r be the index of the variable that switches when entering orthant Q_2 (Fig. 5.1).

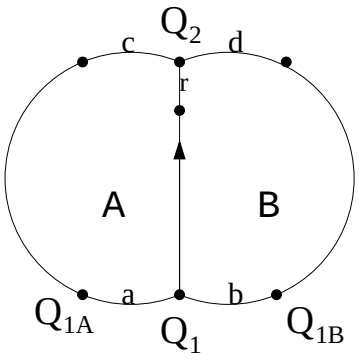

Figure 5.1: Figure-8 cycle with more than one common orthant.

Let C_A denote the returning cone of cycle A and C_B denote the returning cone of cycle B on the starting boundary defined below. Using M_A to denote the mapping of cycle A and M_B to denote the mapping of cycle B by Eq. (2.6) and (2.7), we have the following nine different image types of the returning cones of cycles A and B (Fig. 5.2):

1. $M_A(C_A) \subseteq C_A$, $M_B(C_B) \subseteq C_B$;
2. $M_A(C_A) \subseteq C_B$, $M_B(C_B) \subseteq C_A$;
3. $M_A(C_A) \subseteq C_B$, $M_B(C_B) \subseteq C_B$;
4. $M_A(C_A) \subseteq C_A$, $M_B(C_B) \subseteq C_A$;
5. $M_A(C_A) \subseteq C_A$, $M_B(C_B) \cap C_B \neq \emptyset$, $M_B(C_B) \cap C_A \neq \emptyset$;
6. $M_A(C_A) \subseteq C_B$, $M_B(C_B) \cap C_B \neq \emptyset$, $M_B(C_B) \cap C_A \neq \emptyset$;
7. $M_A(C_A) \cap C_B \neq \emptyset$, $M_A(C_A) \cap C_A \neq \emptyset$, $M_B(C_B) \subseteq C_B$;
8. $M_A(C_A) \cap C_B \neq \emptyset$, $M_A(C_A) \cap C_A \neq \emptyset$, $M_B(C_B) \subseteq C_A$;
9. $M_A(C_A) \cap C_B \neq \emptyset$, $M_A(C_A) \cap C_A \neq \emptyset$, $M_B(C_B) \cap C_B \neq \emptyset$, $M_B(C_B) \cap C_A \neq \emptyset$.

In this chapter, we focus on the cases when there is more than one common orthant on the figure-8 pattern since we want to consider the image types of the returning cones of cycles A and B on the common boundary. We have obtained some results about the figure-8 pattern with only one common orthant in Chapter 4. For more results about the figure-8 pattern with only one common orthant see [15].

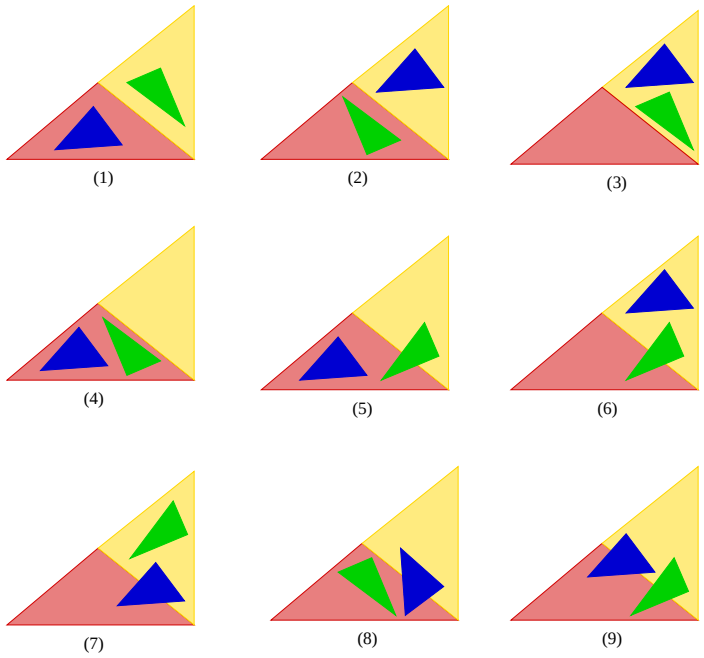

Figure 5.2: Possible image types of cycles A and B, where the red triangles are the returning cones C_A of cycle A projected onto a plane, the yellow triangles are the returning cones C_B of cycle B projected onto a plane, the blue triangles are $M_A(C_A)$ projected onto a plane and the green triangles are $M_B(C_B)$ projected onto a plane.

In the following discussion, we will use $x_i^{(k)}$ to denote the ith coordinate of point x at step k of cycle A and use $y_i^{(k)}$ to denote the ith coordinate of point y at step k of cycle B, even though these are actually the same variables. And we will use Q_{1B} to denote the orthant on cycle B before Q_1 and use Q_{1A} to denote the orthant on cycle A before Q_1 (Fig. 5.1).

Note that in previous chapters, we use $f_i^{(k-1)}$ to denote the ith coordinate of the focal point associated with the kth orthant being entered. In order to refer to a specific orthant clearly, we will use a new notation to denote the focal points in this chapter. Before we define the notation, let us label each orthant on the hypercube with a digit. We have denoted each orthant by the corresponding $\tilde{x}$. For example, we use orthant (0 0 0) to denote the orthant in $\mathbb{R}^3$ where $x_i < 0$, $i = 1, 2, 3$. If we regard each $\tilde{x}$ as a binary sequence, we can label each orthant by the following formula:

$$\text{orthant number} = (\text{the corresponding decimal of the binary sequence } \tilde{x}) + 1 \quad (5.1)$$

Table 5.1 for example shows the numbering of the orthants in $\mathbb{R}^3$. Now we use $F(i, j)$ to denote the jth coordinate of the focal point associated with orthant i, where i is

a digit obtained by Eq. (5.1).

$\tilde{x}$	000	001	010	011	100	101	110	111
numbering (i)	1	2	3	4	5	6	7	8

Table 5.1: Numbering of orthants in $\mathbb{R}^3$.

For the switching variables a, b, c and d defined above, we separate them into five different cases:

1. $a = c$ and $b = d$;
2. $a = d$ and $b = c$;
3. $a = c$ and $b \neq d$ ($a \neq c$, $b = d$ similar by symmetry);
4. $a = d$ and $b \neq c$ ($a \neq d$, $b = c$ similar by symmetry);
5. $a \neq c$, $a \neq d$, $b \neq c$ and $b \neq d$.

Note that $a \neq b$, $c \neq d$ by definition of the figure-8 pattern (see Fig. 5.1 for illustration).

We will discuss the possible image types for each case after outlining a basic construction procedure below.

1. We will always choose the last common boundary as the starting boundary, i.e., the entry wall for Q_2.
2. For focal points $F(i, j)$ which are not defined explicitly below, we will always define $|F(i, j)| = \gamma$ if the jth variable switches when entering or leaving othant i and define $|F(i, j)| = 1$ for others. For Q_1, which has two inward pointing arrows, we will define $|F(Q_1, a)| = |F(Q_1, b)| = \gamma$ if they are not defined particularly. We will define $|F(Q_2, c)| = |F(Q_2, d)| = \gamma$. Thus, C_A and C_B are separated by the hyperplane $c = d$. If $|x_c| > |x_d|$, then cycle B is taken. If $|x_c| < |x_d|$, then cycle A is taken. The sign of $F(i, j)$ is determined by the orthant and the corresponding arrow direction.

Remark 5.1.1. Constant γ used in the construction of focal points in this chapter can be any positive number since we assume that other directed edges which are not on the figure-8 pattern are all pointing inward towards the figure-8 pattern. But practically, since we define most other focal points as ± 1, we recommend using $\gamma > 1$.

We see the reason from the proof of the following Theorems. For example, sometimes we need $\delta_1 < F(i,j) < \delta_2$ to get the required image type, but a small γ makes δ_1 and δ_2 close to each other, and then the choice of $F(i,j)$ will be subtle.

Remark 5.1.2. The construction ideas are not unique. There may exist many methods to get the needed image types. We only use the most obvious idea in the proof of the following theorems.

Remark 5.1.3. From Eq. (2.3), if $f_i^{(k)}$ and $y_i^{(k)}$ have the same sign, then we obtain the following equation since $y_j^{(k)}$ and $f_j^{(k)}$ have different sign.

$$|y_i^{(k+1)}| \;=\; \frac{|f_i^{(k)} y_j^{(k)}| + |f_j^{(k)} y_i^{(k)}|}{|y_j^{(k)}| + |f_j^{(k)}|},$$

where y_j is the switching variable and $i = 1, \ldots, n$. It is clear that we can make $|y_i^{(k+1)}|$ as large as we want by using large $|f_i^{(k)}|$. However, if $y_i^{(k)}$ is not zero and $f_i^{(k)}$ and $y_i^{(k)}$ have the same sign, then

$$|y_i^{(k+1)}| = \frac{|f_i^{(k)} y_j^{(k)}| + |f_j^{(k)} y_i^{(k)}|}{|y_j^{(k)}| + |f_j^{(k)}|} > \frac{|f_j^{(k)}||y_i^{(k)}|}{|y_j^{(k)}| + |f_j^{(k)}|}.$$

We can not make $|y_i^{(k+1)}|$ as small as we want only by using small $|f_i^{(k)}|$. For this reason, we will always, for example, make the cth variable large instead of making the dth variable small in order to get $y_c \geq y_d$ in the following discussion.

If $y_i^{(k)} = 0$, then

$$|y_i^{(k+1)}| = \frac{|f_i^{(k)} y_j^{(k)}| + |f_j^{(k)} y_i^{(k)}|}{|y_j^{(k)}| + |f_j^{(k)}|} = \frac{|f_i^{(k)}||y_j^{(k)}|}{|y_j^{(k)}| + |f_j^{(k)}|}.$$

We can choose suitable $|f_i^{(k)}|$ to get any $|y_i^{(k+1)}|$ required. In the notation of this chapter $f_i^{(k)} = F(K,i)$, where K is the unique digit associating to each orthant as given in Table 5.1, whereas k denoted the kth step along a cycle.

It is hard to control the trajectories in the common orthants for both cycles A and B at the same time since focal points for cycle A may not work for cycle B. We will always assume that neither c nor d switches in common boundaries. From the basic construction idea (2), we get $|F(i,c)| = |F(i,d)| = 1$ for all the common orthants except Q_1 and Q_2.

Lemma 5.1.1. *If $|F(i,c)| = |F(i,d)|$ for all the common orthants except Q_1 and neither c nor d switches in common boundaries, then for any point x (or y) following cycle A (or B), the ordering between $|x_c|$ and $|x_d|$ ($|y_c|$ and $|y_d|$) on the common boundaries is always the same.*

Proof. Denoting the common orthant after Q_1 by Q^*, we will prove that the ordering between $|x_c|$ and $|x_d|$ on the second common boundary (the exiting wall for Q^*) is the same as the first common boundary (the exiting wall for Q_1). For other common boundaries, the result is proved similarly.

On the exiting wall for Q_1, it is the $(M+2)$th step on cycle A. If $x_c^{(M+2)}$ and $x_d^{(M+2)}$ have different sign, say $x_c^{(M+2)} > 0$ and $x_d^{(M+2)} < 0$, then $F(Q^*, c) = 1$ and $F(Q^*, d) = -1$. From Eq. (2.2), we get

$$\begin{aligned}
& |x_c^{(M+3)}| - |x_d^{(M+3)}| \\
= \; & |F(Q^*,c) + (x_c^{(M+2)} - F(Q^*,c))e^{-t}| - |F(Q^*,d) + (x_d^{(M+2)} - F(Q^*,d))e^{-t}| \\
= \; & 1 + (x_c^{(M+2)} - 1)e^{-t} + (-1) + (x_d^{(M+2)} + 1)e^{-t} \\
= \; & (x_c^{(M+2)} + x_d^{(M+2)})e^{-t} \\
= \; & (|x_c^{(M+2)}| - |x_d^{(M+2)}|)e^{-t}
\end{aligned}$$

That is $|x_c^{(M+3)}| - |x_d^{(M+3)}|$ will have the same sign as $|x_c^{(M+2)}| - |x_d^{(M+2)}|$. The case when $x_c^{(M+2)}$ and $x_d^{(M+2)}$ have the same sign is got from the same reasoning. Similarly for $|y_c|$ and $|y_d|$. This completes the proof.

We will see in the proof of Theorem 5.2.3 that when $|F(i,c)| \neq |F(i,d)|$ in some common orthant, the ordering between $|x_c|$ and $|x_d|$ (or $|y_c|$ and $|y_d|$) on the common boundaries may change.

From Lemma 5.1.1, we get

Lemma 5.1.2. *If $|F(i,c)| = |F(i,d)|$ for all the common orthants except Q_1 and neither c nor d switches in common boundaries, then we only need to consider points from step one up to step $M+2$ and $N+2$ for cycles A and B, respectively.*

Since r is the index of the variable that switches when entering orthant Q_2, the rth variable is zero on the last common boundary. Denote

$$C_a = \{\sum_{i \neq r} |x_i| = 1\} \cap C_A \text{ and } C_b = \{\sum_{i \neq r} |x_i| = 1\} \cap C_B.$$

Lemma 5.1.3. *Images of points in C_a and C_b determine the image type of the returning cones of cycles A and B.*

Proof. This comes from Proposition 2.3.3.

In the following discussion, we will use point p to denote the vertex of the simplex at the starting boundary with $|p_c| = 1$, use q to denote the vertex of the simplex at the starting boundary with $|q_d| = 1$, use v to denote the point on the simplex at the starting boundary with $|v_c| = |v_d| = 1/2$ and use $u^{(i)}$, where $i \in \{1, \ldots, n\}$, $i \neq c$, $i \neq d$ and $i \neq r$, to denote all the other vertices with $|u_i^{(i)}| = 1$ on the simplex at the starting boundary. Figure 5.3 illustrates these points when $n = 4$. Point p is on the boundary of C_b since all the points near p in the starting boundary satisfy $|p_c| > |p_d|$ and they will follow cycle B. Similarly, q is on the boundary of C_a. Points v are on the boundary of C_a and C_b since $v_c = v_d$. Similarly, all the $u^{(i)}$s defined above are on the boundary of C_a and C_b.

Since mappings M_A and M_B are continuous and one to one, they map the boundary of C_a and C_b to the boundary of $M_A(C_a)$ and $M_B(C_b)$, respectively. Therefore, in the 4-cube for example (Fig. 5.3), the images of points p, q, u and v determine the image type of the returning cones. If, for example, $M_B(p) \in C_B$, $M_B(u) \in C_B$ and $M_B(v) \in C_B$ then $M_B(C_B) \subseteq C_B$, but if $M_B(p) \in C_A$, $M_B(u) \in C_B$ and $M_B(v) \in C_B$ then $M_B(C_B) \cap C_B \neq \emptyset$, $M_B(C_B) \cap C_A \neq \emptyset$. If the image of an extremal point of a cycle's returning cone lies on the boundary between the two returning cones, then only the images of the other extremal points determine the image type.

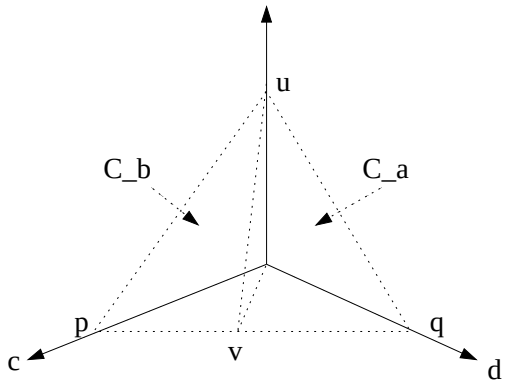

Figure 5.3: Returning cone of cycles A and B in a 4-cube.

Lemma 5.1.4. *For point p defined above, if the cth coordinate never switches in cycle B, then p is a fixed point for mapping M_B and image types 2, 4 and 8 are impossible.*

Proof. We prove this lemma by using the mapping for cycle B given in Eq. (2.6) and

(2.7), i.e., $M_B : \mathbb{R}^n \to \mathbb{R}^n$,

$$M_B p = \frac{B^{(m,0)} p}{1 + \langle \psi^{(m,0)}, p \rangle},$$

where B is an $n \times n$ matrix and ψ is and $n \times 1$ vector.

From the calculation of $B^{(k)}$ in Eq. (2.5), we have

$$B^{(k)} e_c = I e_c - \frac{f^{(k)} e_j^T}{f_j^{(k)}} e_c = e_c - 0 = e_c, \text{ for each k,}$$

where e_c denotes the standard basis vector in $\mathbb{R}^n$. Then by Eq. (2.7), we obtain

$$B^{(k,0)} e_c = B^{(k-1)} \dots B^{(1)} B^{(0)} e_c = B^{(k-1)} \dots B^{(1)} e_c = \dots = B^{(k-1)} e_c = e_c$$

for each $k = 1, \dots, m$. $B^{(k,0)} e_c = e_c$ means that the cth column of matrix $B^{(k,0)}$ is e_c.

By Eq. (2.5), we know that the cth coordinate of $\psi^{(k)}$ is zero, then the cth coordinate of $\sum_{k=1}^{m-1} B^{(k,0)^T} \psi^{(k)}$ is zero since the cth column of $B^{(k,0)}$ is e_c for each $k = 1, \dots, m$. By Eq. (2.7), we know that the cth coordinate of $\psi^{(m,0)}$ is zero. Therefore $1 + \langle \psi^{(m,0)}, p \rangle = 1$ and $B^{(m,0)} p = p$. That is $M_B(p) = p$. It is clear that if point p is a fixed point for cycle B, then image types 2, 4 and 8 are impossible.

Lemma 5.1.5. *For point q defined above, if the dth coordinate never switches in cycle A, then q is a fixed point for mapping M_A and image types 2, 3 and 6 are impossible.*

Lemma 5.1.6. *Any point $u^{(i)}$, where $i \neq c$, $i \neq d$ and $i \neq r$ defined above with $|u_i^{(i)}| = 1$, is a fixed point for cycle A, if the ith coordinate never switch in cycle A. Similarly, any $u^{(i)}$ with $|u_i^{(i)}| = 1$ where $i \neq c$, $i \neq d$ and $i \neq r$ is a fixed point for cycle B, if the ith coordinate never switches in cycle B.*

Unlike points p and q, point fixed point $u^{(i)}$ will not restrict the image type of cycles A and B since when $u^{(i)}$ is a fixed point, the image of $u^{(i)}$, $u^{(i)}$ itself, is on the boundary of the returning cones of both cycles.

If $|u_i^{(i)}| = 1$, $i \neq c$, $i \neq d$ and $i \neq r$ only switches in the common boundaries other than the first common boundary, the image of $u^{(i)}$ will have $|u_c^{(i)}| = |u_d^{(i)}|$ when returning to the starting boundary and therefore the image of $u^{(i)}$ will again be on the boundary of the returning cones of both cycles by Lemma 5.1.1, since we will always define the focal points of common orthants other than the first common orthant by $|F(i,c)| = |F(i,d)|$ in our construction. Therefore this kind of point $u^{(i)}$ also will not restrict the image type of cycles A and B.

For later reference, we will denote by $u^{(A_1)}$, ..., $u^{(A_i)}$ those $u^{(i)}$ for which $u_i^{(i)}$ switches in some of the first $M+2$ steps on cycle A and by $u^{(B_1)}$, ..., $u^{(B_i)}$ those $u^{(i)}$ for which $u_i^{(i)}$ switches in some of the first $N+2$ steps on cycle B. Let $P_A = \{q, v, u^{(A_1)}, \ldots, u^{(A_i)}\}$ and $P_B = \{p, v, u^{(B_1)}, \ldots, u^{(B_i)}\}$. Since at least two variables must switch to have a cycle, P_A and P_B are not empty sets.

To sum up, we have Lemma 5.1.7.

Lemma 5.1.7. *P_A and P_B are not empty sets and the images of points in P_A and P_B will determine the image type of cycles A and B.*

Remark 5.1.4. In the following proof, we use $\forall\ x \in P_A$ or $\forall\ y \in P_B$ to simplify the notation, but if d doesn't switch in cycle A, we don't include q in P_A and if c doesn't switch in cycle B, we don't include p in P_B.

If only two variables switching in cycle A, then one variable is c and the other variable is r, the one which switches on entry to Q_2. Thus, x_d does not switch in A, so q is fixed. And all $u^{(i)}$ are also fixed since the corresponding x_i do not switch in A. In fact, the cycle consists only 4 orthants, $M = 2$ and 2 common orthant. Thus, there is only one point in P_A. Then that point must be v. This is also true for cycle B, and we have the following lemma.

Lemma 5.1.8. If there is only one point in P_A (P_B), that is point v.

5.2 Results

5.2.1 Case 1

Theorem 5.2.1. *When $a = c$ and $b = d$, and neither c nor d switches in common boundaries, then*

1. *image types 1, 5 and 7 are possible;*
2. *if d switches in cycle A, image type 3 is possible;*
3. *if c switches in cycle B, image type 4 is possible.*

Proof.

- Image type 1 is obtained by defining $|F(Q_1, c)| = |F(Q_1, d)| = \gamma$.

  For each $x \in P_A$, $x_c = 0$ and $|x_d| > 0$ on entry to Q_1. Then we will have $|x_d| \geq |x_c|$ on all the common boundaries by Lemma 5.1.1. This means that x_c

must switch on exiting Q_2 since $|F(Q_2,c)| = |F(Q_2,d)| = \gamma$, i.e. $M_A(x) \subseteq C_A$. By Lemma 5.1.7, we have $M_A(C_A) \subseteq C_A$.

Similarly, for each $y \in P_B$, $y_d = 0$ and $|y_c| > 0$ on entry to Q_1. Then we will have $|y_c| \geq |y_d|$ on all the common boundaries. This means that y_d must switch on exiting Q_2, i.e. $M_B(y) \subseteq C_B$. By Lemma 5.1.7, we have $M_B(C_B) \subseteq C_B$.

- Image type 3 is obtained by defining $|F(Q_1,c)| \gg |F(Q_1,d)| = \gamma$.

  Variable d switching in cycle A ensures that point q is not a fixed point for mapping M_A and image type 3 is possible. For each $x \in P_A$, we define $|F(Q_1,c)| \gg |F(Q_1,d)|$ such that $|x_c| \geq |x_d|$ on the first common boundary even if $x_c = 0$ on entry to Q_1. Then we will have $|x_c| \geq |x_d|$ on all the common boundaries. This means that x_d must switch on exiting Q_2, i.e. $M_A(x) \subseteq C_B$. By Lemma 5.1.7, we have $M_A(C_A) \subseteq C_B$.

  On cycle B, for each $y \in P_B$, $y_d = 0$ and $|y_c| > 0$ on entry to Q_1. Then we will have $|y_c| \geq |y_d|$ on all the common boundaries, since $|F(Q_1,c)| \gg |F(Q_1,d)|$. This means that y_d must switch on exiting Q_2, i.e. $M_B(y) \subseteq C_B$. By Lemma 5.1.7, we have $M_B(C_B) \subseteq C_B$.

  In the above discussion, we need $|F(Q_1,c)| \gg |F(Q_1,d)| = \gamma$. Now, we will show how to find the possible interval of $|F(Q_1,c)|$ such that image type 3 is obtained. By Lemma 5.1.7, we get the suitable interval of $|F(Q_1,c)|$ by the mapping of $M_A^{(M+1)} \dots M_A^{(0)}$ at points in P_A.

  Assume the ith variable switches on exiting Q_1. From Remark 5.1.3, for each $x \in P_A$ there exists $|F_x^A(Q_1,c)| \stackrel{\triangle}{=} \mu$, such that $|x_c^{(M+2)}| = |x_d^{(M+2)}|$ on cycle A. To get the $|F_x^A(Q_1,c)|$, consider the mapping for cycle A over the first $M+2$ steps

$$M_A^{(M+1)} \dots M_A^{(0)}(x) = \frac{A^{(M+2,0)}x}{1 + \langle \phi^{(M+2,0)}, x \rangle},$$

  where $A^{(M+2,0)} = A^{(M+1)}A^{(M)} \cdots A^{(0)}$ is an $n \times n$ matrix, and $\phi^{(M+2,0)}$ is an $n \times 1$ vector. The denominator $1 + \langle \phi^{(M+2,0)}, x \rangle$ is not zero and scales x_c and x_d in the same way, therefore we only need to consider the numerator $A^{(M+2,0)}x$. From the definition of $A^{(M+1)}$ in Eq. (2.5), i.e.,

$$A^{(M+1)} = I - \frac{F(Q_1,:)e_i^T}{F(Q_1,i)}.$$

  It is clear that only one coordinate $a_{ci}^{(M+1)}$ of $A^{(M+1)}$ involves variable μ. There-

fore, μ only occurs in the cth row of matrix $A^{(M+2,0)}$ and it appears linearly. Now solve the simple linear equation $|A^{(M+2,0)}x|_c = |A^{(M+2,0)}x|_d$ for μ, where $|A^{(M+2,0)}x|_c$ ($|A^{(M+2,0)}x|_d$) denote the cth (dth) coordinate of $|A^{(M+2,0)}x|$, we get the required $|F_x^A(Q_1, c)|$.

Then, image type 3 is obtained by defining $|F(Q_1, d)| = \gamma$ and $|F(Q_1, c)| \geq \mu_1$, where

$$\mu_1 = \max\{|F_x^A(Q_1, c)|,\ \forall x \in P_A\}.$$

- Image type 4 is obtained by defining $|F(Q_1, d)| \gg |F(Q_1, c)| = \gamma$.

  Variable c switching in cycle B ensures that point p is not a fixed point for mapping M_B. Using the same idea as in type 3, we get the suitable interval of $|F(Q_1, d)|$ by the mapping of $M_B^{(N+1)} \ldots M_B^{(0)}$ at points in P_B. Then, image type 4 is obtained by defining $|F(Q_1, c)| = \gamma$ and $|F(Q_1, d)| \geq \mu_2$, where

$$\mu_2 = \max\{|F_y^B(Q_1, d)|,\ \forall y \in P_B\}.$$

- From the discussion of type 1 and type 4, we get type 5.

  Since we get $M_B(C_B) \subseteq C_B$ by defining $|F(Q_1, d)| = |F(Q_1, c)|$ and get $M_B(C_B) \subseteq C_A$ by defining $|F(Q_1, d)| \gg |F(Q_1, c)|$. We have $M_A(C_A) \subseteq C_A$, $M_B(C_B) \cap C_A \neq \emptyset$, $M_B(C_B) \cap C_B \neq \emptyset$ by continuity of $M_B^{(N+1)} \ldots M_B^{(0)}$ as a function of the changing focal point parameter $F(Q_1, d) \stackrel{\triangle}{=} \mu$. That is, image type 5 is obtained by defining $|F(Q_1, c)| = \gamma$ and $\mu_3 < |F(Q_1, d)| < \mu_2$, where

$$\mu_3 = \min\{|F_y^B(Q_1, d)|,\ \forall y \in P_B\}.$$

  If there is only one point v in P_B by Lemma 5.1.8, then define $|F(Q_1, c)| = \gamma$ and $|F(Q_1, d)| > |F_v^B(Q_1, d)|$ get type 5.

- Image type 7 is obtained from type 1 and type 3 by the same idea as in type 5.

  Defining $|F(Q_1, d)| = \gamma$ and $\mu_4 < |F(Q_1, c)| < \mu_1$, where

$$\mu_4 = \min\{|F_x^A(Q_1, c)|,\ \forall x \in P_A\}.$$

  If there is only one point v in P_A by Lemma 5.1.8, then image type 7 is obtained by defining $|F(Q_1, d)| = \gamma$ and $|F(Q_1, c)| > |F_v^A(Q_1, c)|$.

  From the above discussion, we get another two construction ideas for type 1.

- Image type 1 is obtained by defining $|F(Q_1, d)| = \gamma$ and $\gamma \leq |F(Q_1, c)| \leq \mu_4$.
- Image type 1 can also obtained by defining $|F(Q_1, c)| = \gamma$ and $\gamma \leq |F(Q_1, d)| \leq \mu_3$.

The above analysis together with Lemma 5.1.4 and Lemma 5.1.5 completes the proof.

Theorem 5.2.2. *For the figure-8 pattern described above, when $a = c$ and $b = d$, if there are only two common orthants in total, then image types 2, 6, 8 and 9 are impossible.*

Proof. We will prove this result by showing that it is impossible to have $M_A(x) \in C_B$ and $M_B(y) \in C_A$ at the same time for any $x \in C_A$ and $y \in C_B$ when there are only two common orthants.

Following the notation of Theorem 5.2.1, we consider $x^{(M+1)}$ to be an arbitrary point on the boundary between orthant Q_{1A} and Q_1 and $y^{(N+1)}$ an arbitrary point on the boundary between orthant Q_{1B} and Q_1. Then $x^{(M+2)} = M_A^{(M+1)}(x^{(M+1)})$ and $y^{(N+2)} = M_B^{(N+1)}(y^{(N+1)})$, where $M_A^{(M+1)}$ and $M_B^{(N+1)}$ are as defined in Eq. (2.4).

Without loss of generality, we assume that both the ath coordinate and the bth coordinate on the common boundary are positive. Then $F(Q_2, a)$ and $F(Q_2, b)$ are negative, $F(Q_1, a)$ and $F(Q_1, b)$ are positive, $x_b^{(M+1)}$ and $y_a^{(N+1)}$ are positive and $x_a^{(M+1)} = y_b^{(N+1)} = 0$.

In order to have the bth coordinate of $x^{(M+2)}$ switching in orthant Q_2 and the ath coordinate of $y^{(N+2)}$ switching in orthant Q_2, we need

$$\begin{cases} \log(1 - \frac{x_b^{(M+2)}}{F(Q_2,b)}) < \log(1 - \frac{x_a^{(M+2)}}{F(Q_2,a)}), \\ \\ \log(1 - \frac{y_b^{(N+2)}}{F(Q_2,b)}) > \log(1 - \frac{y_a^{(N+2)}}{F(Q_2,a)}). \end{cases}$$

that is

$$\begin{cases} F(Q_2, a) > \frac{x_a^{(M+2)} F(Q_2,b)}{x_b^{(M+2)}}, \\ \\ F(Q_2, b) > \frac{y_b^{(N+2)} F(Q_2,a)}{y_a^{(N+2)}}. \end{cases}$$

Hence

$$F(Q_2, b) > \frac{y_b^{(N+2)} F(Q_2, a)}{y_a^{(N+2)}} > \frac{y_b^{(N+2)} x_a^{(M+2)} F(Q_2, b)}{x_b^{(M+2)} y_a^{(N+2)}},$$

that is, we need

$$x_b^{(M+2)} y_a^{(N+2)} < x_a^{(M+2)} y_b^{(N+2)}, \tag{5.2}$$

since $F(Q_2, b)$ is negative.

But by Eq. (2.2), we know that

$$\begin{cases} x_b^{(M+2)} = F(Q_1,b) + (x_b^{(M+1)} - F(Q_1,b))e^{-t_x^{(M+1)}}, \\ x_a^{(M+2)} = F(Q_1,a) + (x_a^{(M+1)} - F(Q_1,a)e^{-t_x^{(M+1)}} = F(Q_1,a) - F(Q_1,a)e^{-t_x^{(M+1)}}, \\ y_b^{(N+2)} = F(Q_1,b) + (y_b^{(N+1)} - F(Q_1,b))e^{-t_y^{(N+1)}} = F(Q_1,b) - F(Q_1,b)e^{-t_y^{(N+1)}}, \\ y_a^{(N+2)} = F(Q_1,a) + (y_a^{(N+1)} - F(Q_1,a))e^{-t_y^{(N+1)}}, \end{cases}$$

where $t_x^{(M+1)}$ and $t_y^{(N+1)}$ are the switching times of point x and y in orthant Q_1 respectively. Then

$$\begin{aligned} & x_b^{(M+2)}y_a^{(N+2)} - x_a^{(M+2)}y_b^{(N+2)} \\ = \;& F(Q_1,b)y_a^{(N+1)}e^{-t_y^{(N+1)}} - F(Q_1,b)y_a^{(N+1)}e^{-t_x^{(M+1)}}e^{-t_y^{(N+1)}} + F(Q_1,a)x_b^{(M+1)}e^{-t_x^{(M+1)}} \\ & -F(Q_1,a)x_b^{(M+1)}e^{-t_x^{(M+1)}}e^{-t_y^{(N+1)}} + x_b^{(M+1)}y_a^{(N+1)}e^{-t_x^{(M+1)}}e^{-t_y^{(N+1)}} \\ = \;& F(Q_1,b)y_a^{(N+1)}e^{-t_y^{(N+1)}}(1 - e^{-t_x^{(M+1)}}) + F(Q_1,a)x_b^{(M+1)}e^{-t_x^{(M+1)}}(1 - e^{-t_y^{(N+1)}}) \\ & +x_b^{(M+1)}y_a^{(N+1)}e^{-t_x^{(M+1)}}e^{-t_y^{(N+1)}} \\ > \;& 0, \end{aligned}$$

i.e. $x_b^{(M+2)}y_a^{(N+2)} > x_a^{(M+2)}y_b^{(N+2)}$.

This is a contradiction to Eq. (5.2) and completes the proof.

In contrast to the above theorem, if there are at least three common orthants, we have the following result.

Theorem 5.2.3. *Under the same conditions as in Thm. 5.2.1, if there are at least three common orthants, then*

1. *image types 1, 5, 7 and 9 are possible;*
2. *if d switches in cycle A, image types 3 and 6 are possible;*
3. *if c switches in cycle B, image types 4 and 8 are possible;*
4. *if d switches in cycle A and c switches in cycle B, image type 2 is possible;*

Proof. Denote the common orthant after Q_1 by Q^*. Assume variable i switches in Q_1 and variable j switches in Q^*. In orthant Q_1, let $|F(Q_1,d)| = \gamma$, then for each point $x \in P_A$, this determines $x_d^{(M+2)}$. Let $F_x^A(Q_1,c)$ denote a corresponding $F(Q_1,c)$ for point x such that $|x_c^{(M+2)}| > |x_d^{(M+2)}|$ and define

$$|F(Q_1,c)| \geq \max\{|F_x^A(Q_1,c)|, \forall\ x \in P_A\}. \tag{5.3}$$

It is clear that (see Figure 5.4 (a) for illustration) $|F(Q_1,c)| > |F(Q_1,d)|$ since for each point $x \in P_A$, we have

$$\begin{aligned} |x_c^{(M+2)}| &= \frac{|F_x^A(Q_1,c)x_i^{(M+1)} - F(Q_1,i)x_c^{(M+1)}|}{|x_i^{(M+1)} - F(Q_1,i)|} \\ &= \frac{|x_i^{(M+1)}|}{|x_i^{(M+1)}| + |F(Q_1,i)|}|F_x^A(Q_1,c)| \end{aligned}$$

and

$$\begin{aligned} |x_d^{(M+2)}| &= \frac{|F(Q_1,d)x_i^{(M+1)} - F(Q_1,i)x_d^{(M+1)}|}{|x_i^{(M+1)} - F(Q_1,i)|} \\ &= \frac{|F(Q_1,d)||x_i^{(M+1)}| + |F(Q_1,i)||x_d^{(M+1)}|}{|x_i^{(M+1)}| + |F(Q_1,i)|}. \end{aligned}$$

The preceding follows, because $F(Q_1,i)$ and $x_i^{(M+1)}$ have different sign, $F_x^A(Q_1,c)$ and $x_c^{(M+1)}$ have the same sign and $F(Q_1,d)$ and $x_d^{(M+1)}$ have the same sign.

Hence

$$|F(Q_1,c)| - |F(Q_1,d)| \geq |F_x^A(Q_1,c)| - |F(Q_1,d)| \geq \frac{|F(Q_1,i)||x_d^{(M+1)}|}{|x_i^{(M+1)}|} > 0.$$

For each point $y \in P_B$ by the same formula, we have $|y_c^{(N+2)}| > |y_d^{(N+2)}|$ since $|F(Q_1,c)| > |F(Q_1,d)|$ and $y_d^{(N+1)} = 0$ (see Figure 5.4 (b) for illustration). Therefore, on the entry to Q^*, we always have the cth coordinate larger than the dth coordinate for all the points in P_A and P_B. In orthant Q^*, define

$$|F(Q^*,c)| = \min\{\min\{|x_d^{(M+2)}|, \forall\ x \in P_A\}, \min\{|y_d^{(N+2)}|, \forall\ y \in P_B\}\}$$

and

$$|F(Q^*,d)| = \max\{\max\{|x_c^{(M+2)}|, \forall\ x \in P_A\}, \max\{|y_c^{(N+2)}|, \forall\ y \in P_B\}\}.$$

The construction idea of this theorem is considering the trajectories backwards. First, for each point $x \in P_A$, we will get a t_x such that $|x_c^{(M+3)}| = |x_d^{(M+3)}|$. Second, using t_x to find the required $|F_x^{(t_x)}(Q_{1A},j)|$ for each $x \in P_A$ such that the passage time in Q^* is t_x. Third, by choosing suitable $|F(Q_{1A},j)|$ which is decided by all the

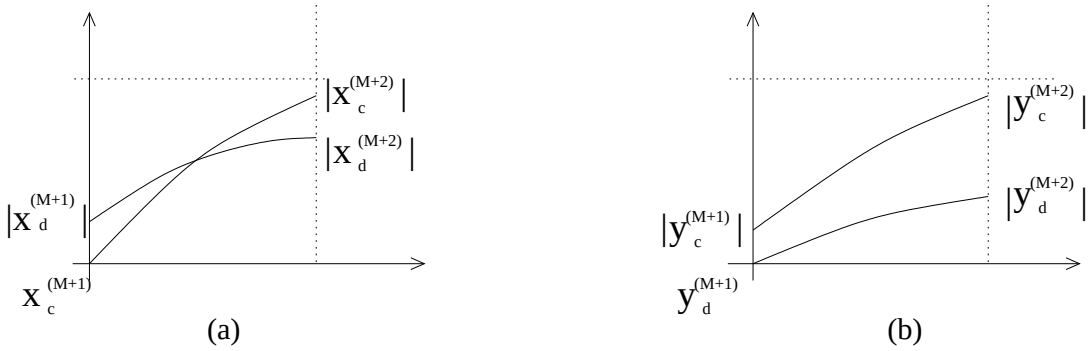

Figure 5.4: Evolution of x_c, x_d, y_c, y_d as they pass through orthant Q_1. In figure (a), in order to have $|x_c^{(M+2)}| > |x_d^{(M+2)}|$, the absolute value of the cth coordinate must increase faster than the dth coordinate. That is we need to define $|F(Q_1, c)| > |F(Q_1, d)|$. In figure (b), since we have already defined $|F(Q_1, c)| > |F(Q_1, d)|$ in figure (a) and $|y_c^{(N+1)}| > |y_d^{(N+1)}|$, we will have $|y_c^{(N+2)}| > |y_d^{(N+2)}|$.

$|F_x^{(t_x)}(Q_{1A}, j)|$s, we force the trajectories starting in C_a to follow the cycle we want. For each point $y \in P_B$, we do the same construction to get $|F_y^{(t_y)}(Q_{1B}, j)|$. Then by choosing suitable $|F(Q_{1B}, j)|$ which is decided by all the $|F_y^{(t_y)}(Q_{1B}, j)|$s, we force the trajectories starting in C_b to follow the cycle we want.

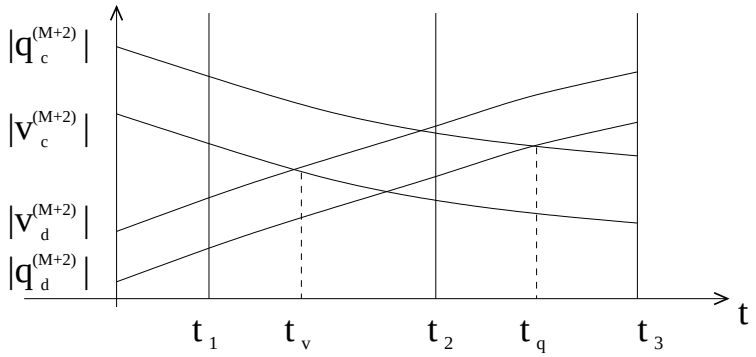

Figure 5.5: Illustration of the construction idea.

Before we start the construction for general case, we use one example (see Figure 5.5) to illustrate the idea. Assume $P_A = \{q,\ v\}$ and the jth variable will switch in Q^*. First, we get t_q and t_v by solving $|q_c^{(M+3)}| = |q_d^{(M+3)}|$ and $|v_c^{(M+3)}| = |v_d^{(M+3)}|$. Second, find $|F_q^{(t_q)}(Q_{1A}, j)|$ and $|F_v^{(t_v)}(Q_{1A}, j)|$ such that the passage time is t_q and t_v, respectively. Third, define $|F(Q_{1A}, j)|$ based on $|F_q^{(t_q)}(Q_{1A}, j)|$ and $|F_v^{(t_v)}(Q_{1A}, j)|$ to get the required image types.

1. When

$$|F(Q_{1A}, j)| < \min\{|F_q^{(t_q)}(Q_{1A}, j)|,\ |F_v^{(t_v)}(Q_{1A}, j)|\}$$

The passage time in Q^* will be shorter than t_v, say at t_1, then $|q_c^{(M+3)}| > |q_d^{(M+3)}|$ and $|v_c^{(M+3)}| > |v_d^{(M+3)}|$. That is we have $M_A(C_A) \subseteq C_B$.

2. When
$$|F(Q_{1A}, j)| > \max\{|F_q^{(t_q)}(Q_{1A}, j)|,\ |F_v^{(t_v)}(Q_{1A}, j)|\}$$
The passage time in Q^* will be longer than t_q, say at t_3, then $|q_c^{(M+3)}| < |q_d^{(M+3)}|$ and $|v_c^{(M+3)}| < |v_d^{(M+3)}|$. That is we have $M_A(C_A) \subseteq C_A$.

3. When
$$\begin{aligned}\min\{|F_q^{(t_q)}(Q_{1A}, j)|,\ |F_v^{(t_v)}(Q_{1A}, j)|\} &< |F(Q_{1A}, j)| \\ &< \max\{|F_q^{(t_q)}(Q_{1A}, j)|,\ |F_v^{(t_v)}(Q_{1A}, j)|\}\end{aligned}$$
The passage time in Q^* will be between t_v and t_q, say at t_2, then $|q_c^{(M+3)}| > |q_d^{(M+3)}|$ and $|v_c^{(M+3)}| < |v_d^{(M+3)}|$. That is we have $M_A(C_A) \cap C_B \neq \emptyset$, $M_A(C_A) \cap C_A \neq \emptyset$.

Now, we start the construction. First, by Eq. (2.2), we get the corresponding passage time t_x for each $x \in P_A$, such that $|x_c^{(M+3)}| = |x_d^{(M+3)}|$. From
$$|x_c^{(M+3)}| = |F(Q^*, c) + (x_c^{(M+2)} - F(Q^*, c))e^{-t_x}|$$
and
$$|x_d^{(M+3)}| = |F(Q^*, d) + (x_d^{(M+2)} - F(Q^*, d))e^{-t_x}|,$$
t_x can be solved since $|x_c^{(M+2)}| > |x_d^{(M+2)}|$ and $|F(Q^*, d)| > |F(Q^*, c)|$ (see Figure 5.5.

Second, for each point $x \in P_A$, using Eq. (2.11), we have
$$\log\left(1 - \frac{x_j^{(M+2)}}{F(Q^*, j)}\right) = t_x.$$
We obtain the required $x_j^{(M+2)}$.

Then using
$$x_j^{(M+2)} = \frac{F(Q_1, j)x_i^{(M+1)} - F(Q_1, i)x_j^{(M+1)}}{x_i^{(M+1)} - F(Q_1, i)},$$
we get the required $x_j^{(M+1)}$. Using the above formula again
$$x_j^{(M+1)} = \frac{F(Q_{1A}, j)x_c^{(M)} - F(Q_{1A}, c)x_j^{(M)}}{x_c^{(M)} - F(Q_{1A}, c)},$$

we obtain the required $F(Q_{1A}, j)$ for each $x \in P_A$ denoted by $F_x^{(t_x)}(Q_{1A}, j)$.

Third, let

$$|F_1(Q_{1A}, j)| = \min\{|F_x^{(t_x)}(Q_{1A}, j)|,\ \forall\ x \in P_A\}$$

and

$$|F_2(Q_{1A}, j)| = \max\{|F_x^{(t_x)}(Q_{1A}, j)|,\ \forall\ x \in P_A\}.$$

Similarly, we get $|F_y^{(t_y)}(Q_{1B}, j)|$ for each $y \in P_B$. Then, let

$$|F_3(Q_{1B}, j)| = \min\{|F_y^{(t_y)}(Q_{1B}, j)|,\ \forall\ y \in P_B\}$$

and

$$|F_4(Q_{1B}, j)| = \max\{|F_y^{(t_y)}(Q_{1B}, j)|,\ \forall\ y \in P_B\}.$$

Now, the last step in the construction, i.e., choosing $|F(Q_{1A}, j)|$ and $|F(Q_{1B}, j)|$,

1. if $|F(Q_{1A}, j)| = |F_1(Q_{1A}, j)|$, we have $|x_c^{(M+3)}| \geq |x_d^{(M+3)}|$ for $\forall x \in P_A$. Cycle A will be followed by cycle B, i.e., $M_A(C_A) \subseteq C_B$.

2. if $|F(Q_{1A}, j)| = |F_2(Q_{1A}, j)|$, we have $|x_c^{(M+3)}| \leq |x_d^{(M+3)}|$ for $\forall x \in P_A$. Cycle A will be followed by cycle A, i.e., $M_A(C_A) \subseteq C_A$.

3. if $|F_1(Q_{1A}, j)| < |F(Q_{1A}, j)| < |F_2(Q_{1A}, j)|$, we have $|x_c^{(M+3)}| > |x_d^{(M+3)}|$ for some points x in P_A and $|x_c^{(M+3)}| < |x_d^{(M+3)}|$ for other points x in P_A. That is $M_A(C_A) \cap C_B \neq \emptyset$, $M_A(C_A) \cap C_A \neq \emptyset$.

4. if $|F(Q_{1B}, j)| = |F_3(Q_{1B}, j)|$, we have $|y_c^{(N+3)}| \geq |y_d^{(N+3)}|$ for $\forall y \in P_B$. Cycle B will be followed by cycle B, i.e., $M_B(C_B) \subseteq C_B$.

5. if $|F(Q_{1B}, j)| = |F_4(Q_{1B}, j)|$, we have $|y_c^{(N+3)}| \leq |y_d^{(N+3)}|$ for $\forall y \in P_B$. Cycle B will be followed by cycle A, i.e., $M_B(C_B) \subseteq C_A$.

6. if $|F_3(Q_{1B}, j)| < |F(Q_{1B}, j)| < |F_4(Q_{1B}, j)|$, we have $|y_c^{(N+3)}| > |y_d^{(N+3)}|$ for some points y in P_B and $|y_c^{(N+3)}| < |y_d^{(N+3)}|$ for other points y in P_B. That is $M_B(C_B) \cap C_B \neq \emptyset$, $M_B(C_B) \cap C_A \neq \emptyset$.

Note that if $|F_1(Q_{1A}, j)| = |F_2(Q_{1A}, j)|$ while there are more than one point in P_A, then we use a different γ in the construction to avoid this. If $|F_1(Q_{1A}, j)| = |F_2(Q_{1A}, j)|$ and there is only one point in P_A, we know that d doesn't switch in cycle A and the only point in P_A is v by Lemma 5.1.8. Then,

1. if $|F(Q_{1A}, j)| \geq |F_v^{(t_v)}(Q_{1A}, j)|$, we have $|x_c^{(M+3)}| \leq |x_d^{(M+3)}|$ for $\forall x \in P_A$. Cycle A will be followed by cycle A, i.e., $M_A(C_A) \subseteq C_A$.

2. if $|F(Q_{1A}, j)| < |F_v^{(t_v)}(Q_{1A}, j)|$, we have $|x_c^{(M+3)}| > |x_d^{(M+3)}|$ for some points x in P_A and $|x_c^{(M+3)}| < |x_d^{(M+3)}|$ for other points x in P_A. That is $M_A(C_A) \cap C_B \neq \emptyset$, $M_A(C_A) \cap C_A \neq \emptyset$.

Similarly, if there is only one point in P_B, we know that c doesn't switch in cycle B and the only point in P_B is v by Lemma 5.1.8. Then,

1. if $|F(Q_{1B}, j)| \leq |F_v^{(t_v)}(Q_{1B}, j)|$, we have $|y_c^{(N+3)}| \geq |y_d^{(N+3)}|$ for $\forall y \in P_B$. Cycle B will be followed by cycle B, i.e., $M_B(C_B) \subseteq C_B$.

2. if $|F(Q_{1B}, j)| > |F_v^{(t_v)}(Q_{1B}, j)|$, we have $|y_c^{(N+3)}| < |y_d^{(N+3)}|$ for some points y in P_B and $|y_c^{(N+3)}| < |y_d^{(N+3)}|$ for other points y in P_B. That is $M_B(C_B) \cap C_B \neq \emptyset$, $M_B(C_B) \cap C_A \neq \emptyset$.

By Lemma 5.1.4 and Lemma 5.1.5, suitable values of $|F(Q_{1A}, j)|$ and $|F(Q_{1B}, j)|$ according to the above itemization will give us all the image types. □

5.2.2 Case 2

From Lemma 5.1.4 and Lemma 5.1.5, we need d to switch in cycle A and c to switch in cycle B to get image type 2, d to switch in cycle A to get image types 3 and 6 and c to switch in cycle B to get image types 4 and 8, but in case 2 ($a = d$ and $b = c$), d switches in cycle A and c switches in cycle B. So we have Thm. 5.2.4.

Theorem 5.2.4. *When $a = d$ and $b = c$, if neither c nor d switches in common boundaries, then image types 2, 3, 4, 6 and 8 are possible,*

Proof.

- Image type 2 can be obtained by defining $|F(Q_1, d)| = |F(Q_1, c)| = \gamma$.

  For each $x \in P_A$, $x_d = 0$ and $|x_c| > 0$ on entry to Q_1. Then we will have $|x_c| \geq |x_d|$ on all the common boundaries, which means that x_d switches on exiting Q_2, i.e. $M_A(x) \in C_B$. By Lemma 5.1.7, we have $M_A(C_A) \subseteq C_B$.

  Similarly, for each $y \in P_B$, $y_c = 0$ and $|y_d| > 0$ on entry to Q_1. Then we will have $|y_d| \geq |y_c|$ on all the common boundaries, which means that y_c switches on exiting Q_2, i.e. $M_B(y) \in C_A$. By Lemma 5.1.7, we have $M_B(C_B) \subseteq C_A$.

- Image type 4 is obtained by defining $|F(Q_1, d)| \gg |F(Q_1, c)| = \gamma$.

  For each $x \in P_A$, we define $|F(Q_1, d)| \gg |F(Q_1, c)|$ such that $|x_d| \geq |x_c|$ on the first common boundary even if $x_d = 0$ on entry to Q_1. Then we will have $|x_d| \geq |x_c|$ on all the common boundaries. This means that x_c switches on exiting Q_2, i.e. $M_A(x^{(0)}) \subseteq C_A$. By Lemma 5.1.7, we have $M_A(C_A) \subseteq C_A$.

  On cycle B, for each $y \in P_B$, $y_c = 0$ and $|y_d| > 0$ on entry to Q_1. Then we will have $|y_d| \geq |y_c|$ on all the common boundaries, since $|F(Q_1, d)| \gg |F(Q_1, c)|$. This means that y_c switches on exiting Q_2, i.e. $M_B(y) \subseteq C_A$. By Lemma 5.1.7, we have $M_B(C_B) \subseteq C_A$.

  Assume the ith variable switches in Q_1. From Remark 5.1.3, there exists $F_x^A(Q_1, d)$ for each point $x \in P_A$ such that $x_c^{(M+2)} = x_d^{(M+2)}$ on cycle A.

  Then, image type 4 is obtained by defining $|F(Q_1, c)| = \gamma$ and $|F(Q_1, d)| \geq \xi_1$, where

  $$\xi_1 = \max\{|F_x^A(Q_1, d)|, \ \forall \ x \in P_A\}.$$

- Image type 3 is obtained by defining $|F(Q_1, c)| \gg |F(Q_1, d)| = \gamma$.

  By Remark 5.1.3, let $F_y^B(Q_1, c)$ denote the required $F(Q_1, c)$ for each point $y \in P_B$ to have $y_c^{(N+2)} = y_d^{(N+2)}$ on cycle B. Using the same idea as in type 4, we get the suitable interval of $|F(Q_1, c)|$ by the mapping of $M_B^{(N+1)} \dots M_B^{(0)}$ at points in P_B. Then, image type 3 is obtained by defining $|F(Q_1, d)| = \gamma$ and $|F(Q_1, c)| \geq \xi_2$, where

  $$\xi_2 = \max\{|F_y^B(Q_1, c)|, , \ \forall \ y \in P_B\}.$$

- From the discussion of type 2 and type 3, we get type 6.

  Since we get $M_B(C_B) \subseteq C_A$ by defining $|F(Q_1, d)| = |F(Q_1, c)|$ and get $M_B(C_B) \subseteq C_B$ by defining $|F(Q_1, c)| \gg |F(Q_1, d)|$. We have $M_A(C_A) \subseteq C_B$, $M_B(C_B) \cap C_B \neq \emptyset$, $M_B(C_B) \cap C_A \neq \emptyset$ by continuity of $M_B^{(N+1)} \dots M_B^{(0)}$ as a function of the changing focal point parameter $F(Q_1, c) \stackrel{\triangle}{=} \xi$. That is, image type 6 is obtained by defining $|F(Q_1, d)| = \gamma$ and $\xi_3 < |F(Q_1, c)| < \xi_2$, where

  $$\xi_3 = \min\{|F_y^B(Q_1, c)|, \ \forall \ y \in P_B\}.$$

- Image type 8 is obtained from type 2 and type 4 by the same idea as in type 6.

Defining $|F(Q_1, c)| = \gamma$ and $\xi_4 < |F(Q_1, d)| < \xi_1$, where

$$\xi_4 = \min\{|F_x^A(Q_1, d)|, \ \forall \ x \in P_A\}.$$

From the above discussion, we get another two construction ideas for type 2. More generally,

- Image type 2 is obtained by defining $|F(Q_1, d)| = \gamma$ and $\gamma \leq |F(Q_1, c)| \leq \xi_3$.
- Image type 2 is obtained by defining $|F(Q_1, c)| = \gamma$ and $\gamma \leq |F(Q_1, d)| \leq \xi_4$.

This completes the proof.

Similarly, we have the following results for case $a = d$ and $b = c$.

Theorem 5.2.5. *Under the same conditions as in Thm. 5.2.4, if there are only two common orthants in total, then image types 1, 5, 7 and 9 are impossible.*

Proof. In Theorem 5.2.2, we have proved that there are no points $x \in P_A$ and $y \in P_B$ such that $M_A(x) \subseteq C_B$ and $M_B(y) \subseteq C_A$ at the same time, which means that it is impossible to have a trajectory from C_a with the cth coordinate switching in Q_2 and trajectory from C_b with the dth coordinate switching in Q_2 at the same time. Therefore, we don't have $M_A(x) \subseteq C_A$ and $M_B(y) \subseteq C_B$ at the same time in case 2 when there are only two common orthants. That is, image types 1, 5, 7 and 9 are impossible.

Theorem 5.2.6. *Under the same conditions as in Thm. 5.2.4, if there are at least three common orthants, then all the image types are possible.*

Proof. The proof is similar to Theorem 5.2.3.

5.2.3 Case 3

Theorem 5.2.7. *When $a = c$ and $b \neq d$, if neither c nor d switches in common boundaries, then*

1. *image types 1, 5, 7 and 9 are possible;*
2. *if d switches in cycle A, image types 3 and 6 are possible;*
3. *if c switches in cycle B, image types 4 and 8 are possible;*
4. *if d switches in cycle A and c switches in cycle B, image type 2 is possible;*

Proof.

- Suitable $|F(Q_1, c)|$ and $|F(Q_{1B}, d)|$ give us types 3, 2 and 6.

  Idea: If we let $|F(Q_1, c)|$ be very large such that for each point $x \in P_A$ and $y \in P_B$ we will always have $|x_c| \geq |x_d|$ and $|y_c| \geq |y_d|$ on common boundaries no matter which cycle we follow, then we have type 3, $M_B(C_B) \subseteq C_B$ and $M_A(C_A) \subseteq C_B$. Now if we let $F(Q_{1B}, d)$ be very large such that if we start with a point $y \in P_B$, we will always have $|y_d| \geq |y_c|$ on common boundaries even if $|y_c|$ is very large in Q_1 because $|F(Q_1, c)|$ is very large, then we have type 2. We have $M_B(C_B) \cap C_B \neq \emptyset$ and $M_B(C_B) \cap C_A \neq \emptyset$ by continuity of M_B as a function of the changing focal point parameter $F(Q_{1B}, d)$.

  Calculation: By Remark 5.1.3, let $|F_x^A(Q_1, c)|$ denote the required $F(Q_1, c)$ for each point $x \in P_A$ to have $|x_c^{(M+2)}| = |x_d^{(M+2)}|$ on cycle A. Define

  $$\alpha_1 = \max\{|F_x^A(Q_1, c)|, \ \forall\ x \in P_A\}.$$

  It is clear that $\alpha_1 > \gamma$. Let $|F_y^B(Q_1, c)|$ denote the required $F(Q_1, c)$ for each point $y \in P_B$ to have $|y_c^{(N+2)}| \geq |y_d^{(N+2)}|$. For each point $y \in P_B$, if $|y_c^{(N+1)}| < |y_d^{(N+1)}|$, then from Remark 5.1.3, there exists $F_y^B(Q_1, c)$ such that $|y_c^{(N+2)}| = |y_d^{(N+2)}|$, and if $|y_c^{(N+1)}| > |y_d^{(N+1)}|$, let $|F_y^B(Q_1, c)| = \gamma$ can ensure $|y_c^{(N+2)}| > |y_d^{(N+2)}|$. Then image type 3 is obtained by defining $|F(Q_1, d)| = \gamma$ and $|F(Q_1, c)| \geq \alpha_2$, where

  $$\alpha_2 = \max\{\alpha_1, |F_y^B(Q_1, c)|, \ \forall\ y \in P_B\}.$$

  Let $F_y^B(Q_{1B}, d)$ denote the required $F(Q_{1B}, d) \stackrel{\triangle}{=} \alpha$ for each point $y \in P_B$ to have $|y_c^{(N+2)}| = |y_d^{(N+2)}|$ on cycle B when $|F(Q_1, c)| \geq \alpha_2$. Since $|y_c^{(N+2)}| \geq |y_d^{(N+2)}|$ before changing $F_y^B(Q_{1B}, d)$, we need a large $|y_d^{(N+2)}|$. The existence of $F_y^B(Q_{1B}, d)$ for equation $|y_c^{(N+2)}| = |y_d^{(N+2)}|$ is ensured by the continuity of M_B as a function of the changing focal point parameter α and Remark 5.1.3. The calculation is not complicated even though the variable α appears in $M_B^{(N)}$ instead of $M_B^{(N+1)}$. For mapping

  $$M_B^{(N+1)} M_B^{(N)} \dots M_B^{(0)}(y) = \frac{B^{(N+2,0)} y}{1 + \langle \phi^{(N+2,0)}, y \rangle},$$

  where $B^{(N+2,0)} = B^{(N+1)} B^{(N)} \cdots B^{(0)}$ is an $n \times n$ matrix, and $\phi^{(N+2,0)}$ is an $n \times 1$ vector, we only need to consider the numerator $B^{(N+2,0)} y$, since the denominator

$1 + \langle \phi^{(N+2,0)}, y \rangle$ is not zero and scales y_c and y_d in the same way. From the definition of $B^{(N)}$ by Eq. (2.5), only one coordinate in the dth row of $B^{(N)}$ involves variable α. Therefore, α only occurs in one row of matrix $B^{(N+1,0)}$ and it appears linearly. Note that the dth column of $B^{(N+1)}$ is e_d since the dth coordinate doesn't switch in common orthant Q_1. Then α still occurs in only one row of matrix

$$B^{(N+2,0)} = B^{(N+1)} B^{(N+1,0)},$$

and it appears linearly. Now solving the simple linear equation $[B^{(N+2,0)} y]_c = [B^{(N+2,0)} y]_d$ for α, we get the required $F_y^B(Q_{1B}, d)$. Then, image type 2 is obtained by defining $|F(Q_{1B}, d)| \geq \alpha_3$ and $|F(Q_1, c)| \geq \alpha_2$, where

$$\alpha_3 = \max\{|F_y^B(Q_{1B}, d)|, \ \forall \ y \in P_B\}.$$

And image type 6 is obtained by defining $\alpha_4 < |F(Q_{1B}, d)| < \alpha_3$ and $|F(Q_1, c)| \geq \alpha_2$, where

$$\alpha_4 = \min\{|F_y^B(Q_{1B}, d)|, \ \forall \ y \in P_B\}.$$

For type 6, if there is only one point in P_B (lemma 5.1.8), then image type 6 is obtained by defining $|F(Q_1, c)| \geq \alpha_2$ and $|F(Q_{1B}, d)| > |F_v^B(Q_{1B}, d)|$.

From the discussion above, image type 3 can also be obtained by defining $\omega \leq |F(Q_{1B}, d)| \leq \alpha_4$ and $|F(Q_1, c)| \geq \alpha_2$, where ω may be 1 or γ depending on whether d switches on entry to Q_{1B} or not.

- Suitable $|F(Q_{1B}, c)|$ and $|F(Q_{1A}, d)|$ give us type 1.

  Idea: Let $|F(Q_{1B}, c)|$ be large enough such that, we will always have $|y_c| \geq |y_d|$ on common boundaries for each $y \in P_B$ and let $|F(Q_{1A}, d)|$ be large enough such that we will always have $|x_d| \geq |x_c|$ on common boundaries for each $x \in P_A$. That is $M_B(C_B) \subseteq C_B$ and $M_A(C_A) \subseteq C_A$ at the same time.

  Calculation: Let $|F_y^B(Q_{1B}, c)|$ denote the required $F(Q_{1B}, c)$ for each point $y \in P_B$ to have $|y_c^{(N+2)}| \geq |y_d^{(N+2)}|$ on cycle B. For each point $y \in P_B$, if $|y_c^{(N+2)}| < |y_d^{(N+2)}|$ before changing $F(Q_{1B}, c)$, then by Remark 5.1.3 and the continuity of mapping M_B as a function of $F(Q_{1B}, c)$, there exists $|F_y^B(Q_{1B}, c)|$ such that $|y_c^{(N+2)}| = |y_d^{(N+2)}|$. If $|y_c^{(N+2)}| > |y_d^{(N+2)}|$, we don't need to define $|F_y^B(Q_{1B}, c)|$ particularly. Then we get $M_B(C_B) \subseteq C_B$.

  Similarly, let $|F_x^A(Q_{1A}, d)|$ denote the required $F(Q_{1A}, d)$ for each point $x \in P_A$ to have $|x_c^{(M+2)}| \leq |x_d^{(M+2)}|$ on cycle A. Then image type 1 is obtained by

defining $|F(Q_{1B}, c)| \geq \alpha_5$ and $|F(Q_{1A}, d)| \geq \alpha_6$ where

$$\alpha_5 = \max\{|F_y^B(Q_{1B}, c)|,\ \forall\ y \in P_B\}.$$

and

$$\alpha_6 = \max\{|F_x^A(Q_{1A}, d)|,\ \forall\ x \in P_A\}.$$

- Suitable $|F(Q_{1B}, d)|$ and $|F(Q_{1A}, d)|$ give us type 4.

  Let $|F_y^B(Q_{1B}, d)|$ denote the required $F(Q_{1B}, d)$ for each point $y \in P_B$ to have $|y_c^{(N+2)}| \leq |y_d^{(N+2)}|$ on cycle B. For each $y \in P_B$, the calculation of $|F_y^B(Q_{1B}, d)|$ is similar to the calculation of $|F_y^B(Q_{1B}, c)|$ in image type 1. Then image type 4 is obtained by defining $|F(Q_{1A}, d)| \geq \alpha_6$ and $|F(Q_{1B}, d)| \geq \alpha_7$ where

  $$\alpha_7 = \max\{|F_y^B(Q_{1B}, d)|,\ \forall\ y \in P_B\}.$$

- From image type 1, suitable $|F(Q_{1B}, c)|$, $|F(Q_{1A}, d)|$ and $|F(Q_{1B}, d)|$ give us type 5.

  Note that when $|F(Q_{1B}, c)| \geq \alpha_5$ and $|F(Q_{1A}, d)| \geq \alpha_6$, we have type 1, i.e., $|y_c^{(N+2)}| \geq |y_d^{(N+2)}|$, $\forall y \in P_B$. By Remark 5.1.3 and the continuity of mapping M_B as a function of $F(Q_{1B}, d)$, there exist $F(Q_{1B}, d)$ for each point $y \in P_B$ such that $|y_c^{(N+2)}| = |y_d^{(N+2)}|$. Let $|G_y^B(Q_{1B}, d)|$ denote the required $F(Q_{1B}, d)$ for each point $y \in P_B$ to have $|y_c^{(N+2)}| = |y_d^{(N+2)}|$ on cycle B when $|F(Q_{1B}, c)| \geq \alpha_5$ and $|F(Q_{1A}, d)| \geq \alpha_6$. Then image type 5 is obtained by defining $|F(Q_{1B}, c)| \geq \alpha_5$, $|F(Q_{1A}, d)| \geq \alpha_6$ and $\alpha_8 < |F(Q_{1B}, d)| < \alpha_9$ where

  $$\alpha_8 = \min\{|G_y^B(Q_{1B}, d)|,\ \forall\ y \in P_B\}.$$

  and

  $$\alpha_9 = \max\{|G_y^B(Q_{1B}, d)|,\ \forall\ y \in P_B\}.$$

  If there is only one point in P_B, then image type 5 is obtained by defining $|F(Q_{1B}, c)| \geq \alpha_5$, $|F(Q_{1A}, d)| \geq \alpha_6$ and $|F(Q_{1B}, d)| > |G_v^B(Q_{1B}, d)|$ by Lemma 5.1.8.

- From image type 3, suitable $|F(Q_1, c)|$ and $|F(Q_{1A}, d)|$ give us type 7; From image type 2, suitable $|F(Q_1, c)|$, $|F(Q_{1B}, d)|$ and $|F(Q_{1A}, d)|$ give us type 8; From image type 6, suitable $|F(Q_1, c)|$, $|F(Q_{1B}, d)|$ and $|F(Q_{1A}, d)|$ give us type 9.

The above analysis together with Lemma 5.1.4 and Lemma 5.1.5 completes the proof.

5.2.4 Case 4 and Case 5

Since the calculations are similar, we will just give the construction ideas in the proofs of Theorem 5.2.8 and Theorem 5.2.9.

Theorem 5.2.8. *When $a = d$ and $b \neq c$, if neither c nor d switches in common boundaries, then*

1. *image types 1, 3, 5, 6, 7 and 9 are possible;*

2. *if c switches in cycle B, image types 2, 4 and 8 are possible;*

Proof.

- Suitable $|F(Q_{1A}, c)|$ and $|F(Q_{1B}, a)|$ give us type 2. Let $|F(Q_{1B}, a)|$ be large enough such that for each $y \in P_B$, we will always have $|y_a| \geq |y_c|$ on common boundaries and let $|F(Q_{1A}, c)|$ be large enough such that for each $x \in P_A$, we will always have $|x_c| \geq |x_a|$ on common boundaries. That is $M_B(C_B) \subseteq C_A$ and $M_A(C_A) \subseteq C_B$ at the same time.

- Suitable $|F(Q_1, a)|$ and $|F(Q_{1B}, c)|$ give us types 4, 1 and 5. Let $|F(Q_1, a)|$ be very large such that we will always have $|x_a| \geq |x_c|$ and $|y_a| \geq |y_c|$ on common boundaries for each point $x \in P_A$ and $y \in P_B$ no matter which cycle we follow. That is we have type 4: $M_B(C_B) \subseteq C_A$ and $M_A(C_A) \subseteq C_A$. Then, let $F(Q_{1B}, c)$ be very large such that for each $y \in P_B$, we will always have $|y_c| \geq |y_a|$ on common boundaries even if $|y_a|$ is very large in Q_1 since $|F(Q_1, a)|$ is very large. That is, we have type 1. Then we have $M_B(C_B) \cap C_B \neq \emptyset$ and $M_B(C_B) \cap C_A \neq \emptyset$ by continuity of M_B as a function of the changing focal point parameter $F(Q_{1B}, c)$.

- Suitable $|F(Q_{1A}, c)|$ and $|F(Q_{1B}, c)|$ give us type 3. Let $|F(Q_{1B}, c)|$ be large enough such that for each $y \in P_B$, we will always have $|y_c| \geq |y_a|$ on common boundaries and let $|F(Q_{1A}, c)|$ be large enough such that for each $x \in P_A$, we will always have $|x_c| \geq |x_a|$ on common boundaries. That is $M_B(C_B) \subseteq C_B$ and $M_A(C_B) \subseteq C_B$ at the same time.

- From image type 3, suitable $|F(Q_{1A}, c)|$, $|F(Q_{1B}, c)|$ and $|F(Q_{1B}, d)|$ give us type 6. From image type 1, suitable $|F(Q_1, a)|$, $|F(Q_{1B}, c)|$ and $|F(Q_{1A}, c)|$ give us type 7; From image type 4, suitable $|F(Q_1, a)|$ and $|F(Q_{1A}, c)|$ give us

type 8; From image type 5, suitable $|F(Q_1, a)|$, $|F(Q_{1B}, c)|$ and $|F(Q_{1A}, c)|$ give us type 9.

The above analysis together with Lemma 5.1.4 and Lemma 5.1.5 completes the proof.

Theorem 5.2.9. *When $a \neq c$, $a \neq d$, $b \neq c$ and $b \neq d$, if neither c nor d switches in common boundaries, then*

1. *image types 1, 5, 7 and 9 are possible;*
2. *if d switches in cycle A, image types 3 and 6 are possible;*
3. *if c switches in cycle B, image types 4 and 8 are possible;*
4. *if d switches in cycle A and c switches in cycle B, image type 2 is possible;*

Proof.

- Suitable $|F(Q_{1B}, c)|$ and $|F(Q_{1A}, d)|$ give us type 1.

  Let $|F(Q_{1B}, c)|$ be large enough such that when we start with a point y in P_B, we will always have $|y_c| \geq |y_d|$ on common boundaries and let $|F(Q_{1A}, d)|$ be large enough such that when we start with a point x in P_A, we will always have $|x_d| \geq |x_c|$ on common boundaries. That is $M_B(C_B) \subseteq C_B$ and $M_A(C_A) \subseteq C_A$ at the same time.

- Suitable $|F(Q_{1B}, d)|$ and $|F(Q_{1A}, c)|$ give us type 2.

  Let $|F(Q_{1B}, d)|$ be large enough such that when we start with a point y in P_B, we will always have $|y_c| \leq |y_d|$ on common boundaries and let $|F(Q_{1A}, c)|$ be large enough such that when we start with a point x in P_A, we will always have $|y_d| \leq |y_c|$ on common boundaries. That is $M_B(C_B) \subseteq C_A$ and $M_A(C_A) \subseteq C_B$ at the same time.

- Suitable $|F(Q_{1B}, c)|$ and $|F(Q_{1A}, c)|$ give us type 3.

  Let $|F(Q_{1B}, c)|$ be large enough such that when we start with a point y in P_B, we will always have $|y_c| \geq |y_d|$ on common boundaries and let $|F(Q_{1A}, c)|$ be large enough such that when we start with a point x in P_A, we will always have $|x_c| \geq |x_d|$ on common boundaries. That is $M_B(C_B) \subseteq C_B$ and $M_A(C_A) \subseteq C_B$ at the same time.

  From the discussion in type 1 and type 2, type 3 is obtained by defining $|F(Q_{1B}, c)| \geq \beta_1$ and $|F(Q_{1A}, c)| \geq \beta_4$.

- Suitable $|F(Q_{1B}, d)|$ and $|F(Q_{1A}, d)|$ give us type 4.

  Let $|F(Q_{1B}, d)|$ be large enough such that when we start with a point y in P_B, we will always have $|y_d| \geq |y_c|$ on common boundaries and let $|F(Q_{1A}, d)|$ be large enough such that when we start with a point x in P_A, we will always have $|x_d| \geq |x_c|$ on common boundaries. That is $M_B(C_B) \subseteq C_A$ and $M_A(C_A) \subseteq C_A$ at the same time.

- From image type 1, suitable $|F(Q_{1B}, c)|$, $|F(Q_{1A}, d)|$ and $|F(Q_{1B}, d)|$ give us type 5. From image type 2, suitable $|F(Q_{1B}, d)|$, $|F(Q_{1A}, c)|$ and $|F(Q_{1B}, c)|$ give us type 6. From image type 1, suitable $|F(Q_{1B}, c)|$, $|F(Q_{1A}, d)|$ and $|F(Q_{1A}, c)|$ give us type 7. From image type 2, suitable $|F(Q_{1B}, d)|$, $|F(Q_{1A}, c)|$ and $|F(Q_{1A}, d)|$ give us type 8. From image type 5, suitable $|F(Q_{1A}, c)|$, $|F(Q_{1A}, d)|$, $|F(Q_{1B}, c)|$ and $|F(Q_{1B}, d)|$ give us type 9.

The above analysis together with Lemma 5.1.4 and Lemma 5.1.5 completes the proof.

5.2.5 Corollaries

In Chapter 4, we got the existence and stability of a periodic orbit for a figure-8 pattern with nonadjacent common orthants. From what has been discussed above, we have the following Corollary for the figure-8 pattern with adjacent common orthants.

Corollary 5.2.1. *For the figure-8 pattern described above, when $a \neq c$ or $b \neq d$, if neither c nor d switches on the common boundaries, it is possible to have a periodic orbit following AB.*

Proof. From the results above (Thm. 5.2.4, Thm. 5.2.7-Thm. 5.2.9), we know that we always have image type 2, $M_A(C_A) \subseteq C_B$, $M_B(C_B) \subseteq C_A$. That is, $M_B M_A(C_A) \subset C_A$, where $M_B M_A$ is a continuous mapping from C_A to C_A. Then there exists a fixed point for cycle AB by Brouwer's fixed point theorem.

Corollary 5.2.2. *For the figure-8 pattern described above, if neither c nor d switches on the common boundaries, it is possible to have a periodic orbit following AB when there are more than two common orthants on the figure-8 pattern.*

Since image types 6, 8 and 9 may contain complex dynamical behavior, and this is a main reason why we consider the image types of figure-8 pattern, we give the following corollary to sum up.

Corollary 5.2.3. *For the figure-8 pattern described above, if neither c nor d switches on the common boundaries,*

1. *when $a = c$, $b = d$ and there are only two common orthants, image types 6, 8 and 9 are impossible.*

2. *when if $a = d$, $b = c$ and there are only two common orthants, image types 6 and 8 are possible but image type 9 is impossible.*

3. *for all other cases,*

   (a) *image type 9 is possible.*

   (b) *if d switches in cycle A, image type 6 is possible.*

   (c) *if c switches in cycle B, image type 8 is possible.*

5.3 Examples

Example 5.3.1. Here we give one example which shows how to get different image types for a given n-cube.

We consider a 4-net example, with structure given in Fig. 5.6 and Table 5.2. In our figure-8 pattern with adjacent common orthants, we assumed that directed edges which are not on the figure-8 pattern are all pointing inward towards the figure-8 pattern since we want cycles A and B to be the only two cycles on the hypercube. Note, in this example, in order to ensure that only cycles A and B are possible, we use white walls (arrows pointing in two directions on some edges) as discussed in 5.1.

Orthant ($\tilde{x}_i$)				Focal points (F_i)			
0	0	0	0	-1	-1	-10	10
0	0	0	1	-10	10	-1	10
0	0	1	0	-10	-1	-10	-1
0	0	1	1	1	-1	-1	-1
0	1	0	0	10	1	-1	-10
0	1	0	1	10	10	-1	-10
0	1	1	0	1	-1	-1	1
0	1	1	1	1	-1	-1	1
1	0	0	0	1	-10	-1	10
1	0	0	1	-10	-1	-1	10
1	0	1	0	-10	-1	1	-10
1	0	1	1	1	-10	1	-10
1	1	0	0	10	-10	-1	-1
1	1	0	1	10	1	10	1
1	1	1	0	1	-1	-1	1
1	1	1	1	1	-10	10	1

Table 5.2: Focal point structure for example 5.3.1.

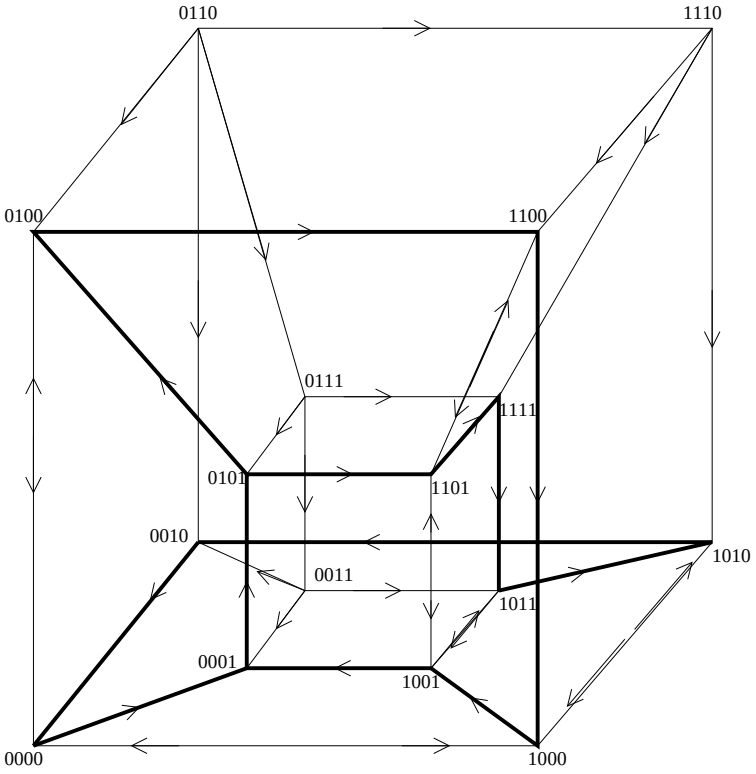

Figure 5.6: Digraph on the 4-cube for the network in Example 5.3.1. The figure-8 pattern is shown by bold edges with 0001 and 0101 as common vertices.

Let cycle $A = [6\ 5\ 13\ 9\ 10\ 2]$ and cycle $B = [6\ 14\ 16\ 12\ 11\ 3\ 1\ 2]$ on the 4-cube. We know that $a = d = 1$, $c = b = 4$, $Q_1 = 2$, $Q_2 = 6$, $q = [-1\ 0\ 0\ 0]^T$, $p = [0\ 0\ 0\ 1]^T$, $v = [-\frac{1}{2}\ 0\ 0\ \frac{1}{2}]^T$ and $u = [0\ 0\ -1\ 0]^T$. This example belongs to case 2, $a = d$ and $b = c$. Since $d = 1$ switches in cycle A and $c = 4$ switches in cycle B, we get image type 2, 3, 4, 6 and 8 from the analysis in Theorem 5.2.4.

Consider the mapping for cycle A

$$M_A(x) = \frac{A^{(6,0)}x}{1 + \langle \psi^{(6,0)}, x \rangle},$$

where $A^{(6,0)} = A^{(5)} \cdots A^{(0)}$ is an $n \times n$ matrix, and $\psi^{(6,0)}$ is an $n \times 1$ vector as given in Eq. (2.7). The denominator $1 + \langle \psi^{(6,0)}, x \rangle$ is not zero and scales x_c and x_d in the same way, therefore we only need to consider the numerator $A^{(6,0)}x$. Similarly, for the mapping of cycle B

$$M_B(y) = \frac{B^{(8,0)}y}{1 + \langle \psi^{(8,0)}, y \rangle},$$

where $B^{(8,0)} = B^{(7)} \cdots B^{(0)}$ is an $n \times n$ matrix, and $\psi^{(8,0)}$ is an $n \times 1$ vector as given

in Eq. (2.7). We only need to consider the numerator $B^{(8,0)}y$.

1. Letting $|F(2,4)| = |F(2,1)| = 10$, we have image type 2 directly.

2. Letting $|F(2,4)| = 10$ and $|F(2,1)| \geq \xi_1$, where

$$\xi_1 = \max\{|F_q^A(2,1)|,\ |F_v^A(2,1)|\},$$

we have image type 4.

Denote $F(2,1)$ by ξ, since

$$A^{(4)} \dots A^{(0)} = \begin{bmatrix} 0 & 0 & 0 & 0 \\ 1.0301 & -0.2010 & 0 & 0.8291 \\ 0.2311 & -0.2110 & 1 & -0.0799 \\ -0.2010 & 1.01 & 0 & 0.8090 \end{bmatrix}$$

and

$$A_A^{(5)} = \begin{bmatrix} 1 & -0.1\xi & 0 & 0 \\ 0 & 0 & 0 & 0 \\ 0 & 0.1 & 1 & 0 \\ 0 & -1 & 0 & 1 \end{bmatrix},$$

$$A^{(5)} \dots A^{(0)} = \begin{bmatrix} -0.10301\xi & 0.0201\xi & 0 & -0.08291\xi \\ 0 & 0 & 0 & 0 \\ 0.3341 & -0.2311 & 1 & 0.003 \\ -1.2311 & 1.2110 & 0 & -0.0201 \end{bmatrix}.$$

For point $q = [-1\ 0\ 0\ 0]^T$

$$q^{(6)} = [A^{(5)} \dots A^{(0)}]q = \begin{pmatrix} 0.10301\xi \\ 0 \\ -0.3341 \\ 1.2311 \end{pmatrix}.$$

In order to get $|q_1^{(6)}| = |q_4^{(6)}|$, solve equation

$$0.10301|\xi| = 1.2311,$$

we get the required $|F(2,1)|$ for point q

$$|F_q^A(2,1)| = \frac{1.2311}{0.10301} = 11.9513.$$

For point $v = [-\frac{1}{2}\ 0\ 0\ \frac{1}{2}]^T$

$$v^{(6)} = [A^{(5)} \dots A^{(0)}]v = \begin{pmatrix} 0.0101\xi \\ 0 \\ -0.1656 \\ 0.6055 \end{pmatrix}.$$

In order to get $|v_1^{(6)}| = |v_4^{(6)}|$, solve equation

$$0.0101|\xi| = 0.6055,$$

we get the required $|F(2,1)|$ for point v

$$|F_v^A(2,1)| = \frac{0.6055}{0.0101} = 59.9505.$$

Since the third variable doesn't switch in cycle A, we don't need to consider point $u = (-1/2\ \ 0\ \ 0\ 1/2)^T$ on the boundary of C_a. Letting $|F(2,4)| = 10$ and $|F(2,1)| \geq \xi_1$, where

$$\xi_1 = \max\{|F_q^A(2,1)|,\ |F_v^A(2,1)|\} = 59.9505,$$

we have type 4.

3. Letting $|F(2,4)| = 10$ and $\xi_2 < |F(2,1)| < \xi_1$, where

$$\xi_2 = \min\{|F_q^A(2,1)|,\ |F_v^A(2,1)|\} = 11.9513,$$

we have image type 8.

Note that for $|F(2,4)| = \gamma$ and $\gamma \leq |F(2,1)| \leq \xi_1$, we always have type 2.

4. Letting $|F(2,1)| = 10$ and $|F(2,4)| \geq \delta_1$, where

$$\delta_1 = \max\{|F_p^B(2,4)|,\ |F_v^B(2,4)|,\ |F_u^B(2,4)|\},$$

we have image type 3.

Denote $F^B(2,4)$ by δ, since

$$B^{(6)} \dots B^{(0)} = \begin{bmatrix} 0.9528 & -1.0422 & 0.3173 & -0.1211 \\ -0.7640 & -0.2343 & 0.3376 & -1.0321 \\ 0.2053 & -0.2121 & 1.0423 & -0.1110 \\ 0 & 0 & 0 & 0 \end{bmatrix}$$

and

$$B^{(7)} = \begin{bmatrix} 1 & 1 & 0 & 0 \\ 0 & 0 & 0 & 0 \\ 0 & 0.1 & 1 & 0 \\ 0 & -0.1\delta & 0 & 1 \end{bmatrix},$$

$$B^{(7)} \dots B^{(0)} = \begin{bmatrix} 0.1888 & -1.2765 & 0.6550 & -1.1532 \\ 0 & 0 & 0 & 0 \\ 0.1289 & -0.2355 & 1.0761 & -0.2142 \\ 0.07640\delta & 0.02343\delta & -0.03376\delta & 0.10321\delta \end{bmatrix}.$$

For point $p = [0\ 0\ 0\ 1]^T$,

$$p^{(8)} = [B^{(7)} \dots B^{(0)}]p = \begin{pmatrix} -1.1532 \\ 0 \\ -0.2142 \\ 0.10321\delta \end{pmatrix}.$$

In order to get $|p_1^{(8)}| = |p_4^{(8)}|$, and since $p_1^{(8)} < 0$, solve equation

$$1.1532 = 0.10321|\delta|,$$

we get the required $|F(2,4)|$ for point p

$$|F_p^B(2,4)| = \frac{1.1532}{0.10321} = 11.1733.$$

For point $v = [-\frac{1}{2}\ 0\ 0\ \frac{1}{2}]^T$,

$$v^{(8)} = [B^{(7)} \dots B^{(0)}]v = \begin{pmatrix} -0.6710 \\ 0 \\ -0.1715 \\ 0.0134\delta \end{pmatrix}.$$

In order to get $|v_1^{(8)}| = |v_4^{(8)}|$, solve equation

$$0.6710 = 0.0134|\delta|,$$

we get the required $|F(2,4)|$ for point v

$$|F_v^B(2,4)| = 50.0746.$$

For point $u = [0\ 0\ -1\ 0]^T$,

$$u^{(8)} = [B^{(7)} \dots B^{(0)}]u = \begin{pmatrix} -0.655 \\ 0 \\ -1.0761 \\ 0.03376\delta \end{pmatrix}.$$

In order to get $|u_1^{(8)}| = |u_4^{(8)}|$, solve equation

$$0.655 = 0.033761|\delta|,$$

we get the required $|F(2,4)|$ for point u

$$|F_u^B(2,4)| = 19.4017.$$

So, let $|F(2,1)| = 10$ and $|F(2,4)| \geq \delta_1$, where

$$\delta_1 = \max\{|F_p^B(2,4)|,\ |F_v^B(2,4)|,\ |F_u^B(2,4)|\} = 50.0746,$$

we have type 3.

5. Let $|F(2,1)| = 10$ and $\delta_2 < |F(2,4)| < \delta_1$, where

$$\delta_2 = \min\{|F_p^B(2,4)|,\ |F_v^B(2,4)|,\ |F_u^B(2,4)|\} = 11.1733,$$

we have image type 6.

Note that for $|F(2,1)| = 10$ and $10 \leq |F(2,4)| \leq \delta_2$, we always have type 2.

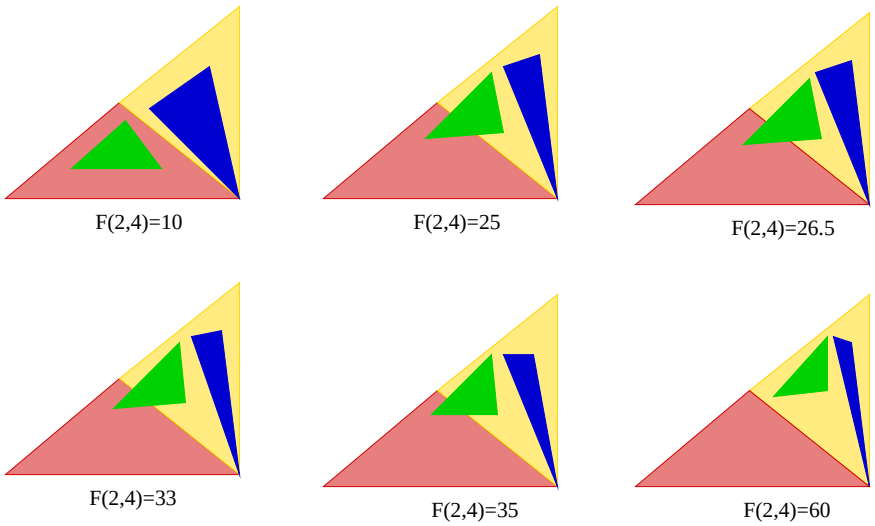

Figure 5.7: Image types of cycles A and B when $|F(2,1)| = 10$, where the red triangles are the returning cones C_A of cycle A projected onto a plane, the yellow triangles are the returning cones C_B of cycle B projected onto a plane, the blue triangles are $M_A(C_A)$ projected onto a plane and the green triangles are $M_B(C_B)$ projected onto a plane.

So far, we have finished the construction of focal points to get different image types. We will give the returning cone images and the trajectories in phase space for some specific values of $|F(2,1)|$ and $|F(2,4)|$ to complete this example.

1. Let $|F(2,1)| = 10$ and $|F(2,4)| = 10$, we get image type 2. There is a stable periodic cycle AB passing through $y^* = [-1.0589 \;\; 0 \;\; -0.6807 \;\; 0.5568]^T$.

2. Let $|F(2,1)| = 10$ and $|F(2,4)| = 25$, we get image type 6. There is a stable periodic cycle AB^3 passing through $y^* = [-1.5451 \;\; 0 \;\; -0.6969 \;\; 1.2666]^T$.

3. Let $|F(2,1)| = 10$ and $|F(2,4)| = 26.5$, we get image type 6. There is a stable periodic cycle AB^4AB^3 passing through $y^* = [-1.6341 \;\; 0 \;\; -0.7039 \;\; 1.5619]^T$.

4. Let $|F(2,1)| = 10$ and $|F(2,4)| = 33$, we get image type 6. There is a stable periodic cycle $AB^{10}AB^9$ passing through $y^* = [-1.3887 \;\; 0 \;\; -0.6759 \;\; 1.3884]^T$.

5. Let $|F(2,1)| = 10$ and $|F(2,4)| = 35$, we get image type 6. There is a stable periodic cycle AB^{34} passing through $y^* = [-1.2468 \;\; 0 \;\; -0.6489 \;\; 1.2240]^T$.

6. Let $|F(2,1)| = 10$ and $|F(2,4)| = 60$, we get image type 3. There is a stable periodic cycle B passing through $y^* = [-3.3531 \;\; 0 \;\; -0.8356 \;\; 14.1769]^T$.

Figure 5.7 shows the returning cones and the returning cone images after projection. Figure 5.8 shows the phase space projections of the periodic orbits.

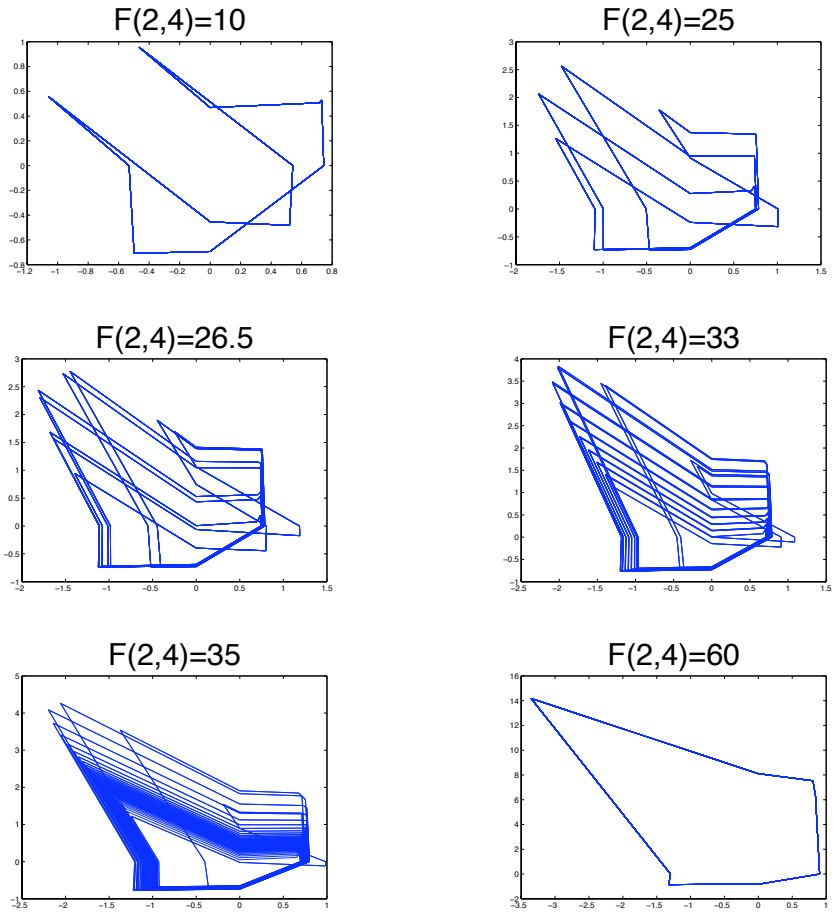

Figure 5.8: 2D phase space projections of the stable periodic orbit in the 4-net of Fig. 5.6 and Table 5.2 when $|F(2,1)| = 10$, where the x-axis is the first coordinate and the y-axis is the fourth coordinate.

We will use the third set of values, $|F(2,1)| = 10$ and $|F(2,4)| = 26.5$, to show that how we find the periodic orbits and fixed points above.

We choose a point on the boundary between orthant 0001 and 0101 randomly, say $y^{(0)} = (-1 \;\; 0 \;\; -1 \;\; 1)$ at first. Then we calculate the mapping of each step by Eq. (2.3). After a few steps, we notice that the trajectory always seems to follow cycle AB^4AB^3. In order to check the existence of a periodic orbit AB^4AB^3, calculating

the cycle map by Eq. (2.6), (2.7) and (2.14), we obtain

$$A \approx \begin{pmatrix} 351.1208 & 90.1756 & 88.1245 \\ 152.9281 & 39.4761 & 39.9950 \\ -326.7360 & -84.5620 & -74.2014 \end{pmatrix}, \quad \phi \approx \begin{pmatrix} -217.3203 \\ -56.0639 \\ -57.5239 \end{pmatrix}.$$

The eigenvalues λ_i, $i = 1, 2, 3$ and their corresponding eigenvectors v_i, $i = 1, 2, 3$ are

$$l_1 \approx 305.7321, \quad l_2 \approx 10.3741, \quad l_3 \approx 0.2894,$$

$$v_1 \approx \begin{pmatrix} -0.6902 \\ -0.2973 \\ 0.6597 \end{pmatrix}, \quad v_2 \approx \begin{pmatrix} 0.2596 \\ -0.0377 \\ -0.9650 \end{pmatrix}, \quad v_3 \approx \begin{pmatrix} -0.2656 \\ 0.9613 \\ 0.0735 \end{pmatrix}.$$

From Proposition 2.3.4 and 2.3.6, we know that this system has one fixed points $y^* = [-1.6341 \;\; 0 \;\; -0.7039 \;\; 1.5619]^T$. By Proposition 2.3.7, y^* is stable because y^* is on the span of v_1 which is the corresponding eigenvector of the dominant eigenvalue l_1.

We use the same 4-net example in Example 5.3.1 to show that how we construct networks that have specific maps (piecewise-linear maps) of two triangles with images of the vertices specified. We still don't know whether we can construct networks such that all the points in P_A and P_B can be mapped to any specified points. If the answer is yes, then given a map with known dynamics, we may be able to construct a network which has that map as a Poincaré map and hence has the same complex dynamics.

Example 5.3.2. Let $q^* = (-1/4 \;\; 0 \;\; -5/8 \;\; 1/8)^T$ and $v^* = (-1/7 \;\; 0 \;\; -4/7 \;\; 2/7)^T$ be two points on $C_a \bigcup C_b$. We will construct a network with piecewise-linear map M_A such that $q^* = M_A(q)$ and $v^* = M_A(v)$, where $q = (-1 \;\; 0 \;\; 0 \;\; 0)^T$ and $v = (-1/2 \;\; 0 \;\; 0 \;\; 1/2)^T$ by Figure 5.6. By Eq. (2.6), we have

$$q^* = M_A q = \frac{A^{(6,0)} q}{1 + \langle \psi^{(6,0)}, q \rangle} \tag{5.4}$$

and

$$v^* = M_A v = \frac{A^{(6,0)} v}{1 + \langle \psi^{(6,0)}, v \rangle}, \tag{5.5}$$

where $A^{(6,0)}$ and $\psi^{(6,0)}$ are as indicated in Eq. (2.7). For these eight equations Eq (5.4) and (5.5), two of them are equalities $0 = 0$. Therefore we only need to solve six

equations. We choose $F(10,2)$, $F(10,3)$, $F(10,4)$, $F(2,1)$, $F(2,3)$ and $F(2,4)$ as six unknowns. Other focal points are defined by Table 5.2.

With all the focal points defined, we write out Eq (5.4) and (5.5) as equations of unknowns $F(10,2)=\alpha$, $F(10,3)=\beta$, $F(10,4)=\delta$, $F(2,1)=\rho$, $F(2,3)=\zeta$ and $F(2,4)=\eta$.

$$\begin{cases} \frac{-0.00201\alpha\rho+0.101\rho}{-0.00201\alpha+1.3321}=-\frac{1}{4}, \\ \frac{-0.00201\alpha\zeta+0.101\zeta+0.0201\beta-0.211}{-0.00201\alpha+1.3321}=-\frac{5}{8}, \\ \frac{-0.00201\alpha\eta+0.101\eta+0.0201\delta}{-0.00201\alpha+1.3321}=\frac{1}{8}, \\ \frac{(-0.00201\alpha\rho+0.101\rho)*0.5+(-0.00809\alpha\rho-0.091\rho)*0.5}{-0.00505\alpha+1.1605}=-\frac{1}{7}, \\ \frac{(-0.00201\alpha\zeta+0.101\zeta+0.0201\beta-0.211)*0.5+(-0.00809\alpha\zeta-0.091\zeta+0.0809\beta+0.001)*0.5}{-0.00505\alpha+1.1605}=-\frac{4}{7}, \\ \frac{(-0.00201\alpha\eta+0.101\eta+0.0201\delta)*0.5+(-0.00809\alpha\eta-0.091\eta+0.0809\delta)*0.5}{-0.00505\alpha+1.1605}=\frac{2}{7}. \end{cases} \tag{5.6}$$

Solve Eq. (5.6), we get two sets of solutions:

$$\begin{aligned} &F(10,2)=1186.9752, \quad F(10,3)=-268.5584, \quad F(10,4)=473.3225, \\ &F(2,1)=-0.1153, \qquad F(2,3)=-2.7431, \qquad F(2,4)=4.2216 \end{aligned}$$

and

$$\begin{aligned} &F(10,2)=-11.6812, \quad F(10,3)=-6.5921, \quad F(10,4)=6.5058, \\ &F(2,1)=-2.7225, \qquad F(2,3)=-4.0468, \qquad F(2,4)=0.3107. \end{aligned}$$

By Figure 5.6, we know that

$$F(10,2)<0, \quad F(10,3)<0, \quad F(10,4)>0, \quad F(2,1)<0, \quad F(2,3)<0, \quad F(2,4)>0.$$

Therefore, the second set of solutions is the right answer.

To verify our result, solving $M_A(q)$ and $M_A(v)$ by Eq. (2.14) with the constructed focal points, we obtain

$$M_A(q)=q^*, \quad M_A(v)=v^*.$$

That is we find the focal points such that the vertices of C_a except $u=(0 \;\; 0 \;\; -1 \;\; 0)^T$ (u is a fixed point in this case) are mapped to some specified points.

Chapter 6

Discussion

It has been more than thirty years since Glass networks were proposed. Five years after the proposing of Glass networks, Glass and Pasternack obtained a structural principle about a special cycle on the n-cube called 'cyclic attractor'. Networks with cyclic attractor will either have a stable limit cycle attractor or approach the origin in the limit $t \to \infty$. During these years, although many researches have paid attention to Glass networks, most of the results are about the existence and stability of periodic orbits of given Glass networks. Results for the structural principles of Glass networks are left behind.

All the results in this thesis are about structural principles of Glass networks. We know that the dynamical behavior of any Glass network can be represented symbolically on the n-cube. However, the digraph on the n-cube only shows the possible trajectory transition direction in the phase space. The domain for a cycle map may be empty, i.e., not every cycle on the n-cube can have trajectories passing through the corresponding orthant in the phase space.

In this thesis, starting with different given cycles on the n-cube, we obtain the following structural principles:

1. for any simple cycle on the n-cube with a non-branching vertex, Thm. 3.1.1 and Thm. 3.1.2 prove that it is possible to have a stable periodic orbit passing through the corresponding orthants for some sets of focal points F in Glass networks;

2. when the simple cycle on the n-cube doesn't have a non-branching vertex, the existence of periodic orbit depends on the structure of the n-cube. A structural principle is given to determine whether it is possible to have a periodic oribit for some sets of suitable focal points (Thm. 3.2.1 and Thm. 3.2.2);

3. another structural principle is given in Thm. 4.1.1 for the existence of figure-8

orbits with only one common orthant. The result is generalized to cycles with multiple nonadjacent common vertices (Thm. 4.2.1);

4. in Chapter 5, by considering all the possible image types of the Poincaré map for a figure-8 pattern with more than one common orthant, we obtain structural principles for the Glass networks to have complex periodic orbits or possibly chaos.

Despite the above progress in the structural principles, there are questions left behind to think about in the future.

1. In Chapter 5, the figure-8 pattern with more than one common orthant, we only consider the case that other directed edges which are not on the figure-8 pattern are all pointing inward towards the figure-8 pattern. Although this is the simplest case in figure-8 pattern with more than one common orthant, they have rich dynamical behaviors as show in Example 5.3.1. Figure-8 patterns without this restriction should be more interesting. Another restriction, used in this chapter, is that neither the cth nor the dth element switches on common boundaries. Using the construction idea in Thm. 3.1.1, i.e., controlling the trajectory direction by choosing suitable focal points, the first restriction may be conquered. But a figure-8 pattern without the second restriction is hard to analyze.

2. After finding structural principles for periodic orbits, another interesting problem is to find structural principles for chaos, i.e. what kind of digraph on the n-cube allows chaos. In Chapter 5, we focus on figure-8 patterns on the n-cube. By considering all the different image types, we narrow the image types down to image types 6, 8 and 9 which may contain complex dynamical behavior including chaos. As shown in Example 5.3.1, we have successfully constructed a network with complex periodic cycles, but structural principles for chaos are considered as future work.

The relevance of the results obtained in this thesis to gene networks is the following:

1. assessing dynamical possibilities for gene networks with certain structures (in the state space diagram), particularly when parameters in real networks are poorly known;

2. engineering possibilities: our type of approach may allow construction of synthetic networks with certain dynamical properties or may one day contribute to the ability to alter malfunctioning gene networks such that they recover their intended dynamical behavior.

Bibliography

[1] F. Jacob and J. Monod, *Genetic Regulatory Mechanisms in the Synthesis of Proteins*, J. Mol. Biol., **3** (1961), 318-356.

[2] L. Glass and S. A. Kauffman, *The logical analysis of continuous, non-linear biochemical control networks*, J. theor. Biol., **39** (1973), 103-129.

[3] L. Glass, *Classification of biological networks by their qualitative dynamics*, J. theor. Biol., **54** (1975), 85-107.

[4] L. Glass, *Combinatorial and topological methods in nonlinear chemical kinetics*, The Journal of Chemical Physics, **63(4)** (1975), 1325-1335.

[5] L. Glass and J. S. Pasternack, *Prediction of limit cycle in mathematical models of biological oscillations*, Bulletin of Mathematical Biology, **40** (1978), 27-44.

[6] L. Glass, *Global analysis of nonlinear chemical kinetics*, B. J. Berne(Ed.), Statistical Mechanics, Part B: Time-dependent Processes, Plenum Press, New York,1977, 311-349.

[7] L. Glass, *Combinatorial aspects of dynamics in biological systems*, Statistical Mechanics and Statistical Methods in Theory and Application, Plenum Publishing Corporation, 1977.

[8] L. Glass and J. S. Pasternack, *Stable oscillations in mathematical models of biological control systems*, J. Math. Biology, **6** (1978), 207-223.

[9] H. De Jong, *Modeling and simulation of genetic regulatory system: a literature review*, Journal of Computational Biology, **9(1)** (2002), 67-103.

[10] H. De Jong, J. Geiselmann, G.Batt, C. Hernandez and M. Page, *Qualitative simulation of the initiation of sporulation in bacillus subtilis*, Bulletin of Mathematical Biology, **66** (2004), 261-299.

[11] E. Farcot and J.-L. Gouzé, *Periodic solutions of piecewise affine gene network models: the case of a negative feedback loop*, Institut National De Recherche En Informatique Et En Automatique(INRIA), **6018** (Nov. 2006).

[12] T. Mestl, E. Plahte and S. W. Omholt, *Periodic solutions in systems of piecewise linear differential equations*, Dynamics and Stability of Systems, **10(2)** (1995), 179-193.

[13] R. Edwards, H. T. Siegelmann, K. Aziza and L. Glass, *Symbolic dynamics and computation in model gene networks*, Chaos, **11(1)** (2001), 160-169.

[14] R. Edwards and L. Glass, *Combinatorial explosion in model gene networks*, Chaos, **10(3)** (2000), 691-704.

[15] T. Gedeon, *Attractors in continuous-time switching networks*, Communications on Pure and Applied Analysis, **2(2)** (2003), 187-209.

[16] T. Mestl, C. Lemay and L. Glass, *Chaos in high-dimensional neural and gene networks*, Physica D, **98** (1996), 33-52.

[17] R. Edwards, *Analysis of continuous-time switching networks*, Physica D, **146** (2000), 165-199.

[18] R. Edwards, *Chaos in neural and gene networks with hard switching*, Differential Equations and Dynamical Systems, **9(3-4)** (2001), 187-220.

[19] M. B. Elowitz and S. Leibler, *A synthetic oscillatory network of transcriptional regulators*, Nature, **403** (2000), 335-338.

[20] T. S. Gardner, C. R. Cantor and J. J. Collins *Construction of a genetic toggle switch in Escherichia coli*, Nature, **403** (2000), 339-342.

[21] E. Plahte and S. Kjϕglum, *Analysis and generic properties of gene regulatory networks with graded response functions*, Phys. D, **201** (2005), 150-176.

[22] E. Farcot, *Geometric properties of a class of piecewise affine biological network models*, J. Math. Biol., **52** (2006), 373-418.

[23] R. Edwards and L. Glass, *A calculus for relating the dynamics and structure of complex biological networks*, Adventures in Chemical Physics: A Special Volume in Advances in Chemical Physics, **132** (2006), 151-178.

[24] R. Edwards, P. van den Driessche and L. Wang, *Periodicity in piecewise-linear switching networks with delay*, J. Math. Biol, **55** (2007), 271-298.

[25] R. Casey, H. de Jong and J. Gouzé, *Piecewise-linear models of genetic regulatory networks: equilibria and their stability*, J. Math. Biol, **52** (2006), 27-56.

[26] S. A. Kauffman, J. theor. Biol., **22** (1969), 437.

[27] S. A. Kauffman, *In current topics in developmental biology*, New York: academic press, **6** (1971).

[28] S. A. Kauffman, *Lectures on mathematics in the life sciences*, Providence R. I.: American mathematical society, **3** (1971).

[29] M. Sugita, J. Theor. bio., **4** (1963), 179.

[30] E. H. Snoussi, Qualitative dynamics of piecewise-linear differential equations: a discrete mapping approach, Dyn. Stability Syst., **4** (1989), 189-207.

[31] D. Ropers, H. De Jong, M. Page, D. Schneider, J. Geiselmann, Qualitative simulation of the carbon starvation response in Escherichia coli, BioSystems, **84 (2)** (2006), 124-152.

[32] D. W. Jordan and P. Smith, Nonlinear ordinary differential equations: An introduction to dynamical systems (third edition), Oxford University Press, 277-278.

[33] R. Thomas, D. Thieffry and M. Kaufman, Dynamical behaviour of biological regulatory networks-I. Biological role of feedback loops and practical use of the concept of the loop-characteristic state, Bull. Math. Biol., **57 (2)** (1995), 247-276.